2012

The Expression of the Zinc Finger Transcription Factor zDC Defines the Classical Dendritic Cell Lineage

Matthew M. Meredith

THE EXPRESSION OF THE ZINC FINGER TRANSCRIPTION FACTOR zDC DEFINES THE CLASSICAL DENDRITIC CELL LINEAGE

A Thesis Presented to the Faculty of

The Rockefeller University

in Partial Fulfillment of the Requirements for

the degree of Doctor of Philosophy

by

Matthew M. Meredith

June 2012

THE EXPRESSION OF THE ZINC FINGER TRANSCRIPTION FACTOR zDC DEFINES THE CLASSICAL DENDRITIC CELL LINEAGE

Matthew M. Meredith, Ph.D.

The Rockefeller University 2012

Classical dendritic cells (cDCs) are a critical component of the immune system due to their roles in the maintenance of immune tolerance and the induction of adaptive immune responses. However, distinguishing cDCs from other myeloid populations is complicated by the lack of highly specific cDC markers. For example, high expression of the integrin CD11c is used to define cDCs, but this marker is also expressed at lower levels by plasmacytoid dendritic cells, monocyte and macrophage subsets, and some lymphocytes. Similarly, the use of the CD11c promoter to drive the expression of different reporters in cDCs likewise affects these additional populations.

To identify a novel and more specific cDC marker, I compared the gene expression profiles of differentiated cDCs, committed cDC precursors (pre-DCs), monocytes, and myeloid progenitor populations by gene array. Enriching cDC-specific genes identified an uncharacterized zinc finger transcription factor that I call zDC (Zbtb46, Btbd4). This factor is expressed by cDCs but not other myeloid or lymphoid immune populations.

The characterization of zDC expression and function involved three major directions. (1) To exploit cDC-specific expression of zDC, I produced zDC-DTR knock-in mice that express diptheria toxin receptor (DTR) regulated by the zDC locus. Consistent with zDC expression, DTR expression is limited to cDCs among hematopoietic cells and diptheria toxin (DT) injection depletes cDCs but not other populations. (2) To identify the target genes occupied and regulated by zDC, I performed chromatin immunoprecipitation-sequencing (ChIP-seq) on zDC from steady state cDCs. zDC bound upstream of the transcription start sites of over 1,000 genes at sequence-specific motifs. (3) To interrogate zDC function, I generated zDC-deficient mice by knocking out the second exon of the zDC locus. cDC development is unimpaired in $zDC^{-/-}$ mice, but steady state zDC-deficient cDCs upregulated zDC target genes identified by ChIP-seq in addition to maturation gene pathways. This steady state maturation results in impaired peripheral tolerance as well as enhanced skin-draining lymph node vascularization. Therefore, the zinc finger transcription factor zDC uniquely defines the cDC lineage and serves as a transcriptional repressor which maintains cDC quiescence in the steady state.

ACKNOWLEDGMENTS

I would like to thank foremost my advisor, Michel Nussenzweig, for his guidance and support. I also want thank past and present members of the Nussenzweig lab for their unwavering generosity and kindness: Kang Liu for her thoughtfulness and mentorship since my first days in the lab; Alice Kamphorst for her wholehearted friendship and advice; Davide Robbiani for his patience and training in molecular biology; Kai-Hui Yao for her invariable generosity and enthusiasm; Tom Eisenreich and David Bosque for their help with the mouse colonies; Pierre Guermonprez for his reassuring optimism and critical suggestions; Heidi Schreiber for her generous collaboration with microscopy; Guillaume Darrasse-Jeze for his helpful suggestions; Mila Jankovic for her unfailing compassion and perspective; Zoran Jankovic for his kindness and thoughtfulness; Anna Gazumyan for her infectious enthusiasm and endless encouragement; Anne Bothmer for her honesty and friendship; Klara Velinzon for her patience and skill during cell sorts; and Virginia Menendez for her kindness and efficiency.

I would additionally like to thank friends and colleagues in other labs at Rockefeller and in the area: Juliana Idoyaga in Ralph Steinman's lab for her cheerful insights and generous contribution of protocols and reagents including DEC-OVA; Cheolho Cheong in Ralph Steinman's lab for his collaboration to set

up mixed leukocyte reactions; Rachel Niec in Alexander Rudensky's lab for her help setting up *Toxoplasma gondii* infections; and Suzannah Rihn from Paul Bieniasz's lab for her collaboration running gel shift assays during her rotation in our lab.

I would also like to thank the members of my thesis committee: Ralph Steinman for his contagious curiosity; Howard Hang for his thoughtful questions and suggestions; Nina Papavasiliou for her encouragement; and Miriam Merad for her time and consideration.

Finally, I am grateful to the David Rockefeller Graduate Program and the members of Dean's Office for their consideration, patience, and support.

TABLE OF CONTENTS

List of Figures vi

Chapter 1. Introduction 1

Chapter 2. Results Part I: zDC expression 21

Chapter 3. Results Part II: zDC-DTR mice 31

Chapter 4. Results Part III: zDC target genes 65

Chapter 5. Results Part IV: zDC function 74

Chapter 6. Discussion 96

Chapter 7. Methods 117

Appendix I. zDC target genes: Total 127

Appendix II. zDC target genes: Nucleic acid metabolism 132

Appendix III. zDC target genes: Protein metabolism 133

References 134

LIST OF FIGURES

Figure 1. Myeloid development and CD11c expression 5
Figure 2. Gene array identification of zDC 23
Figure 3. zDC transcript and protein is expressed by cDCs 26
Figure 4. zDC expressed by human cDCs and highly conserved 29
Figure 5. zDC-DTR mice 33
Figure 6. DTR expression in zDC-DTR mice 36
Figure 7. DT dose titration in zDC-DTR mice 39
Figure 8. cDC ablation in lymphoid and non-lymphoid organs 41
Figure 9. Flt3L and cDC reconstitution 43
Figure 10. cDC ablation: zDC-DTR vs CD11c-DTR 46
Figure 11. Immune populations: zDC-DTR vs CD11c-DTR 49
Figure 12. LPS-induced lymph node $CD14^{+}$ dendritic cells 53
Figure 13. Splenic macrophages 56
Figure 14. Lymph node macrophages 58
Figure 15. Antigen presentation and MLR stimulation 61
Figure 16. *Toxoplasma gondii* infection 64
Figure 17. zDC binds upstream of the TSS at specific motifs 67
Figure 18. Functional classification of zDC target genes 70
Figure 19. zDC targets concentrated at MHC locus 72
Figure 20. zDC knockout mice 76
Figure 21. cDCs do not depend on zDC for development 78
Figure 22. zDC-deficient cDCs upregulate zDC target genes 81
Figure 23. zDC-deficient cDCs upregulate maturation pathways 84
Figure 24. TLR stimulation does not downregulate zDC-DTR 87
Figure 25. OT-I deletion impaired in zDC-deficient mice 90
Figure 26. Hyperplastic lymph nodes from zDC-deficient mice 92
Figure 27. Elevated VEGF expression by zDC-deficient cDCs 95
Figure 28. Myeloid development, and CD11c and zDC expression 100

Chapter 1.

INTRODUCTION

Classical dendritic cells (cDCs) are professional antigen presenting cells that constantly sample and process antigen for presentation to T cells. In the steady state, cDCs help mediate tolerance for self and innocuous antigens. Conversely, in response to infection and inflammatory responses, cDCs undergo maturation and initiate adaptive immune responses. Thus, cDCs influence the transition from steady state tolerance to adaptive immunity.

Since their initial description in 1973, distinguishing cDCs from other myeloid populations has proven challenging and controversial. For example, cDCs, plasmacytoid dendritic cells (pDCs), monocytes, and macrophages share multiple phenotypic markers, and arise from shared progenitors in the bone marrow. However, cDCs represent a functionally distinct population. Most notably, antigen presentation by cDCs is orders of magnitude more efficient than other myeloid populations.

The integrin CD11c is the most reliable surface marker of the cDC lineage, but its expression is also shared by other immune populations including pDCs, monocytes, and macrophages. This promiscuous expression results in mislabeling various populations as cDCs. Therefore, new markers are needed to more genuinely identify cDCs from other myeloid populations.

In this thesis, I outline the identification of a novel cDC marker called zDC for 'zinc finger expressed by cDCs.' zDC expression is unique to cDCs but absent in other cells of the immune system, most importantly pDCs, monocytes, and macrophages. Utilizing this cDC-specific promoter, I introduced a diphtheria toxin receptor (DTR) coding sequence into the zDC locus to generate zDC-DTR knock-in. To address zDC function, I performed chromatin immunoprecipitation-sequencing (ChIP-seq) to define the set of genes bound by zDC in steady state cDCs. Furthermore, I produced a conditional knockout of the second exon of the zDC locus to interrogate the effect of zDC deletion on cDC development and function.

Discovery of classical dendritic cells

In 1967, it was reported that lymphocytes alone are unable to respond to cognate antigen, and that unidentified 'accessory cells' are required for the formation of antibody responses *in vitro* (Mosier 1967). Subsequent microscopic evaluation of the accessory cells demonstrated that they were composed mostly of macrophages, but a small proportion exhibited uniquely elongated and branched cell bodies. In 1973, these rare cells were officially named 'dendritic cells,' derived from the Greek word for tree, *dendron* (Steinman and Cohn 1973).

cDCs were quickly appreciated as the potent immune accessory cells mediating the mixed leukocyte reaction (Steinman and Witmer 1978) and the induction of T

cell responses (Nussenzweig et al. 1980). Compared to macrophages, which were thought to be the critical accessory cells for these processes, cDCs were 100-fold more potent at initiating antigen-specific T cell proliferation. In addition to high MHC II expression (Nussenzweig et al. 1981; Steinman et al. 1979), various markers were subsequently characterized to more specifically identify cDCs, most notably the integrin CD11c (Metlay et al. 1990), and even cDC subsets, including the lectins DCIR2, which is recognized by the antibody 33D1 (Nussenzweig et al. 1982), and DEC-205 (Kraal et al. 1986).

cDC development and homeostasis

Like all immune cells, cDCs derive from bone marrow-resident hematopoietic stem cells. Macrophage and dendritic cell progenitors (MDPs) are myeloid-restricted progenitor cells that give rise to monocytes, plasmacytoid dendritic cells (pDCs), and cDCs (Figure 1) (Fogg et al. 2006; Varol et al. 2007). This population consists of proliferating cells that express the cytokine/chemokine receptors CX_3CR1, M-CSF-R (CD115), c-kit (CD117), and Flt3 (CD135) and lack the expression of lineage markers and the stem cell marker Sca-1 (Auffray et al. 2009; Fogg et al. 2006). *In vivo* transfer and *in vitro* cell culture experiments demonstrate that MDPs have the potential to give rise to monocytes, pDCs, and cDCs (Fogg et al. 2006; K. Liu et al. 2009; Waskow et al. 2008). Granulocytes, on the other hand, do not arise from MDPs and are derived instead from earlier myeloid progenitors. MDPs reside in the bone marrow and cannot be found in blood or peripheral lymphoid organs in the steady state (K. Liu et al. 2009).

Figure 1. Development of cDCs, pDCs, and monocytes/macrophages and the expression of CD11c.

Macrophage and **d**endritic cell **p**rogenitors (MDPs) give rise to monocytes and **c**ommon **d**endritic cell **p**rogenitors (CDPs). Both subsets of monocytes circulate the blood to lymphoid and non-lymphoid organs where they contribute to the development of some macrophage subsets in the steady state. In response to inflammatory stimuli, Ly6C^{hi} monocytes differentiate into cells with many features of cDCs, including CD11c, MHC II, and co-stimulatory markers. CDPs, which have lost monocyte potential, give rise to pDCs and pre-DCs. Similar to monocytes, steady state pDCs circulate the blood to lymphoid and non-lymphoid organs. Pre-DCs, which demonstrate only cDC potential, develop in the bone marrow and travel via the blood to lymphoid and non-lymphoid organs. Both subsets of cDCs are derived from pre-DCs. Solid arrows represent differentiation while dotted arrows show migration. Red arrow shows differentiation during inflammation. Blue color indicates CD11c expression.

Figure 1

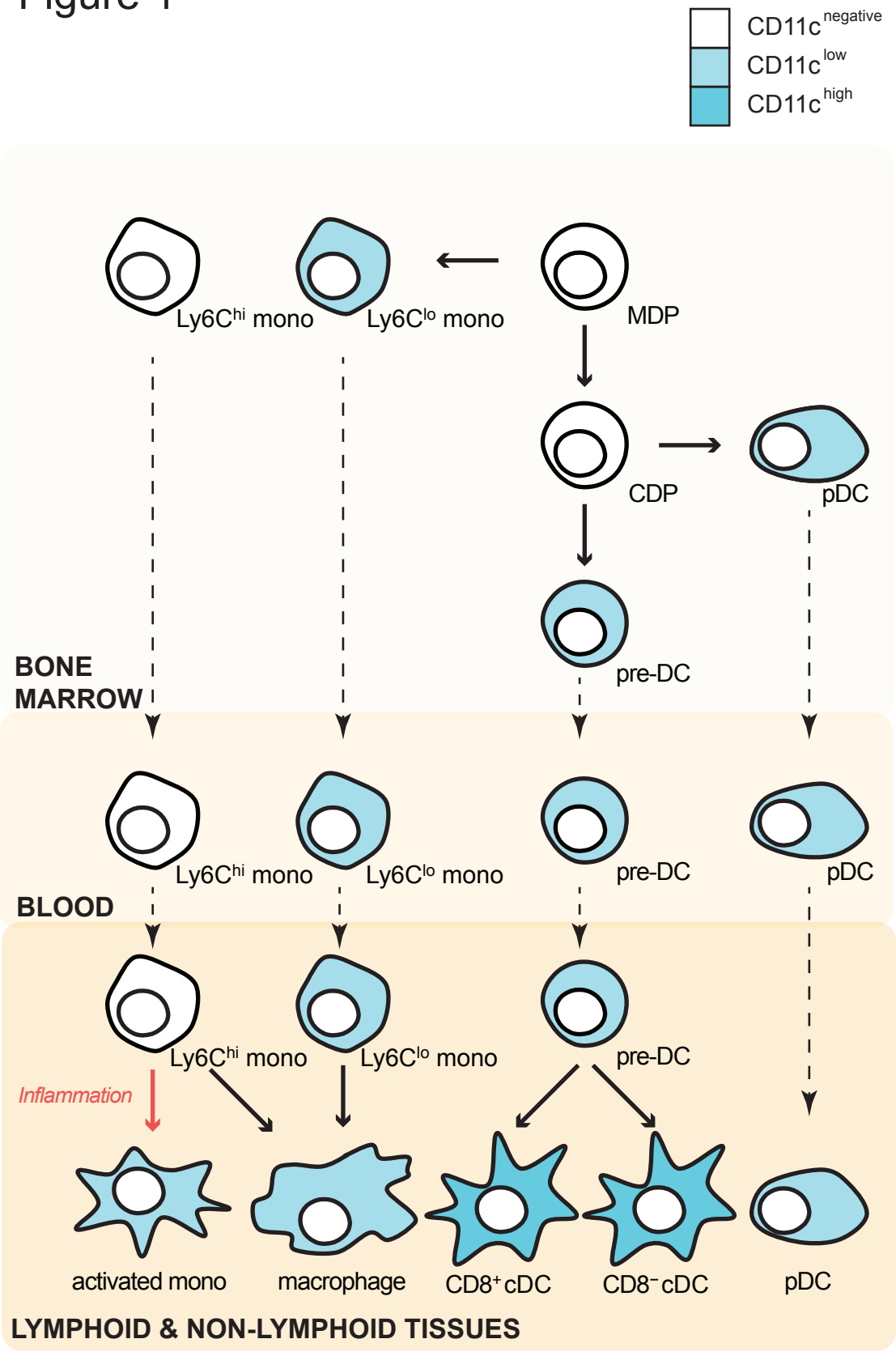
CD11c negative
CD11c low
CD11c high
Ly6C hi mono
Ly6C lo mono
MDP
CDP
pDC
pre-DC
BONE MARROW
Ly6C hi mono
Ly6C lo mono
pre-DC
pDC
BLOOD
Ly6C hi mono
Ly6C lo mono
pre-DC
Inflammation
activated mono
macrophage
CD8+ cDC
CD8− cDC
pDC
LYMPHOID & NON-LYMPHOID TISSUES

Common dendritic cell progenitors (CDPs) subsequently arise from MDPs (K. Liu et al. 2009). CDPs maintain both pDC and cDC potential *in vivo* and *in vitro*, but do not generate monocytes (K. Liu et al. 2009; Naik et al. 2007; Onai et al. 2007). In addition to the loss of monocyte potential, CDPs can be distinguished from MDPs by the downregulation of the cytokine receptor c-kit. Furthermore, CDPs develop and reside in the bone marrow (K. Liu et al. 2009), but can additionally migrate to peripheral lymphoid organs following Toll-like receptor stimulation (Schmid et al. 2011).

Finally, pre-DCs arise from CDPs in the bone marrow (Diao et al. 2004; K. Liu et al. 2009; Naik et al. 2006). Pre-DCs represent fully committed cDC precursors, and can be identified by the expression of the cDC marker CD11c, the cytokine/chemokine receptors Flt3 and CX_3CR1, and the absence of surface MHC II expression (K. Liu et al. 2009; K. Liu and Nussenzweig 2010; Naik et al. 2006). Furthermore, pre-DCs are round cells that have not yet acquired the 'dendritic' morphology of differentiated cDCs (K. Liu et al. 2009). After developing in the bone marrow, pre-DCs migrate via the blood to peripheral lymphoid and non-lymphoid organs. Following several rounds of division, pre-DCs differentiate into both $CD8^+$ and $CD4^+$ cDCs in lymphoid tissues (Diao et al. 2004; K. Liu et al. 2009; Naik et al. 2006). Pre-DCs have also been identified as the precursors of $CD103^+$ cDCs and some $CD11b^+$ DCs in non-lymphoid organs including skin, lung, liver, and intestine (Bogunovic et al. 2009; Ginhoux et al.

2009; Helft et al. 2010). Pre-DC input is constantly required because differentiated cDCs undergo few divisions *in situ* and are replaced every 10-14 days in the spleen and lymph nodes (K. Liu et al. 2007).

cDC development and homeostasis is critically dependent on the cytokine Flt3L (K. Liu et al. 2007; Waskow et al. 2008). Flt3L signaling is recognized by the receptor Flt3, which results in activation of the transcription factor Stat3 (Onai and Manz 2008). The significance of Flt3L signaling to cDCs is demonstrated by the absence of cDC development in $Flt3L^{-/-}$ mice (McKenna et al. 2000). Furthermore, treating wildtype mice with Flt3L *in vivo* results in significant expansion of cDCs (Maraskovsky et al. 1996), and Flt3L likewise increases circulating cDCs in humans (Maraskovsky et al. 2000). Unexpectedly, $Flt3^{-/-}$ mice demonstrate only a partial defect in lymphoid cDC development (Waskow et al. 2008), while this effect is more profound in non-lymphoid tissues (Ginhoux et al. 2009). This incomplete dependence on the Flt3 receptor suggests an additional receptor, possibly expressed more by lymphoid than non-lymphoid cDCs, is able to recognize Flt3L.

All pre-DC-derived cDCs share the expression of CD11c and MHC II, and generally depend on the transcription factors PU.1, Stat3, Gfi1, Ikaros and Xbp1 (Belz and Nutt 2012; Geissmann et al. 2010b). Mutating or deleting any of these factors results in substantial reductions of cDC numbers. PU.1 is required for the induction of Flt3 expression (Carotta et al. 2010) and Stat3 is activated

downstream of Flt3 signaling (Onai and Manz 2008), emphasizing the importance of Flt3L for cDC development and homeostasis. Gfi1 deficiency similarly results in decreased Stat3 activation (Rathinam et al. 2005).

cDC heterogeneity

cDCs are located in lymphoid and non-lymphoid organs and are generally defined as $CD11c^{hi}MHCII^{+}$. Though each tissue's unique combination of intrinsic and extrinsic milieu impact cDC identity, most tissues contain two major subsets of cDCs: $CD8^{+}/CD103^{+}$ and $CD4^{+}/CD11b^{+}$ cDCs. These subsets express distinct phenotypic markers, require different transcription factors, and display functional specializations.

Lymphoid $CD8^{+}$ cDCs localize in the T cell zones of the spleen and lymph nodes (Dudziak et al. 2007). $CD8^{+}$ cDCs also express the lectin DEC-205. This subset depends on the transcription factors Batf3, Id2, and Irf8 (Geissmann et al. 2010b). Antigen targeting via the DEC-205 receptor and Batf3-deficient mice, which lack $CD8^{+}$ cDCs in the steady state, demonstrate that $CD8^{+}$ cDCs are specialized for antigen cross-presentation on MHC I to stimulate $CD8^{+}$ T cell responses (Dudziak et al. 2007; Hildner et al. 2008). Furthermore, this subset endocytoses dead cells via the Clec9a receptor (Sancho et al. 2009) and cross-presents cell-associated antigens (O. Schulz and Reis e Sousa 2002). $CD8^{+}$ cDCs are also capable of MHC II presentation and promote the differentiation of $Foxp3^{+}$ T regulatory cells in the steady state (Yamazaki et al. 2008). Conversely,

following immune stimulation, $CD8^+$ cDCs preferentially induce interferon-γ (IFN-γ)-producing T_H1 responses (Maldonado-Lopez et al. 1999). Their specialization for cross-presentation and T_H1 responses demonstrate $CD8^+$ cDCs are critical to IFNγ-dependent control of intracellular infections by viruses and parasites (Hildner et al. 2008; C. H. Liu et al. 2006). A subset of human cDCs identified by BDCA3 expression similarly express CLEC9A and share global gene expression patterns with mouse $CD8^+$/$CD103^+$cDCs (Hashimoto et al. 2011; Robbins et al. 2008).

$CD4^+$ cDCs in the spleen are found primarily in the bridging channels as well as the red pulp (Dudziak et al. 2007). Furthermore, this subset expresses the lectin DCIR2 in the spleen but not in other lymphoid organs. Mice lacking the transcription factors Irf2, Irf4, and RelB demonstrate significant defects in CD4+ cDC development (Geissmann et al. 2010b). Although this subset is capable of cross-presentation in some situations (Kamphorst et al. 2010; O. Schulz and Reis e Sousa 2002), $CD4^+$/$CD11b^+$ cDCs are specialized for MHC II presentation to produce $CD4^+$ T cell responses (Dudziak et al. 2007; Kamphorst et al. 2010) and promote interleukin-4 (IL-4) and IL-5-producing T_H2 responses. This ability to promote B cell antibody production by inducing T_H2 responses is consistent with $CD4^+$ cDC specialization for the presentation of exogenous antigen on MHC II. Human $BDCA1^+$ cDCs correlate with mouse $CD11b^+$/$CD4^+$ cDCs when comparing global gene expression patterns (Robbins et al. 2008).

In addition to CD11c^{hi}MHCII^{+} cDCs, lymph nodes contain an additional subset of CD11c^{+}MHCII^{hi} migratory DCs (mDCs). These cells undergo CCR7-dependent migration from peripheral tissues to draining lymph nodes (Alvarez et al. 2008). mDCs are a heterogeneous group of cells which include pre-DC-derived CD103^{+} and more heterogeneous CD11b^{+} populations that migrate from non-lymphoid organs. Additionally, the skin-draining lymph nodes contain Langerin^{+} Langerhans cells that migrate from the skin (Romani et al. 2010). Langerhans cells are unique in that they primarily arise from embryonic precursors *in utero* and are subsequently maintained by *in situ* proliferation.

Although most cDC characterization has classically occurred in lymphoid tissues, non-lymphoid organs are also host to a heterogeneous group of cDCs with many similarities to lymphoid populations. CD103^{+} cDCs in non-lymphoid organs are generally recognized as the equivalents of lymphoid CD8^{+} cDCs based on functional and transcriptional profiles (Hashimoto et al. 2011). Both populations are able to cross-present cell-associated antigens and require the transcription factors Batf3, Id2, and Irf8 for development. For example, in the small intestine lamina propria, pre-DC-derived CD103^{+} cDCs support the development of regulatory T cells. Although non-lymphoid CD11b^{+} cDCs are highly similar to lymphoid CD4^{+} cDCs, this population is more heterogeneous in non-lymphoid organs. For example, CD11b^{+} cDCs partially depend on M-CSF-R and can be

generated from both pre-DC and monocyte transfer *in vivo*. Regardless, $CD11b^+$ cDCs seem to serve similar functional roles, including the generation of T_H2 responses (Julia et al. 2002).

cDC function

T cells are only able to recognize antigen in the context of MHC-peptide complexes processed by antigen presenting cells, including B cells, stromal cells, macrophages, and cDCs (Trombetta and Mellman 2005). $CD8^+$ T cells bind MHC I, which present intracellular antigens as well as cross-presented extracellular antigens, while $CD4^+$ T cells bind MHC II presenting extracellular antigenic peptides. T cell receptor (TCR) binding with MHC-peptide complexes triggers T cell proliferation, and the presence or absence of additional cues, including co-stimulatory markers and cytokines, influence the subsequent activation and differentiation of the responding T cell (Steinman et al. 2003b).

In the steady state, cDCs contribute to peripheral tolerance by continuously sampling and presenting antigen to T cells and instructing them to undergo deletion, anergy, or regulatory T cell differentiation (Hawiger et al. 2001; Hawiger et al. 2004; Kretschmer et al. 2005). The mechanisms controlling this decision are still unresolved, but several factors contribute to this process. Immature cDCs express low levels of co-stimulatory molecules, which stabilize cDC:T cell synapses and deliver activation signals to T cells (Dustin et al. 2010; Mellman and Steinman 2001). T cells that do not receive these secondary signals

undergo bim-mediated apoptosis, implying that TCR stimulation activates proapoptotic pathways by default that can be inactivated by additional signals from the antigen presenting cell (Steinman et al. 2003a). Furthermore, immature cDCs produce suppressive cytokines including IL-10, which limits T cell proliferation and is necessary for immune tolerance to respiratory antigens (Akbari et al. 2001; Bouloc et al. 2000). Similarly, regulatory T cell survival and differentiation are in part regulated by cDC signaling (Darrasse-Jeze et al. 2009; Kretschmer et al. 2005; Yamazaki et al. 2008). For example, lymphoid and gut resident cDCs promote regulatory T cell differentiation via transforming growth factor (TGF)-β and retinoic acid signaling (Coombes et al. 2007; Sun et al. 2007; Yamazaki et al. 2008).

cDCs sense the state of the immune system via numerous pathogen recognition receptors, co-stimulatory molecules, and cytokine/chemokine receptors. Most notably, Toll-like receptors (TLRs) recognize conserved pathogen epitopes and signal via the adaptors MyD88 and/or TRIF, which results in the translocation of various cytosol-restricted transcription factors into the nucleus, including NFκB, Irf3, and Irf5 (Kawai and Akira 2006). Maturation also results from CD40 ligation, or signaling from inflammatory cytokines including tumor necrosis factor (TNF)-α, IL-1β, and IL-6 (Gallucci and Matzinger 2001; Mellman and Steinman 2001). As a result of stimulation, cDCs undergo phenotypic and transcriptional changes, including the upregulation of MHC II, co-stimulatory molecules including CD40, CD80, and CD86, and inflammatory cytokines including IL-12 and TNFα.

Dendritic cell differentiation *in vitro*

$CD11c^+$ cells resembling cDCs can be generated from monocytes *in vitro* by culturing with the cytokines granulocyte-macrophage colony stimulating factor (GM-CSF) and IL-4 (Inaba et al. 1992a; Inaba et al. 1992b; Sallusto and Lanzavecchia 1994). Like cDCs, these cells express CD11c and MHC II, and upregulate co-stimulatory markers following maturation. Furthermore, these cells are able to present antigen to T cells *in vitro* and home to T cell zones of lymph nodes when transferred into mice.

The GM-CSF culture system has been, and continues to be, a highly popular and effective means to generate a large number cDC-like cells from blood or bone marrow isolated from mice and humans. However, these GM-CSF-cultured monocyte-derived cells have been more recently shown to be developmentally and functionally distinct from cDCs *in vivo*. Steady state cDCs develop independently of GM-CSF (Waskow et al. 2008) and instead derive from Flt3L-dependent pre-DCs (K. Liu et al. 2009; Naik et al. 2006). Furthermore, GM-CSF-derived $CD11c^+$ cells more closely resemble activated monocytes in terms of gene expression (Robbins et al. 2008) and the production of inflammatory mediators including nitric oxide and tumor necrosis factor-α (Xu et al. 2007). Although GM-CSF-cultured monocytes are able to present antigen to T cells, they do so inefficiently compared to pre-DC-derived cDCs (Kamphorst et al. 2010).

More recently, a culture system supplemented with Flt3L has been described which generates cells more representative of steady state cDCs (Brasel et al. 2000). Culturing bone marrow with Flt3L produces a mixture of three populations which express CD11c: $B220^{+}$, $CD24^{+}Sirp\alpha^{-}$, and $CD24^{-}Sirp\alpha^{+}$. Gene expression analysis demonstrated that $CD11c^{+}B220^{+}$ corresponded to pDCs, $CD24^{+}Sirp\alpha^{-}$ resembled $CD8^{+}$ cDCs, and $CD24^{-}Sirp\alpha^{+}$ are similar to $CD8^{-}$ cDCs (Naik et al. 2005b). Furthermore, subsequent functional studies showed that Flt3L-cultured cDCs could present antigen similar to their splenic counterparts (Kamphorst et al. 2010). For example, LPS stimulation enhanced the ability of Flt3L-cultured cDCs to present antigen similar to to LPS-matured splenic cDCs.

Plasmacytoid dendritic cells (pDCs)

pDCs represent long-lived circulating cells (O'Keeffe et al. 2002) and are most notably responsible for rapid and massive production of type I interferons in response to viral infection (Cella et al. 1999; Fitzgerald-Bocarsly 1993). pDCs arise from CDP progenitors similar to cDCs (K. Liu et al. 2009; Naik et al. 2007; Onai et al. 2007), although there is also evidence that pDCs can be derived from lymphoid progenitors owing to the presence of immunoglobulin rearrangements and the expression of other lymphoid-specific genes including pre-Tα and IL-7R (Corcoran et al. 2003; D'Amico and Wu 2003; Naik et al. 2005a; Rissoan et al. 2002; Schlenner et al. 2010; Shigematsu et al. 2004). Steady state pDCs share the expression of CD11c and Flt3 with cDCs, but can be distinguished from cDCs

based on the expression of Ly6C, B220, and PDCA-1 (Colonna et al. 2004; Krug et al. 2004; Zhang et al. 2006). Following activation, pDCs upregulate the expression of MHC II, CD8α, and co-stimulatory molecules (Asselin-Paturel et al. 2001; Colonna et al. 2004; O'Keeffe et al. 2002), which further increases their phenotypic resemblance to cDCs.

Circulating pDCs monitor lymphoid and non-lymphoid organs, including the spleen, lymph nodes, skin, lung, and liver (Asselin-Paturel et al. 2001; Blasius et al. 2004; Lian et al. 2003; O'Keeffe et al. 2003). pDCs sense viral infection via the expression of TLR7 and TLR9, which recognize viral RNA and DNA, respectively (Barchet et al. 2005; Colonna et al. 2004; Krug et al. 2004). Following TLR stimulation, pDCs rapidly secrete massive amounts of type I interferons, which dually inhibit viral replication in infected cells and activate additional cells of the immune system, including macrophages and NK cells.

Monocytes and macrophages

Given many developmental and phenotypic similarities between cDCs and monocytes/macrophages, there has been extensive confusion and debate regarding their respective roles since the discovery of cDCs in 1973. As mentioned earlier, cDCs and monocytes both arise from MDPs in the bone marrow. Monocytes are defined by the expression of the integrin CD11b and cytokine receptor M-CSF-R (CD115), both of which are heterogeneously expressed at lower levels in both pre-DCs and differentiated cDCs (K. Liu et al.

2009; Naik et al. 2006). Furthermore, the cDC marker CD11c is likewise heterogeneously expressed at lower levels by steady state monocytes and macrophages, and is further upregulated following immune stimulation (Figure 1).

Monocytes circulate the blood to monitor lymphoid and non-lymphoid tissues, providing a reservoir of innate immune cells with proinflammatory and antimicrobial capabilities (Gordon and Taylor 2005). Two subsets of monocytes can be distinguished by the expression of the cell surface antigen Ly6C and the chemokine receptors CX_3CR1 and CCR2: $Ly6C^{hi}CX_3CR1^{lo}CCR2^{+}$ 'inflammatory' and $Ly6C^{lo}CX_3CR1^{hi}CCR2^{-}$ 'resident' monocytes. There is increasing evidence that both monocyte subsets contribute to the steady state development of lymphoid and non-lymphoid macrophages (Hashimoto et al. 2011). Following immune stimulation, $Ly6C^{hi}$ monocytes home to inflamed tissues where they undergo activation and differentiation into highly phagocytic antigen presenting cells (Hohl et al. 2009; Leon et al. 2007; Serbina et al. 2003). Whereas steady state $Ly6C^{hi}$ monocytes do not express CD11c or MHC II, after activation, for example in response to *Listeria monocytogenes* infection, these cells upregulate the expression of CD11c, MHC II, and co-stimulatory markers (Serbina et al. 2003). Although activated $Ly6C^{hi}$ monocytes resemble cDCs phenotypically, they process and present antigen orders of magnitude less efficiently than cDCs (Kamphorst et al. 2010).

Macrophages are present in every lymphoid and non-lymphoid organ, and represent a highly heterogeneous population (Gordon and Taylor 2005; Hashimoto et al. 2011). Although previously assumed to be dependent on monocyte input, recent evidence suggests many macrophage subsets arise during embryogenesis from yolk sac progenitors independently of the hematopoietic system (C. Schulz et al. 2012). Regardless, most macrophage subsets are highly phagocytic and are responsible the clearance of apoptotic cells, pathogens, and other debris (Galli et al. 2011; Gordon and Taylor 2005). Furthermore, some macrophages also have roles in tissue integrity and immune suppression.

Diphtheria toxin receptor (DTR) and CD11c-DTR mice

Cell ablation is a powerful technique that permits the removal of a population to interrogate its function in various experimental settings. Compared to non-genetic systems, including antibody- and clondronate liposome-mediated depletion, the introduction of diphtheria toxin receptor (DTR) expression under a desired gene promoter facilitates highly specific ablation of cells expressing that gene. Diphtheria toxin is produced by the bacterium *Corynebacterium diphtheriae* and is composed of two functional units: DT-A and DT-B (Saito et al. 2001). DT-B mediates internalization by binding membrane-anchored heparin-binding epidermal growth factor-like (HB-EGF-like) growth factor, thus also known as diphtheria toxin receptor (DTR). Internalized DT:DTR are trafficked to late endosomes where low pH allows DT-A to translocate to the cytosol. In the

cytosol, DT-A transfers ADP-ribose moieties onto diphthamide residues of elongation factor-2 (EF-2), which renders it inactive and results in cell death due to translational arrest. This process is so efficient that a single unit of DT-A is sufficient to kill a cell (Yamaizumi et al. 1978). Although mouse EF-2 is sensitive to DT-A modification, DT-B cannot bind mouse HB-EGF-like growth factor (that is, the mouse homolog of DTR) (Mitamura et al. 1995), which makes mouse cells 'insensitive' to DT toxicity. Therefore, the introduction of human DTR expression under the regulation of a particular gene promoter renders cells expressing that gene sensitive to DT-mediated cell death.

In 2002, CD11c-DTR transgenic mice, which express DTR under the regulation of the CD11c promoter, were first described (Jung et al. 2002). DT treatment in these mice results in significant reduction of $CD11c^+$ cDCs and consequently prevents the cross-presentation of cell-associated antigen to $CD8^+$ T cells. In addition to their role in the initiation of $CD8^+$ T cell responses, $CD11c^+$ cells were also shown to be required for the re-stimulation of memory $CD8^+$ T cells (Zammit et al. 2005). The absence of $CD11c^+$ cDCs likewise impairs innate immune responses, including the activation of NK cells that depend on IL-15 production from cDCs (Lucas et al. 2007). The absence of $CD11c^+$ cDC-derived help impairs the control of multiple viral, bacterial, and parasitic pathogens, including Herpes Simplex Virus I (Kassim et al. 2006), *Mycobacterium tuberculosis* (Tian et al. 2005), and *Toxoplasma gondii* (C. H. Liu et al. 2006).

A major caveat of the CD11c-DTR system, however, is the promiscuous expression of CD11c among myeloid, and even lymphoid, cells (Bennett and Clausen 2007; Murphy 2011; Probst et al. 2005; Zammit et al. 2005). As discussed previously, monocyte and macrophage subsets express CD11c heterogeneously and further upregulate it in response to inflammation, and pDCs constitutively express low levels of CD11c (Figure 1). Furthermore, steady state NK cells similarly express low levels of CD11c, and $CD8^+$ T cells upregulate its expression upon activation. This low level of expression must be sufficient to drive DTR expression because many of these populations have been reported to be affected by DT treatment in CD11c-DTR mice (Bennett and Clausen 2007; Probst et al. 2005; Zammit et al. 2005). Importantly, even 'low' DTR expression can have appreciable effects considering the potent toxicity of DT-A (Yamaizumi et al. 1978). Consequently, the interpretation of experimental results using the CD11c-DTR system can be misleading. For example, several macrophage subsets are sensitive to DT ablation in CD11c-DTR, and these cells have also been implicated in the re-stimulation of already primed T cells (Mellman et al. 1998; Trombetta and Mellman 2005) as well as the control of viral and bacterial infections (Aderem and Underhill 1999; Gordon and Taylor 2005).

Lack of unifying marker

Since their initial discovery and in the decades to follow, a major limitation in studying cDC biology has been the lack of highly specific markers to distinguish the cDC lineage from other myeloid populations. CD11c has proven to be a very

useful marker for identifying cDCs, but its expression is present on various other immune populations, particularly myeloid populations that arise from shared progenitors (Figure 1). As a consequence, defining cDCs in various tissues and disease contexts based solely on CD11c can be misleading. Likewise, the use of the CD11c promoter can label cells outside of the cDC lineage. To resolve this confusion, novel and highly restricted cDC-specific markers are needed to better define cDCs.

This thesis outlines the description of a novel cDC marker called 'zDC' for '**z**inc finger expressed by c**DC**s.' Within the immune system, the expression of zDC is highly restricted to pre-DCs and differentiated cDCs. The characterization of zDC expression and function involved three directions: (1) the generation and description of zDC-DTR knock-in mice in which DTR expression is regulated by the zDC locus, (2) the identification of zDC target genes by chromatin immunoprecipitation-sequencing (ChIP-seq), and (3) the generation of $zDC^{lox/lox}$ mice and description of $zDC^{-/-}$ mice.

Chapter 2.

RESULTS (PART I): zDC EXPRESSION

Identification of zDC

To identify gene loci specifically expressed by cDCs, I performed gene array analysis comparing developing and fully differentiated cDCs with monocytes and myeloid cell progenitors (Figure 2) (Fogg et al. 2006; K. Liu et al. 2009; Onai et al. 2007). First, to focus on genes expressed by cells committed to the cDC lineage, I compared the expression of all genes by pre-DCs, which are cDC-committed, and monocytes, which do not demonstrate steady state cDC potential. Due to the development distance between these two distinct populations, I selected genes that were expressed 10-fold or higher in pre-DCs compared to monocytes (Figure 2A). Next, to further enrich cDC-commitment genes, I compared the expression of those pre-DC/monocyte genes in MDP, which demonstrates monocyte and dendritic cell potential, and CDP, which has lost monocyte potential. Assuming that CDP is closer developmentally to cDC commitment compared to MDP, I selected genes which were upregulated in CDP relative to MDP. Due to the small developmental space between the MDP and CDP stages, I chose genes that were expressed at least two-fold higher in CDP compared to MDP (Figure 2B). Finally, to identify genes shared by differentiated cDCs, I compared the expression of those pre-DC/monocyte and CDP/MDP-enriched genes in splenic DEC-205^{+}(CD8^{+}) and DCIR2^{+}(CD4^{+}) cDCs. Because I was interested in genes which were shared by both subsets, I selected genes

Figure 2. Selection of cDC commitment genes identified the zinc finger transcription factor zDC (Zbtb46, Btbd4)

(A) The expression of gene probes represented on Affymetrix Mouse 430 2.0 chip compared in monocytes (x-axis) versus pre-DCs (y-axis). Dark grey line shows equally expressed probes, and outer grey lines indicate probes expressed at greater than ten-fold difference. Yellow dots indicate probes upregulated in pre-DCs relative to monocytes by ten-fold or more.
(B) The expression of gene probes upregulated by pre-DCs determined in (A) compared in MDPs (x-axis) versus CDPs (y-axis). Dark grey line again shows equally expressed probes, and outer grey lines indicate probes expressed at greater than two-fold difference. Red dots indicate probes upregulated in CDPs relative to MDPs by two-fold or more.
(C) The expression of probes upregulated by pre-DCs and CDPs as determined in (B) compared in $CD4^+$ cDCs (x-axis) versus $CD8^+$ cDCs (y-axis). Dark grey line shows probes that are equally expressed, and outer grey lines show probes expressed greater than two-fold difference. Arrows indicate probes for CD11c and zDC (Zbtb46, Btbd4).

Figure 2

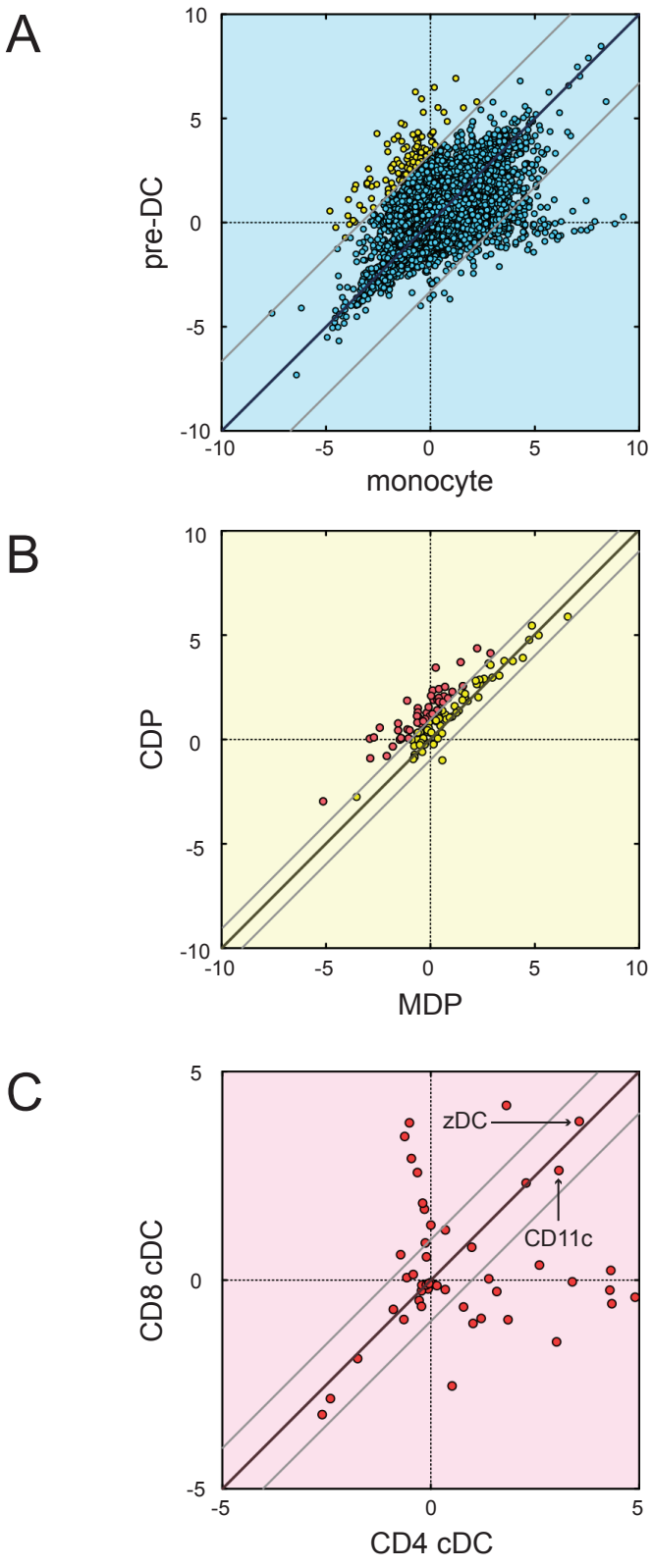
A
10
5
0
-5
-10
pre-DC
-10
-5
0
5
10
monocyte
B
10
5
0
-5
-10
CDP
-10
-5
0
5
10
MDP
C
5
0
-5
CD8 cDC
zDC
CD11c
-5
0
5
CD4 cDC

which were expressed at similar levels. This screen reassuringly identified CD11c, the most reliable cDC phenotypic marker. In addition to CD11c, I found the uncharacterized zinc finger transcription factor Zbtb46 (Btbd4), which I call 'zDC' for '**z**inc finger expressed by c**DC**s' (Figure 2C).

zDC expression is limited to pre-DCs and cDCs

Gene array expression analysis demonstrated zDC is upregulated by pre-DCs (i.e. after the CDP stage of development) and subsequently maintained in both subsets of fully differentiated cDCs. In contrast, B and T lymphocytes, monocytes, and MDP and CDP progenitors express very low or negligible levels of zDC transcript (Figure 3A).

To confirm this pattern of expression and broaden the scope of populations included, I quantified zDC transcript levels in various myeloid populations and their progenitors by Q-PCR (Figure 3B). Very little to no expression was detected in MP, MDP, or CDP progenitors. As suggested by gene array, pre-DCs upregulated zDC more than ten-fold relative to CDPs, and this high level of expression was maintained in both subsets of differentiated cDCs isolated from both lymphoid (spleen) and non-lymphoid (lung) tissues. Importantly, other differentiated myeloid populations, including pDCs and monocytes, expressed very little transcript. Furthermore, activated monocytes isolated from the spleens of *Listeria monocytogenes*-infected mice, despite acquiring a 'cDC-like' phenotype including upregulation of CD11c and MHC II, do not express

Figure 3. zDC transcript and protein is specifically expressed by mouse cDCs but not other immune cell populations.

(A) Heat maps showing normalized zDC expression depicted on $\log_2$ scale from three zDC probes on Affymetrix Mouse 430 2.0 chips.
(B) zDC transcript levels in myeloid progenitors (MPs), MDPs, CDPs, pre-DCs, splenic and lung cDC subsets, pDCs, and steady state and activated monocytes determined by Q-PCR and normalized to GAPDH.
(C) zDC western blot of CD11b-enriched monocytes/macrophages, PDCA-1-enriched pDC, and sorted DEC-205$^+$ and DCIR2$^+$ cDC. Histone H4 blot shown as a loading control.

Figure 3

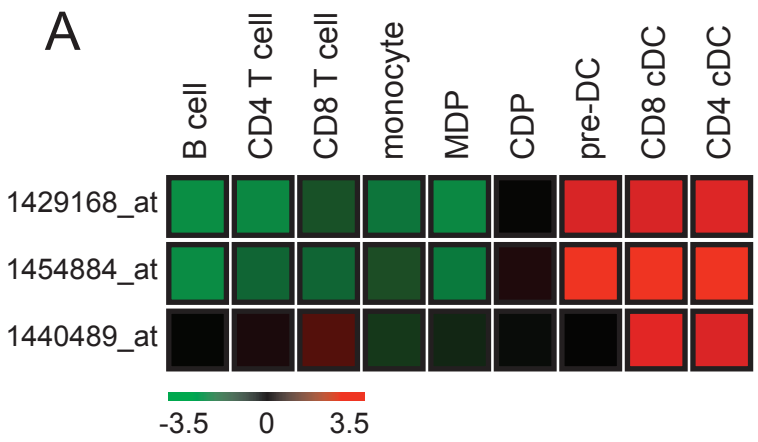
A
B cell
CD4 T cell
CD8 T cell
monocyte
MDP
CDP
pre-DC
CD8 cDC
CD4 cDC
1429168_at
1454884_at
1440489_at
-3.5
0
3.5

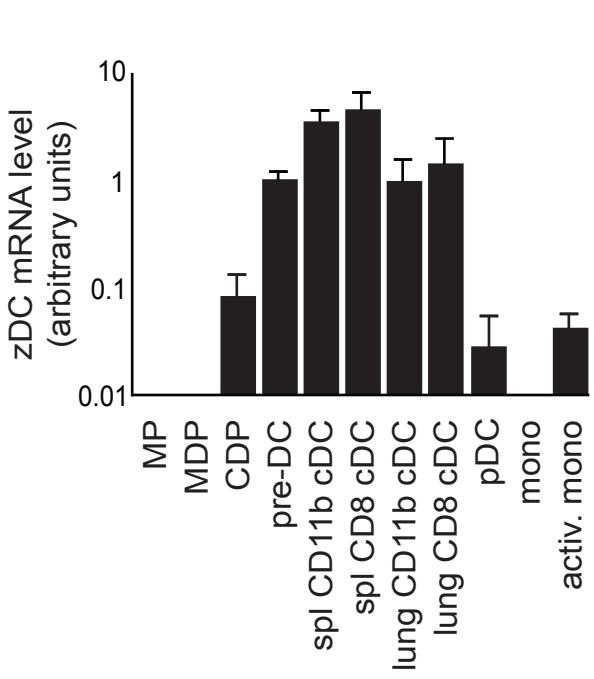
B
zDC mRNA level
(arbitrary units)
10
1
0.1
0.01
MP
MDP
CDP
pre-DC
spl CD11b cDC
spl CD8 cDC
lung CD11b cDC
lung CD8 cDC
pDC
mono
activ. mono

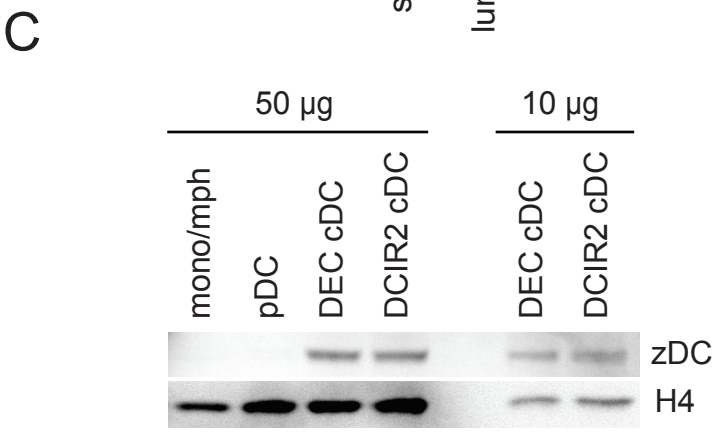
C
50 µg
10 µg
mono/mph
pDC
DEC cDC
DCIR2 cDC
DEC cDC
DCIR2 cDC
zDC
H4

appreciable levels of zDC. I further confirmed this pattern of cDC-specific expression using public online gene array databases (immgen.org and biogps.org). These online databases further demonstrated high expression of zDC by cDCs and the absence of zDC expression by all other assayed immune populations, including early hematopoietic stem cell and lymphoid progenitors, macrophages, neutrophils, and NK cells. Therefore, among steady state immune system cells, zDC expression is highly unique to cDCs.

To develop more reagents with which to characterize zDC expression, I produced recombinant mouse zDC in *Escherichia coli* for immunization in Armenian hamsters to generate an anti-zDC monoclonal antibody. This anti-zDC antibody was used to verify the expression of zDC protein in cDCs by western blot. Consistent with mRNA expression data, zDC protein was detected in cDC but not pDC or monocyte/macrophage whole cell lysates (Figure 3C). The zDC gene therefore produces a protein product that is uniquely utilized by the cDC lineage.

In addition to cDC-restricted expression in mice, human ZDC (ZBTB46, BTBD4) is also highly expressed by human cDCs compared to other blood-circulating immune cells, including B and T lymphocytes, NK cells, pDCs, monocytes, and neutrophils (Figure 4A). Furthermore, in addition to its pattern of expression, the zDC amino acid sequence itself is highly conserved throughout vertebrate

Figure 4. zDC pattern of expression and amino acid sequence is highly conserved in vertebrates.

(A) Gene array expression of human ZDC (probe 227329_at on Affymetrix U133 Plus 2.0) by sorted human blood populations. Adapted from Robbins *et al.*, 2008 {Robbins, 2008 #42}.

(B) Dendrogram of vertebrate zDC amino acid sequences (left) and percent identity to mouse (right).

Figure 4

A

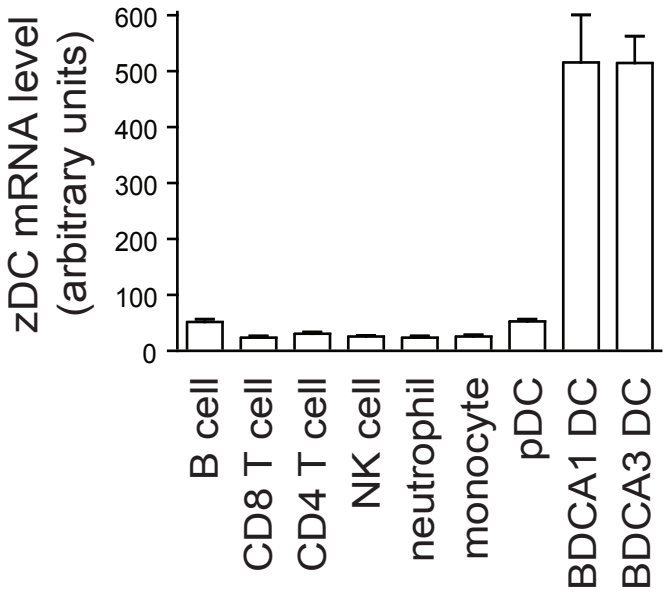
zDC mRNA level
(arbitrary units)
600
500
400
300
200
100
0
B cell
CD8 T cell
CD4 T cell
NK cell
neutrophil
monocyte
pDC
BDCA1 DC
BDCA3 DC

B

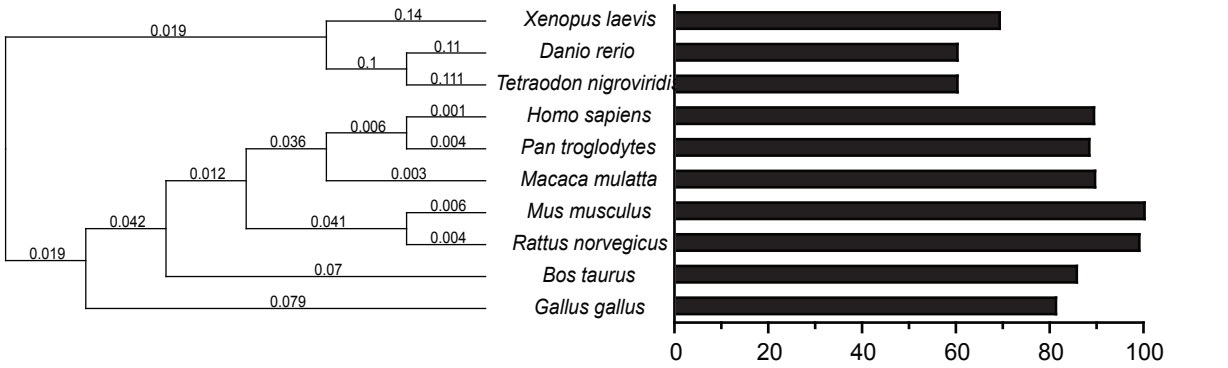
0.019
0.14
0.11
0.1
0.111
0.001
0.006
0.036
0.004
0.012
0.003
0.006
0.042
0.041
0.004
0.019
0.07
0.079
Xenopus laevis
Danio rerio
Tetraodon nigroviridis
Homo sapiens
Pan troglodytes
Macaca mulatta
Mus musculus
Rattus norvegicus
Bos taurus
Gallus gallus
0
20
40
60
80
100
Percent identity to Mus musculus amino acid sequence

evolution (Figure 4B), but not found in cartilaginous fish. Therefore, zDC gene expression by cDCs and amino acid sequence are highly conserved.

In summary, zDC expression is upregulated after the CDP stage in development when the cDC lineage splits from monocytes and pDCs (K. Liu et al. 2009), and that its steady state expression within the hematopoietic system of both mice and humans is restricted to the cDC lineage.

Chapter 3.

RESULTS (PART II): zDC-DTR MICE

zDC-DTR knock-in mice

To further explore zDC regulation and exploit its specific expression pattern, I designed and produced a knock-in mouse expressing DTR under the zDC promoter. To introduce DTR expression into zDC-expressing cells, I inserted a human DTR cDNA into the 3' untranslated region (UTR) of the zDC gene (zDC-DTR; Figure 5A). The zDC-DTR targeting construct was assembled by traditional cloning methods, and targeting was performed in C57BL/6 embryonic stem cells. I chose to introduce the DTR coding sequence, along with an upstream internal ribosome entry site (IRES) sequence, immediately following the zDC stop codon in the 3'UTR of the zDC locus to maintain the structure of the zDC locus intact. In this way, any regulatory regions in the gene body in addition to the promoter are uninterrupted, ensuring the zDC locus regulates DTR expression.

To determine whether the zDC-DTR allele disrupts the expression of zDC, I performed western blots for zDC protein on CD11c-enriched splenic cDCs from $zDC^{+/+}$, $zDC^{+/DTR}$, $zDC^{DTR/DTR}$ mice. As intended, zDC is still expressed from the zDC-DTR allele (Figure 5B). Next, to determine whether DTR expression is restricted to cDCs, I characterized DTR expression among immune system cells

Figure 5. zDC-DTR mice express DTR under the regulation of the zDC locus.

(A) Schematic diagram of wildtype and DTR knock-in zDC loci. 5' and 3' UTR are shown in black, coding sequences in white, and the locations of BTB/POZ and zinc finger domains are indicated with arrows. IRES (gray) and DTR-mCherry (red) are inserted immediately following the endogenous zDC stop codon in exon 5.

(B) Western blots for zDC, hDTR, and Histone H4 loading control on CD11c-enriched splenocytes from $zDC^{+/+}$, $zDC^{+/DTR}$, and $zDC^{DTR/DTR}$ mice.

Figure 5

A

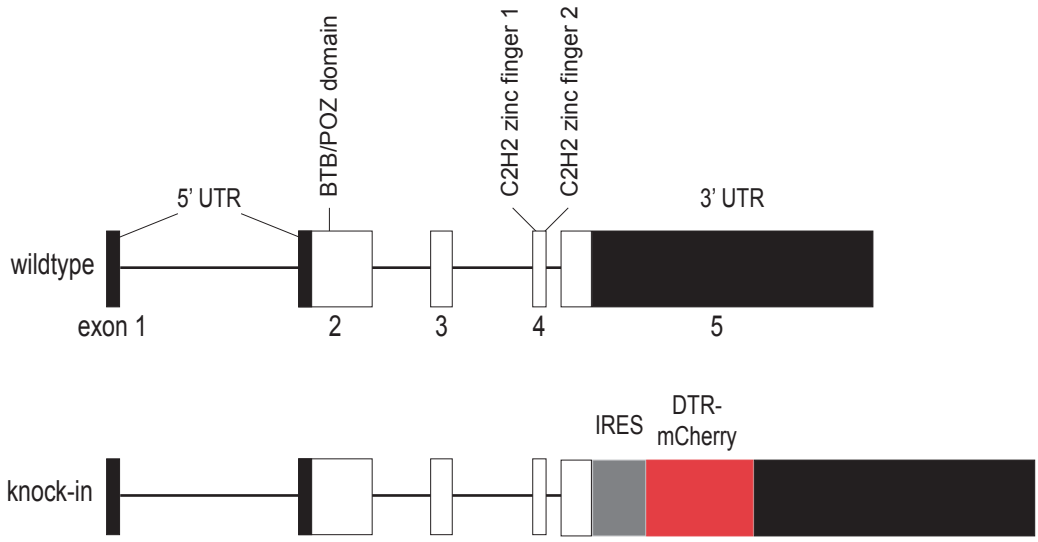
BTB/POZ domain
C2H2 zinc finger 1
C2H2 zinc finger 2
5' UTR
3' UTR
wildtype
exon 1
2
3
4
5
IRES
DTR-
mCherry
knock-in

B

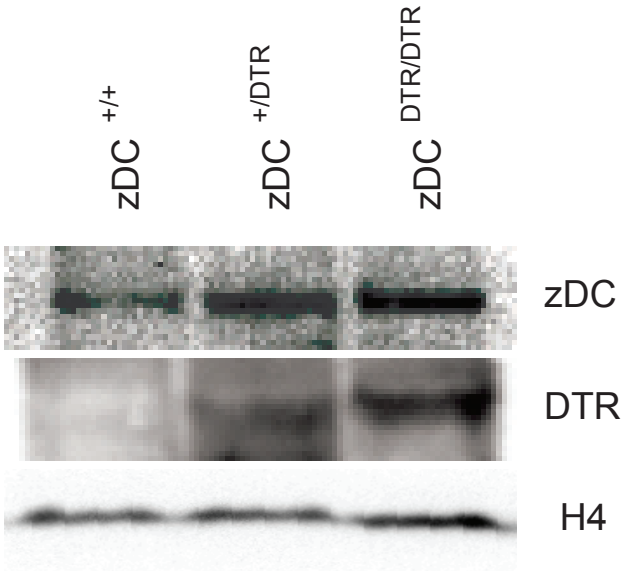
zDC +/+
zDC +/DTR
zDC DTR/DTR
zDC
DTR
H4

by flow cytommetry. Although DTR is expressed as a fusion protein with mCherry, fluorescence could not be detected by flow cytometry, and therefore I used biotinylated anti-DTR antibody to examine zDC-DTR expression. As expected, DTR surface expression was found on $CD8^+$ and $CD4^+$ cDCs in the spleen, skin draining lymph nodes, and mesenteric lymph node in zDC-DTR mice (Figure 6). Consistent with mRNA and protein analysis, DTR expression on pDCs, monocytes, or lymphocytes was not detectable.

Despite highly specific cDC-expression among immune system cells, an essential radioresistant population must also express zDC because injection of a single dose of 20ng diphtheria toxin (DT) per g bodyweight into zDC-DTR knock-in mice and C57BL/6→zDC-DTR bone marrow chimeras is fatal within 24-48 hours. Conversely, zDC-DTR→C57BL/6 bone marrow chimeras survive DT injections every other day for over two weeks. Similarly, DTR expression outside the hematopoietic system requires the use of bone marrow chimeras for extended DT treatment with the CD11c-DTR system (Zaft et al. 2005). Thus, among bone marrow-derived cells, zDC-DTR expression appears to be restricted to cDC, however, it is also expressed by a yet unknown group of essential radioresistant cells.

To confirm cDCs are sensitive to DT-mediated ablation, I injected zDC-DTR→C57BL/6 bone marrow chimeras with various doses of DT and quantified cDC abundance in the spleen and skin-draining lymph nodes by flow cytommetry

Figure 6. zDC-DTR mice introduce DTR expression into cDCs, and DTR expression is not detectable in other immune populations.

Flow cytometry histograms of DTR staining from zDC-DTR mice (black line) and wildtype littermates (gray shaded) splenic $CD8^+$ and $CD4^+$ cDCs ($Lin^-Ly6C^-CD11c^{hi}MHCII^+$), pDCs ($Lin^-CD11c^{int}PDCA\text{-}1^+$), monocytes ($Lin^-CD11b^+CD115^+$), B cells ($CD3^-NK1.1^-CD19^+$), and T cells ($CD3^+CD19^-NK1.1^-$).

Figure 6

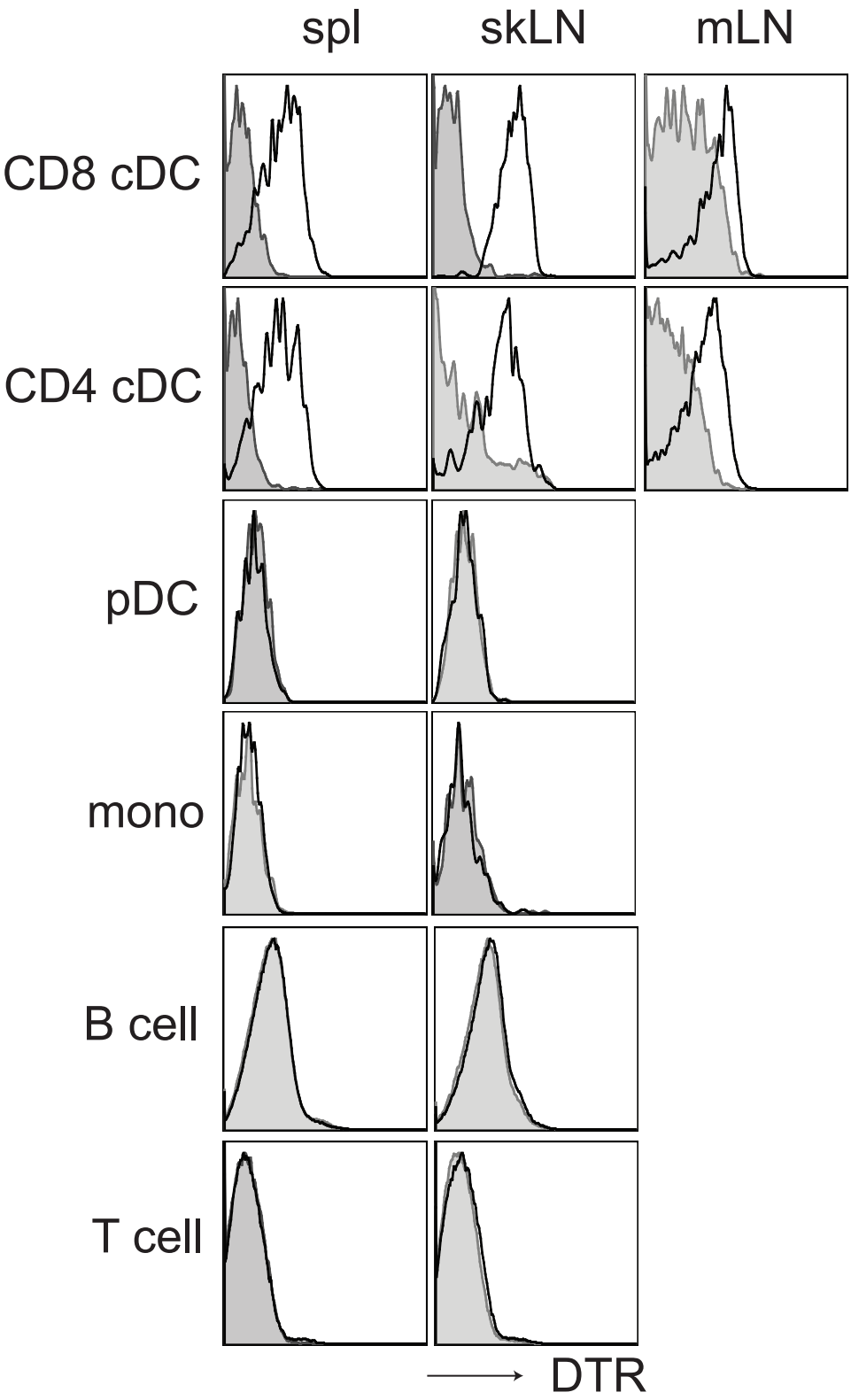

12 hours after DT injection. The lowest dose of DT at which $CD11c^{hi}MHCII^{+}$ cDCs in spleen and skLN, as well as $CD11c^{+}MHCII^{hi}$ mDCs in skLN, were efficiently ablated was 20ng DT per g bodyweight (Figure 7). Therefore, for all transient cDC ablation experiments, I have used 20ng DT per g bodyweight.

DT treatment in zDC-DTR bone marrow chimeras efficiently deletes pre-DC precursors in the bone marrow and differentiated cDCs in the spleen as soon as 12 hours after injection (Figure 8 A-B). zDC-DTR permits the ablation of $CD11c^{hi}MHCII^{+}$ cDCs in multiple lymphoid and non-lymphoid organs, including the skLN, mesenteric lymph node (mLN), lung, and liver (Figure 8C). Furthermore, $CD11c^{+}MHCII^{hi}$ migratory DC (mDC) found in skLN and mLN were similarly decreased after DT treatment. Similar to CD11c-DTR (Schmid et al.), DT injection into zDC-DTR→C57BL/6 bone marrow chimeras resulted in a rapid four-fold increase in serum Flt3L concentration which returned to steady state levels after seven days (Figure 9A). Consistent with increased serum Flt3L and the kinetics of cDC development (K. Liu et al. 2007; Waskow et al. 2008), cDC reconstitution in the spleen was apparent as early as five days after DT injection and complete after seven days (Figure 9B), which is similar to the kinetics observed after ablation in CD11c-DTR mice (Jung et al. 2002). cDC reconstitution in the skin draining lymph nodes was similar to splenic cDC reconstitution, while mDC kinetics were delayed by about two days (Figure 9C). Therefore, DT injection into zDC-DTR bone marrow chimeras resulted in efficient ablation of pre-DCs and their progeny in lymphoid and non-lymphoid tissues.

Figure 7. DT dose titration for cDC ablation in the spleen and skin-draining lymph nodes of zDC-DTR mice.

(A) zDC-DTR bone marrow chimeras were injected with PBS or 4, 8, 20, 30, or 40 ng DT per g body weight. The amount of $CD11c^{hi}MHCII^{+}$ cDC ablation was determined 12 hours later by flow cytometry in the spleen or (B) $CD11c^{hi}MHCII^{+}$ cDC and $CD11c^{+}MHCII^{hi}$ mDC in skin-draining lymph nodes.

Figure 7

A

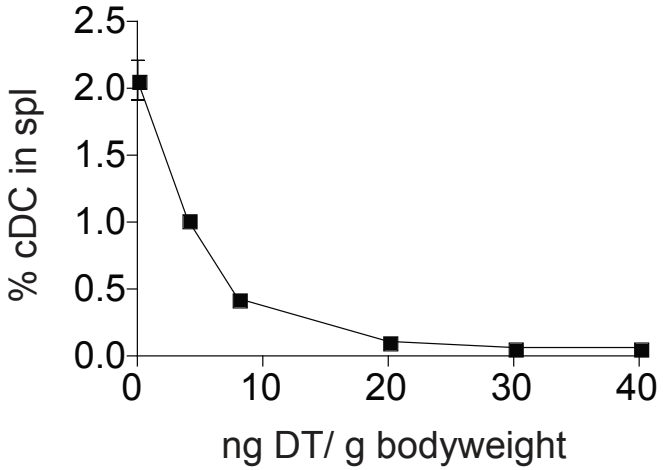
2.5
2.0
1.5
1.0
0.5
0.0
% cDC in spl
0
10
20
30
40
ng DT/ g bodyweight

B

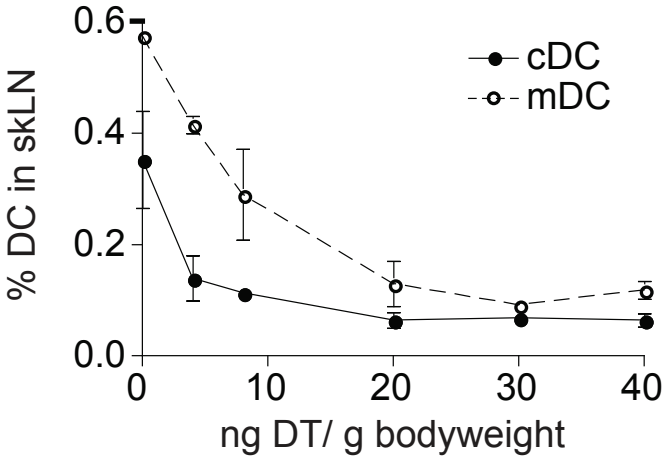
0.6
0.4
0.2
0.0
% DC in skLN
cDC
mDC
0
10
20
30
40
ng DT/ g bodyweight

Figure 8. Pre-DCs and cDCs are depleted with DT injection in zDC-DTR mice.

(A) Flow cytometry plots of bone marrow pre-DCs (gated on $Lin^{-}CD45R^{-}$ $CD11c^{+}MHCII^{-}$) in zDC-DTR bone marrow chimeras injected with PBS or DT. Numbers indicate percent of bone marrow.

(B) $CD11c^{hi}MHCII^{+}$ cDC abundance in spleen, skin draining lymph nodes (skLN), mesenteric lymph node (mLN), lung, and liver in PBS- and DT-treated zDC-DTR bone marrow chimeras. $CD11c^{+}MHCII^{hi}$ mDC also included in skLN and mLN. Gated on Lin^{-} in skLN and mLN, and $Lin^{-}CD45^{+}$ in liver and lung. Numbers indicate percent of organ.

Figure 8

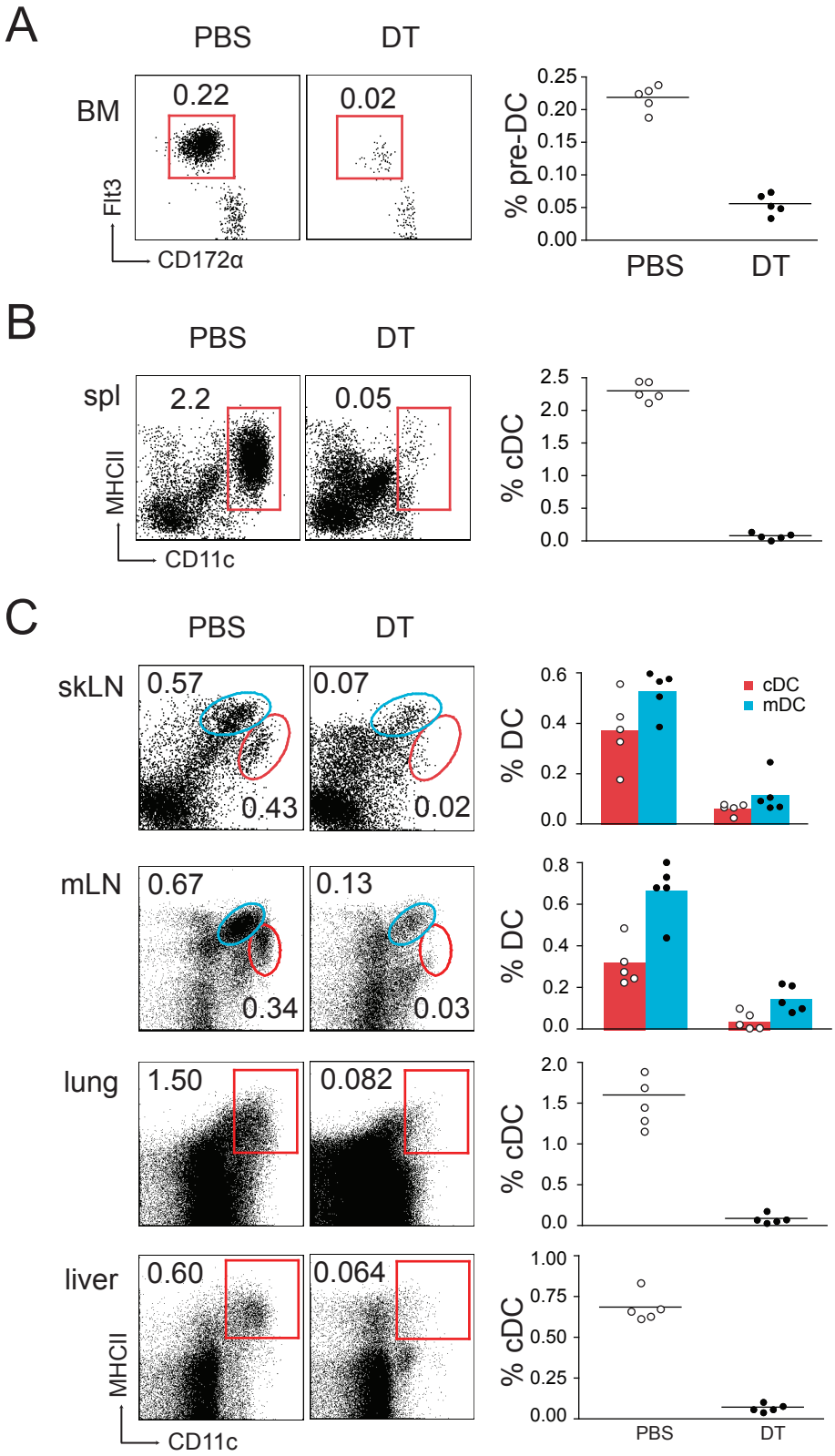
A
PBS
DT
BM
0.22
0.02
Flt3
CD172α
% pre-DC
0.25
0.20
0.15
0.10
0.05
0.00
PBS
DT
B
PBS
DT
spl
2.2
0.05
MHCII
CD11c
% cDC
2.5
2.0
1.5
1.0
0.5
0.0
C
PBS
DT
skLN
0.57
0.43
0.07
0.02
% DC
0.6
0.4
0.2
0.0
cDC
mDC
mLN
0.67
0.34
0.13
0.03
% DC
0.8
0.6
0.4
0.2
0.0
lung
1.50
0.082
% cDC
2.0
1.5
1.0
0.5
0.0
liver
0.60
0.064
MHCII
CD11c
% cDC
1.00
0.75
0.50
0.25
0.00
PBS
DT

Figure 9. DT injection in zDC-DTR mice results in rapidly elevated serum Flt3L levels proceeded by cDC reconstitution in the spleen and skin-draining lymph nodes.

(A) Flt3L concentrations in sera of DT-treated zDC-DTR bone marrow chimeras determined by ELISA at multiple time points after DT injection.
(B) cDC abundance in spleen and (C) skLN at multiple time points after DT injection.

Figure 9

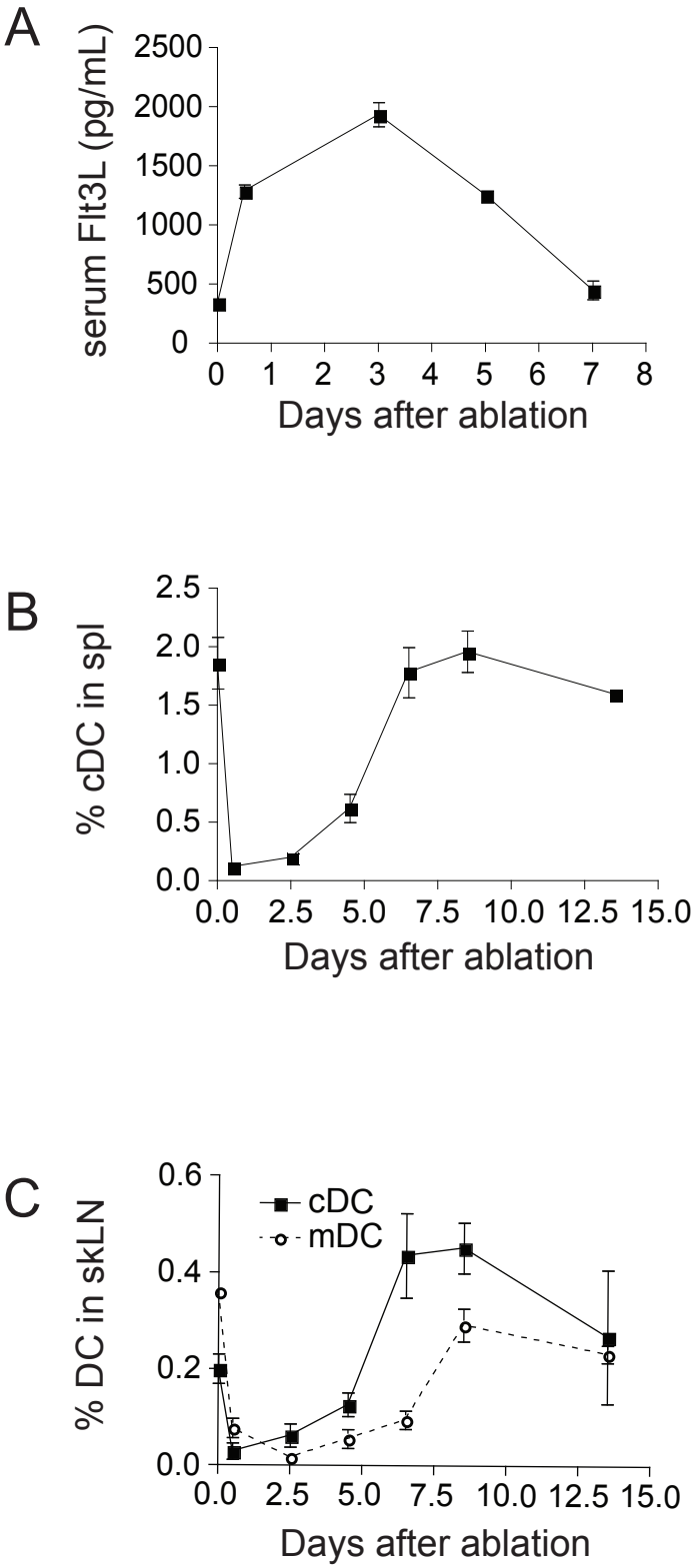
A
serum Flt3L (pg/mL)
2500
2000
1500
1000
500
0
0 1 2 3 4 5 6 7 8
Days after ablation
B
% cDC in spl
2.5
2.0
1.5
1.0
0.5
0.0
0.0 2.5 5.0 7.5 10.0 12.5 15.0
Days after ablation
C
% DC in skLN
0.6
0.4
0.2
0.0
cDC
mDC
0.0 2.5 5.0 7.5 10.0 12.5 15.0
Days after ablation

The CD11c-DTR system has been used extensively to interrogate cDC function during various immune responses. Therefore, to appreciate the differences between these two models, DT treatment in zDC- and CD11c-DTR bone marrow chimeras were directly compared. DT ablation in zDC- and CD11c-DTR bone marrow chimeras resulted in an equivalent loss of splenic cDCs and bone marrow pre-DCs within 12 hours of injection (Figure 10 A-B). While splenic cDCs originate from pre-DC precursors, DCs in some non-lymphoid tissues can arise from pre-DCs or monocytes (Helft et al. 2010; K. Liu and Nussenzweig 2010). For example, in the small intestine lamina propria, $CD103^+$ cDCs are derived exclusively from pre-DCs, while $CD11b^+$ DCs can arise from either pre-DCs or monocytes (Bogunovic et al. 2009; Varol et al. 2009). Due to this monocyte contribution, DT-treatment in zDC-DTR bone marrow chimeras resulted in only a partial reduction of $CD11c^{hi}MHCII^+$ DCs in the small intestine lamina propria (Figure 10C). Specifically, pre-DC-derived $CD103^+CD11b^-$ cDCs were completely depleted in the lamina propria, while only a portion of $CD103^+CD11b^+$ and $CD103^-CD11b^+$ DCs were affected by DT treatment. DT-treatment in CD11c-DTR bone marrow chimeras, however, resulted in a complete ablation of all $CD11c^{hi}MHCII^+$ DCs regardless of pre-DC or monocyte origin. Therefore, DT treatment in zDC-DTR bone marrow chimeras ablates pre-DC-derived cDCs, while not depleting monocyte-derived DCs.

To understand what effect DT treatment has on other immune populations in DT-treated zDC- and CD11c-DTR bone marrow chimeras, I characterized various

Figure 10. zDC-DTR allows efficient depletion of pre-DC-derived cDCs in the spleen and small intestine lamina propria.

(A) Steady state splenic $Lin^{-}CD11c^{hi}MHCII^{+}$ cDCs were quantified 12 hours after PBS or DT injection in zDC-DTR bone marrow chimeras. The ablation of splenic cDCs was also compared in DT-treated WT, zDC-DTR, and CD11c-DTR bone marrow chimeras.

(B) $Lin^{-}CD11c^{+}MHCII^{-}$ $Flt3^{+}$ bone marrow pre-DCs in zDC-DTR bone marrow chimeras were quantified by flow cytometry 12 hours after treatment with PBS or DT. The ablation of bone marrow pre-DCs was compared in DT-treated WT, zDC-DTR, and CD11c-DTR bone marrow chimeras.

(C) Steady state small intestine lamina propria $Lin^{-}CD45^{+}CD11c^{hi}MHCII^{+}$ total DCs (top) and DC subsets (bottom) in zDC-DTR bone marrow chimeras 18 hours after treatment with PBS or DT. The amount of total lamina propria DCs and lamina propria DC subsets were compared in DT-treated WT, zDC-DTR, and CD11c-DTR bone marrow chimeras.

Figure 10

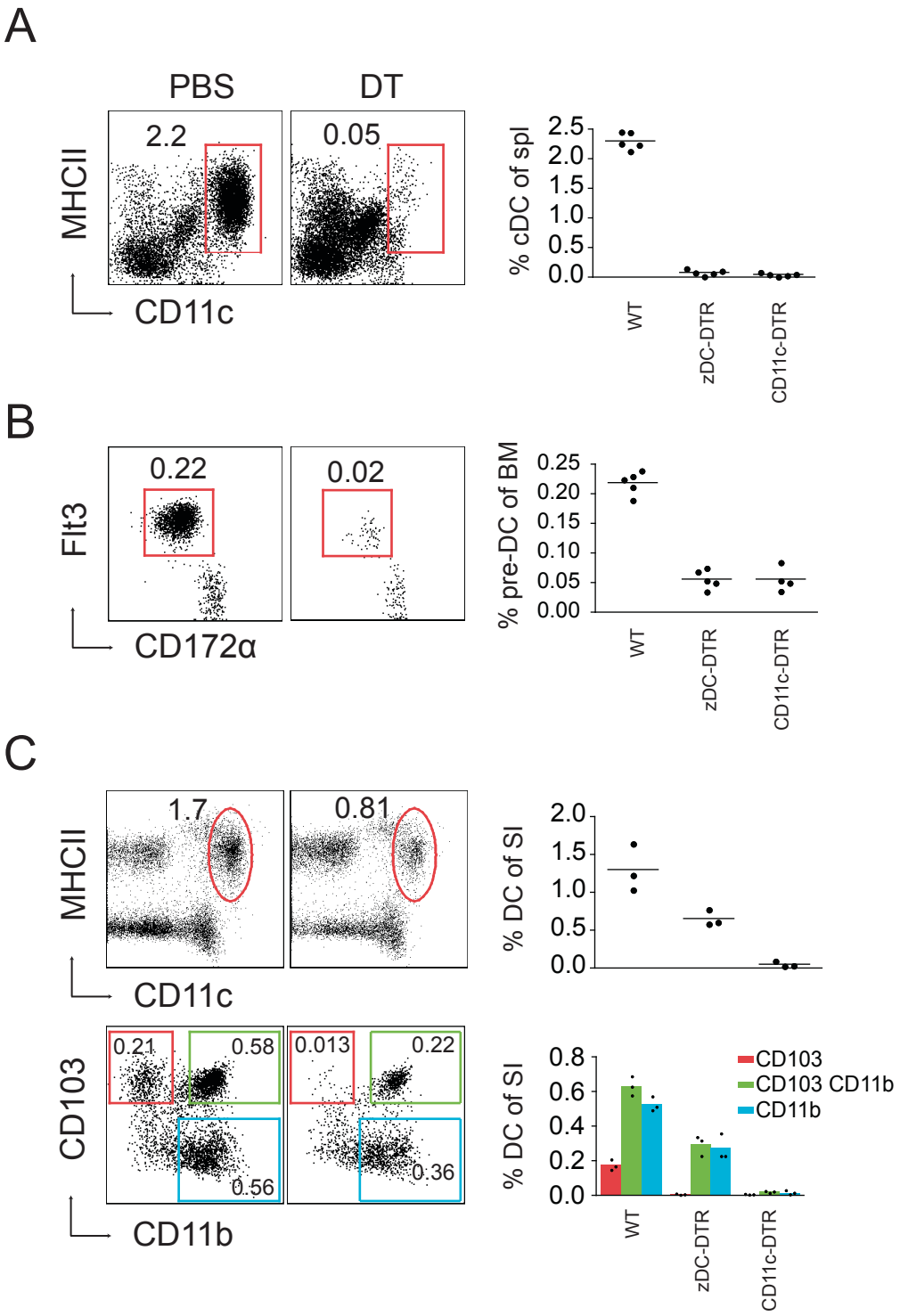
A
PBS
DT
2.2
0.05
MHCII
CD11c
% cDC of spl
2.5
2.0
1.5
1.0
0.5
0.0
WT
zDC-DTR
CD11c-DTR
B
0.22
0.02
Flt3
CD172α
% pre-DC of BM
0.25
0.20
0.15
0.10
0.05
0.00
WT
zDC-DTR
CD11c-DTR
C
1.7
0.81
MHCII
CD11c
% DC of SI
2.0
1.5
1.0
0.5
0.0
0.21
0.58
0.56
0.013
0.22
0.36
CD103
CD11b
% DC of SI
0.8
0.6
0.4
0.2
0.0
CD103
CD103 CD11b
CD11b
WT
zDC-DTR
CD11c-DTR

lymphoid and myeloid populations after DT treatment. Due to the absence of zDC and CD11c expression, steady state B and T lymphocytes were unaffected by DT injection in both zDC- and CD11c-DTR chimeras (Figure 11 A-B). Although activated T cells can upregulate CD11c which renders them sensitive to DT treatment in CD11c-DTR mice (Bennett and Clausen 2007; Jung et al. 2002), zDC expression remains low in activated T cells (immgen.org). Additionally, both zDC- and CD11c-DTR chimeras showed increased numbers of splenic $Ly6G^+$ neutrophils following DT injection (Figure 11C), which is likely due to inflammation resulting from DT-mediated cDC ablation (Birnberg et al. 2008; Tittel et al. 2012). Therefore, DT treatment in both zDC- and CD11c-DTR bone marrow chimeras does not affect steady state B or T lymphocytes, but does result in neutrophilia.

Besides cDCs, many other immune cells express CD11c, albeit at lower levels (Geissmann et al.). Both NK cells and pDCs, which express intermediate levels of CD11c, were unaffected by DT injection in zDC-DTR bone marrow chimeras (Figure 11 D-E). However, both of these populations were reduced in DT-treated CD11c-DTR chimeras. Furthermore, pDCs activated with the TLR9 ligand CpG, which upregulates MHCII and co-stimulatory receptor expression (Iparraguirre et al. 2008), were likewise unaffected by DT treatment in zDC-DTR mice (Figure 11F). Thus, the intermediate levels of CD11c expressed by NK cells and pDCs must be sufficient to induce depletion of these populations after DT treatment in CD11c-DTR mice.

Figure 11. zDC-DTR spares other immune cell populations affected in CD11c-DTR mice, including steady state and activated monocyte-derived populations.

(A) $CD19^+$ splenic B cells, (B) $CD19^-NK1.1^-CD3^+$ T cells, (C) $Lin^-CD11b^+Ly6G^+$ neutrophils, (D) $CD3^-CD19^-NK1.1^+$ NK cells, (E) $Lin^-CD11c^{int}PDCA\text{-}1^+$ steady state pDCs and (F) activated pDCs, and (G) $Lin^-Flt3^-CD11b^+Ly6G^-CD115^+$ steady state monocytes and (H) activated $Ly6C^{hi}$ monocytes in PBS- or DT-treated zDC-DTR bone marrow chimeras. Mice in (F) were injected with 20μg CpG in 15% DOTAP 12 hours before treatment with PBS or DT. Mice in (H) were infected with 5×10^4 *Listeria monocytogenes* CFU i.v. and injected with PBS or DT 24-48 hours post infection. All populations were quantified in WT, zDC-DTR, and CD11c-DTR bone marrow chimeras 12 hours following DT injection.

Figure 11

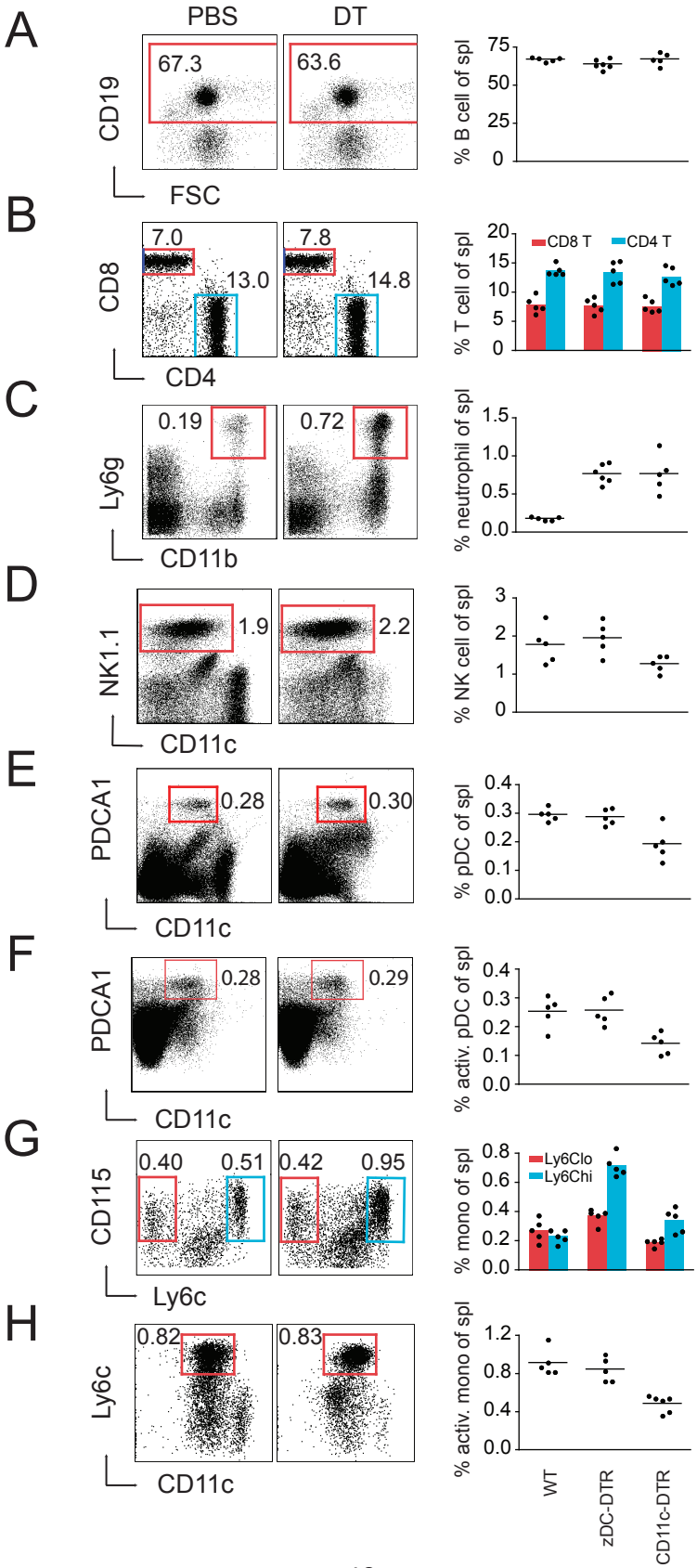
A
PBS
DT
67.3
63.6
CD19
FSC
% B cell of spl
75
50
25
0
B
7.0
13.0
7.8
14.8
CD8
CD4
CD8 T
CD4 T
% T cell of spl
20
15
10
5
0
C
0.19
0.72
Ly6g
CD11b
% neutrophil of spl
1.5
1.0
0.5
0.0
D
1.9
2.2
NK1.1
CD11c
% NK cell of spl
3
2
1
0
E
0.28
0.30
PDCA1
CD11c
% pDC of spl
0.4
0.3
0.2
0.1
0.0
F
0.28
0.29
PDCA1
CD11c
% activ. pDC of spl
0.4
0.3
0.2
0.1
0.0
G
0.40
0.51
0.42
0.95
CD115
Ly6c
Ly6Clo
Ly6Chi
% mono of spl
0.8
0.6
0.4
0.2
0.0
H
0.82
0.83
Ly6c
CD11c
% activ. mono of spl
1.2
0.8
0.4
0.0
WT
zDC-DTR
CD11c-DTR

Similarly, Ly6C^{lo} monocytes also express low levels of CD11c. Consequently, whereas DT treatment in zDC-DTR resulted in a small increase in Ly6C^{lo} monocyte numbers, this monocyte subset is conversely reduced by DT treatment in CD11c-DTR chimeras (Figure 11G). On the other hand, the number of Ly6C^{hi} monocytes, which do not express CD11c in the steady state, increased after DT treatment in both zDC- and CD11c-DTR chimeras. Therefore, steady state cDC ablation is more specifically achieved in zDC-DTR mice compared to CD11c-DTR mice, which has heterogenous effects on other CD11c^{int} cells.

Activation of Ly6C^{hi} monocytes during infection or by stimulation *in vitro* with cytokines and TLR ligands induces CD11c and MHCII expression (Geissmann et al. 2003; Gordon and Taylor 2005; Randolph et al. 1999). For example, during infection with *Listeria monocytogenes*, Ly6C^{hi} monocytes accumulate in the spleen and upregulate CD11c, MHCII, and co-stimulatory markers (Serbina et al. 2003). Because this population also produces TNFα and iNOS, they are also referred to as 'tipDCs.' Despite acquiring a cDC-like phenotype, these activated monocytes are not ablated in zDC-DTR bone marrow chimeras (Figure 11H). However, consistent with their upregulation of CD11c, DT treatment in CD11c-DTR chimeras during *L. monocytogenes* infection reduces the proportion of this population in the spleens of infected mice by about 50%. Thus, during inflammation, DT treatment in zDC-DTR bone marrow chimeras spares activated monocytes that express CD11c and MHCII, which are affected in CD11c-DTR bone marrow chimeras.

Additional populations of $CD11c^+MHCII^+$ cells appear in lymphoid organs during inflammation, and it has been difficult to ascertain their origin from pre-DCs or monocytes. For example, LPS injection results in the appearance of $CD11c^+MHCII^+$DC-SIGN/$CD209^+CD14^+$DEC-205^- cells in skLNs with evidence that they derive from monocytes (Cheong et al. 2010). $CD11c^+MHCII^+CD14^+$DEC-205^- cells do not appear in DT-treated zDC-DTR mice following LPS stimulation (Figure 12A). Furthermore, these cells also fail to accumulate after LPS injection in $Flt3L^{-/-}$ mice despite the presence of normal blood monocyte numbers (Figure 12 B-C), suggesting they arise from cDCs and not from monocytes. However, the lack of $CD11c^+MHCII^+CD14^+$DEC-205^- cell accumulation in DT-treated zDC-DTR and $Flt3L^{-/-}$ mice could also occur due to the absence of cDC-derived help. To address this possibility, I looked at $CD11c^+MHCII^+CD14^+$DEC-205^- cell accumulation after LPS injection in PBS- and DT-treated $CD45.1^+$WT:$CD45.2^+$zDC-DTR mixed bone marrow chimeras, which maintain DT-insensitive $CD45.1^+$ WT cDCs after DT injection. Although DT-treated mixed bone marrow chimeras were able to generate $CD45.1^+$ WT $CD11c^+MHCII^+CD14^+$DEC-205^- cells, few were derived from $CD45.2^+$ zDC-DTR cells (Figure 12D). Therefore, the inability of $CD11c^+MHCII^+CD14^+$DEC-205^- cells to accumulate in DT-treated zDC-DTR mice is cell-intrinsic. Due to their absence in both DT-treated zDC-DTR and $Flt3L^{-/-}$ mice, $CD11c^+MHCII^+CD14^+$DEC-205^- cells are most likely not of monocyte origin, and could be categorized as activated cDCs.

Figure 12. $CD11c^+CD14^+$ cells in the skin-draining lymph nodes are derived from cDCs and not monocytes.

(A) PBS- and DT-treated zDC-DTR bone marrow chimeras were injected with 5 μg LPS i.v. and $CD11c^+MHCII^+CD14^+$ cells were quantified by flow cytometry 24 hours later.

(B) WT and $Flt3L^{-/-}$ mice injected with PBS or LPS i.v. and $CD11c^+MHCII^+CD14^+$ cells were quantified by flow cytometry 24 hours later.

(C) $CD11b^+Flt3^-Ly6G^-CD115^+$ monocytes in blood 24 hours after PBS or LPS injection in WT and $Flt3L^{-/-}$ mice.

(D) $CD45.1^+$ WT versus $CD45.2^+$ zDC-DTR contribution to $CD11c^+MHCII^+CD14^+$ cells in skLN 24 hours after LPS treatment in PBS- or DT-treated WT:zDC-DTR mixed bone marrow chimeras.

Figure 12

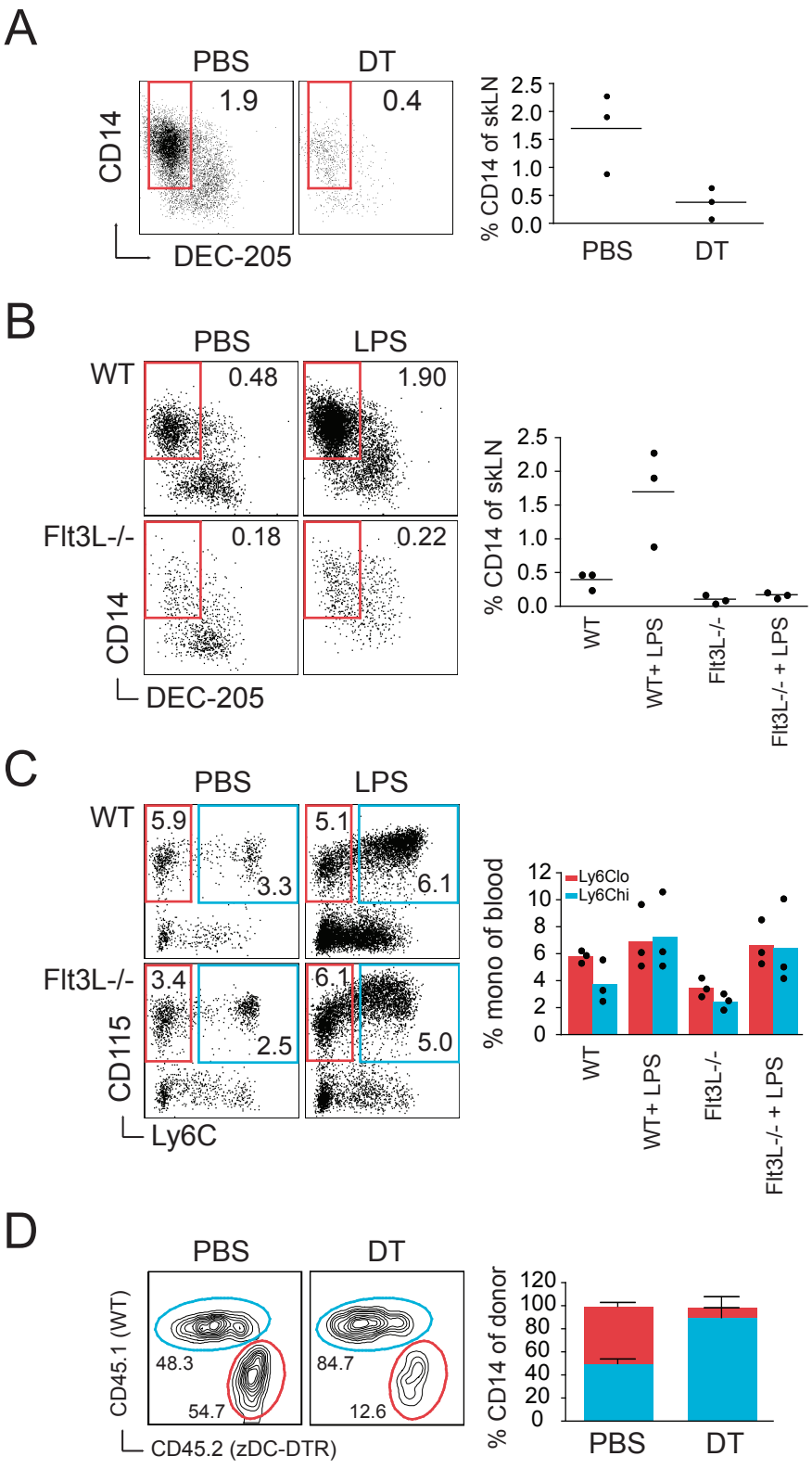
A
PBS
DT
1.9
0.4
CD14
DEC-205
% CD14 of skLN
2.5
2.0
1.5
1.0
0.5
0.0
PBS
DT
B
PBS
LPS
WT
0.48
1.90
Flt3L-/-
0.18
0.22
CD14
DEC-205
% CD14 of skLN
WT
WT+ LPS
Flt3L-/-
Flt3L-/- + LPS
C
PBS
LPS
WT
5.9
3.3
5.1
6.1
Flt3L-/-
3.4
2.5
6.1
5.0
CD115
Ly6C
% mono of blood
Ly6Clo
Ly6Chi
12
10
8
6
4
2
0
WT
WT+ LPS
Flt3L-/-
Flt3L-/- + LPS
D
PBS
DT
CD45.1 (WT)
48.3
54.7
84.7
12.6
CD45.2 (zDC-DTR)
% CD14 of donor
120
100
80
60
40
20
0
PBS
DT

Like their monocyte precursors, many macrophage subsets express low levels of CD11c and have been shown to be sensitive to DT ablation in CD11c-DTR mice (Bennett and Clausen 2007). For example, splenic red pulp macrophages are depleted in DT-treated CD11c-DTR bone marrow chimeras (Figure 13A). In contrast, this population is maintained in zDC-DTR bone marrow chimeras. To better characterize macrophage populations, spleen and skLN sections from DT-treated zDC-DTR knock-in and CD11c-DTR hemizygous mice were analyzed by immunohistochemistry. In agreement with analysis by flow cytommetry, splenic F4/80^{+} red pulp macrophage were unaffected by DT-treatment mice zDC-DTR but were absent in CD11c-DTR mice (Figure 13B). Similarly, CD169^{+} marginal zone macrophages in the spleen were slightly reduced but intact after DT treatment in zDC-DTR mice, while this population was almost absent in DT-treated CD11c-DTR mice (Figure 13C). In the skLN, F4/80^{+} medullar macrophages appeared unaffected by DT treatment in both zDC- and CD11c-DTR (Figure 14A). Similar to their counterpart in the spleen, skLN subcapsular sinus macrophages were intact in DT-treated zDC-DTR mice and reduced in CD11c-DTR mice (Figure 14B). Therefore, DT-treated zDC-DTR mice maintain spleen and skLN macrophage populations, while DT treatment in CD11c-DTR mice results in a substantial loss of multiple macrophage populations.

Figure 13. zDC-DTR spares splenic macrophage populations affected in CD11c-DTR mice.

(A) Flow cytometry plots depicting splenic $Lin^{-}CD11c^{int}CD11b^{lo}F4/80^{+}$ red pulp macrophages in PBS- or DT-treated zDC-DTR bone marrow chimeras. All populations were quantified in WT, zDC-DTR, and CD11c-DTR bone marrow chimeras 12 hours following DT injection.
(B) Spleens from DT-treated WT, zDC-DTR, and CD11c-DTR mice were stained with B220 (green) to visualize B cell zones and F4/80 (red) to identify $F4/80^{+}$ splenic red pulp macrophages.
(C) As in (B), but stained with B220 (green) and CD169 (red) to identify $CD169^{+}$ splenic marginal zone macrophages.

Figure 13

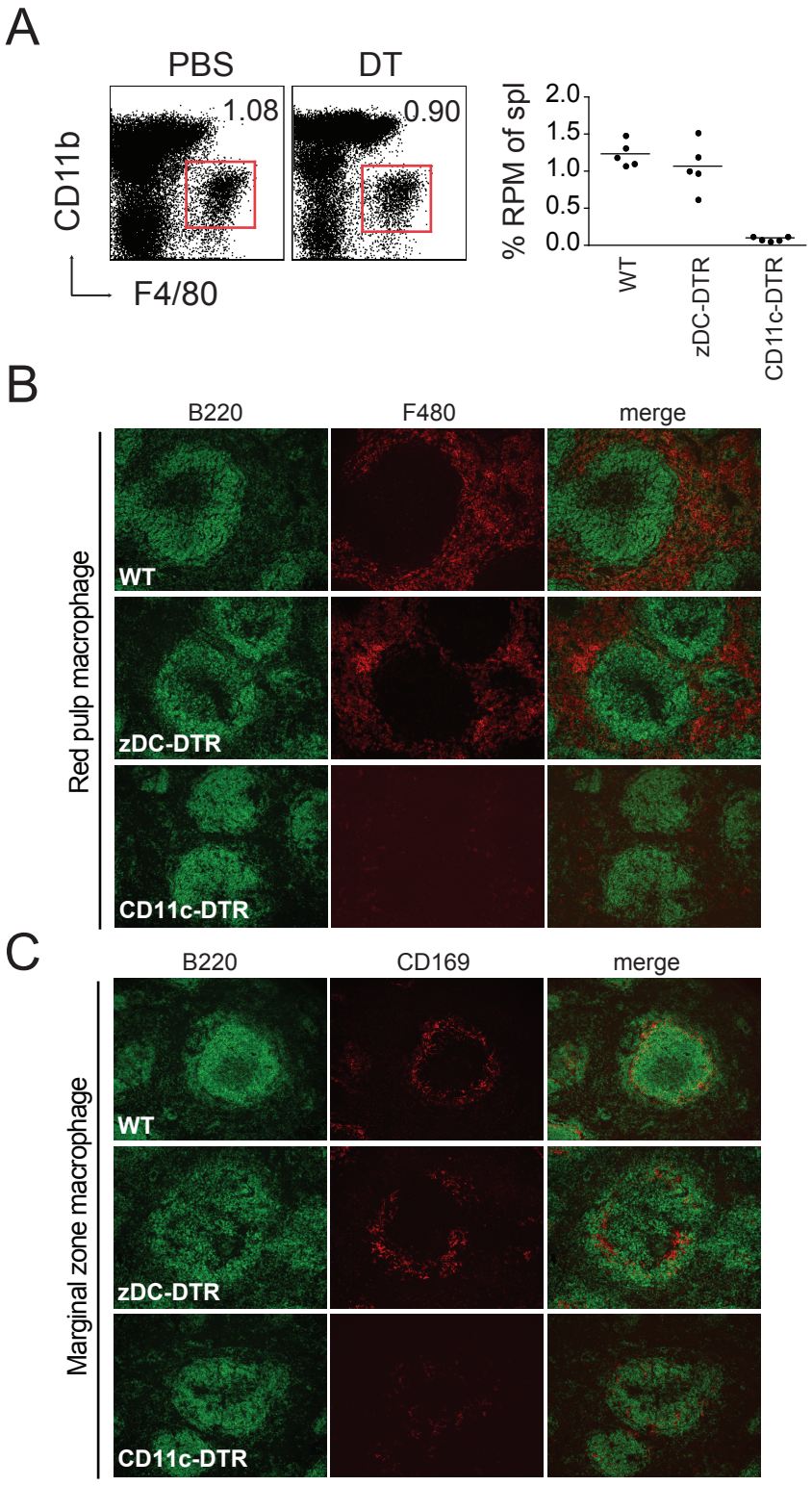
A
PBS
DT
1.08
0.90
CD11b
F4/80
% RPM of spl
2.0
1.5
1.0
0.5
0.0
WT
zDC-DTR
CD11c-DTR
B
B220
F480
merge
Red pulp macrophage
WT
zDC-DTR
CD11c-DTR
C
B220
CD169
merge
Marginal zone macrophage
WT
zDC-DTR
CD11c-DTR

Figure 14. zDC-DTR spares lymph node macrophage populations affected in CD11c-DTR mice.

(A) Skin-draining lymph nodes from DT-treated WT, zDC-DTR, and CD11c-DTR mice were stained with B220 (green) to visualize B cell zones and F4/80 (red) to identify $F4/80^+$ medullar macrophages. Diagram of lymph node included with merged image to represent region of lymph node imaged (box in dashed line) relative to entire lymph node (outlined in solid line).
(B) As in (A), but stained with B220 (green) and $CD169^+$ (red) to identify $CD169^+$ subcapsular sinus macrophages located on the outer border of lymph node sections.

Figure 14

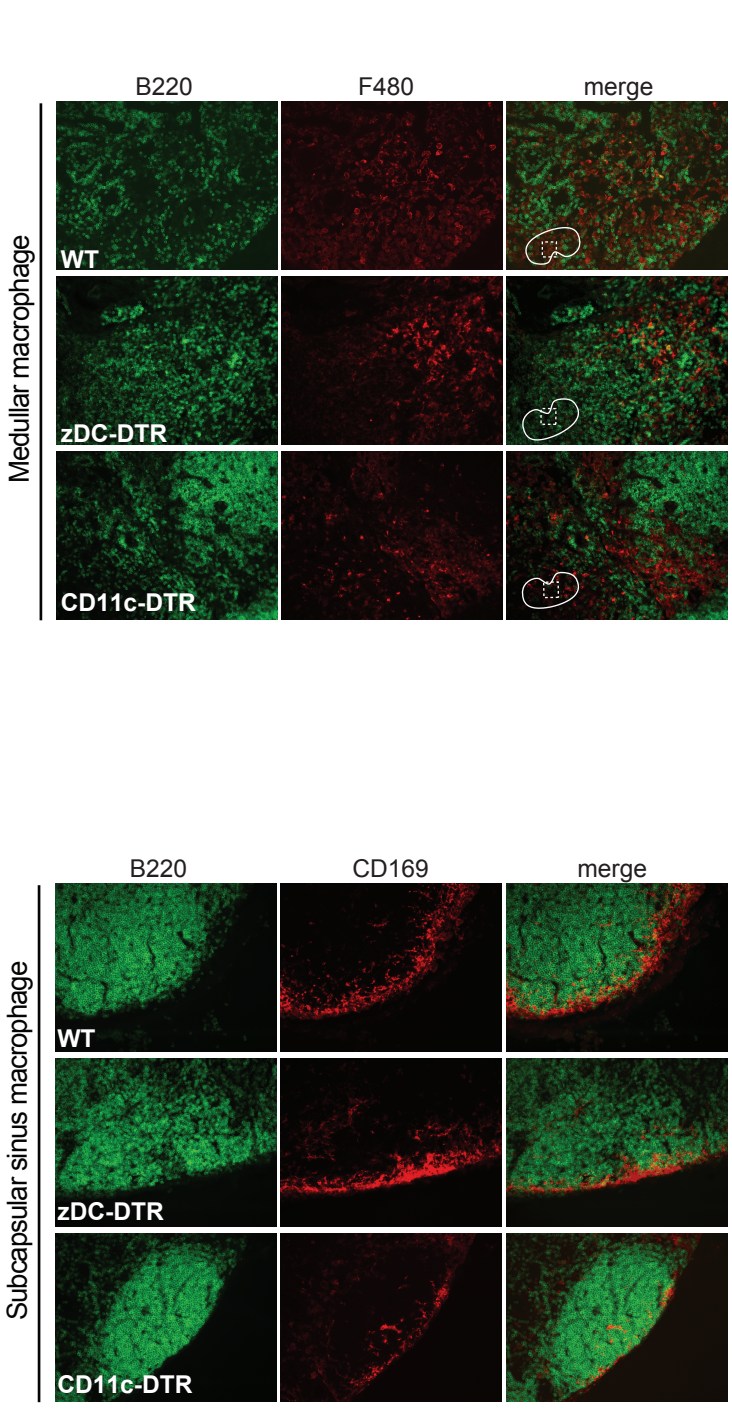
A
B220
F480
merge
Medullar macrophage
WT
zDC-DTR
CD11c-DTR
B
B220
CD169
merge
Subcapsular sinus macrophage
WT
zDC-DTR
CD11c-DTR

In conclusion, zDC-DTR is equivalent to CD11c-DTR in the ablation of pre-DC-derived cDCs. However, zDC-DTR also spares multiple steady state and inflammatory CD11c-expressing non-cDC populations affected by DT treatment in CD11c-DTR mice, most notably cells of the monocyte/macrophage lineage.

Immune responses in DT-treated zDC-DTR and CD11c-DTR mice

cDCs are orders of magnitude more efficient at antigen presentation than other antigen presenting cells including macrophages. To examine the relative contribution of cDCs and other CD11c-expressing cells to the presentation of soluble antigen, I compared OT-I and OT-II proliferation in DT-treated zDC- and CD11c-DTR bone marrow chimeras after immunization with the antigen ovalbumin (OVA). As expected, DT treatment of zDC- and CD11c-DTR bone marrow chimeras prior to immunization with soluble OVA abrogated OT-I and OT-II proliferative responses (Figure 15A). Therefore, as expected, antigen presentation to T cells is mediated by cDCs, and macrophages, which remain intact in DT-treated zDC-DTR mice, are insufficient to induce T cell proliferation. Similarly, splenocytes from DT-treated zDC- and CD11c-DTR mice failed to induce the proliferation of allogeneic T cells in mixed leukocyte reactions (MLRs) *in vitro* (Figure 15B). In this way, other antigen presenting cells, including macrophages and B cells, are unable to coordinate the MLR.

Figure 15. cDCs mediate OVA presentation to OT-I and OT-II T cells as well as the mixed leukocyte reaction, and these responses are abrogated in both zDC- and CD11c-DTR mice.

(A) CFSE-labeled CD45.1$^+$ OT-I and OT-II cells were transferred into CD45.2$^+$ recipients, treated with DT 24 hours later, and injected with 20μg OVA i.v. another 24 hours later. CFSE dilution of CD45.1$^+$ OT-I and OT-II cells was measured by flow cytometry three days after OVA injection.
(B) 500,000 bulk splenocytes from DT-treated CD45.2$^+$ C57BL/6 bone marrow chimeras were co-cultured with 50,000 CFSE-labeled CD45.1$^+$ BALB/c T cells. CFSE dilution of CD45.1$^+$ BALB/c T cells was measured by flow cytometry after five days.

Figure 15

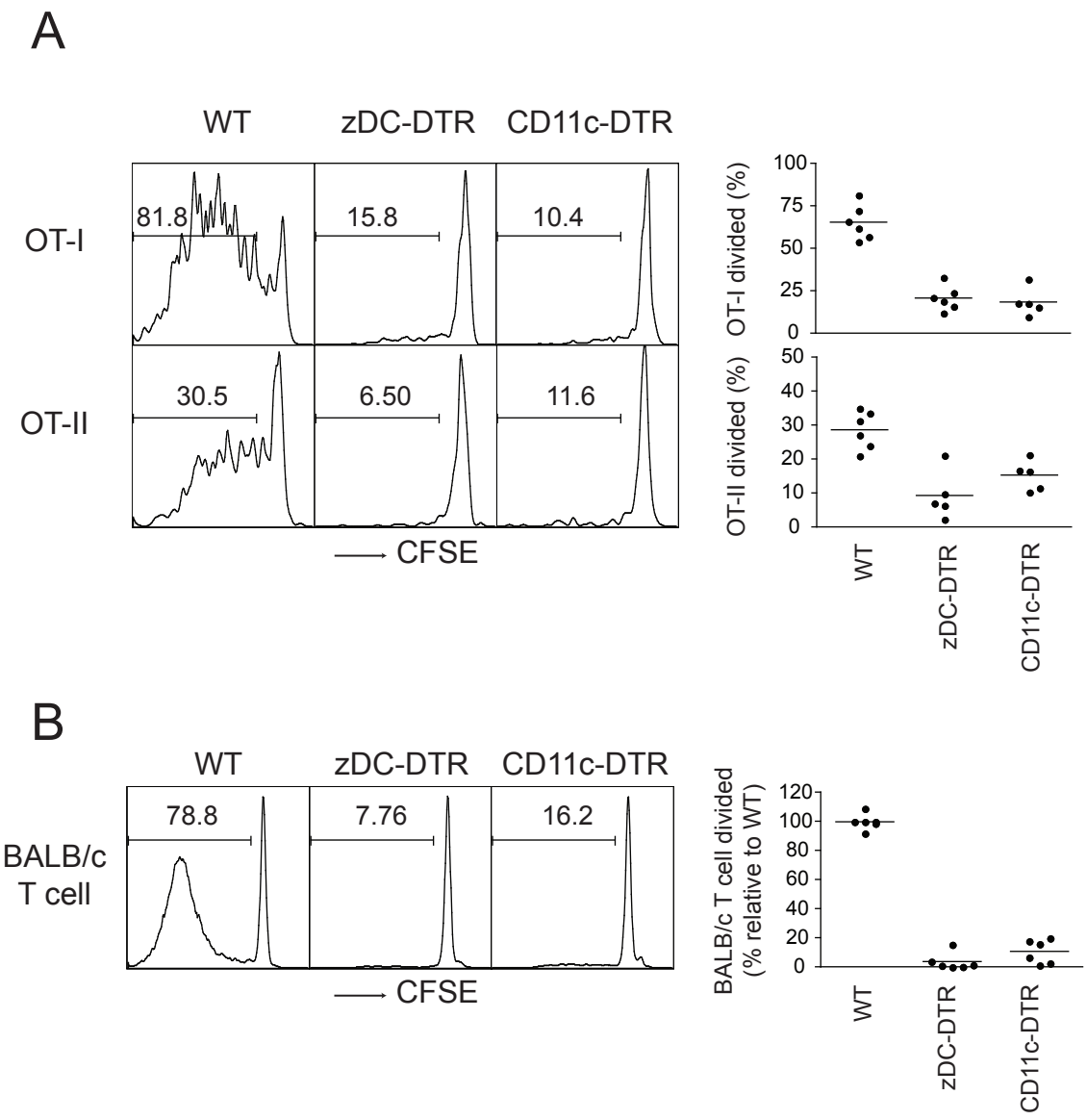
A
WT
zDC-DTR
CD11c-DTR
OT-I
OT-II
81.8
15.8
10.4
30.5
6.50
11.6
CFSE
OT-I divided (%)
OT-II divided (%)
100
75
50
25
0
50
40
30
20
10
0
WT
zDC-DTR
CD11c-DTR
B
WT
zDC-DTR
CD11c-DTR
BALB/c
T cell
78.8
7.76
16.2
CFSE
BALB/c T cell divided
(% relative to WT)
120
100
80
60
40
20
0
WT
zDC-DTR
CD11c-DTR

cDCs are required to initiate immune responses to a various pathogens. To understand the contribution of cDCs and other CD11c-expressing during pathogen challenge, I examined the immune response following *Toxoplasma gondii* infection in zDC- and CD11c-DTR bone marrow chimeras. Clearance of this protozoan parasite depends on IFNγ production by $CD4^+$ T cells (Denkers and Gazzinelli 1998; Lieberman and Hunter 2002; Subauste and Remington 2001). zDC- and CD11c-DTR bone marrow chimeras were injected with DT one day prior to infection and every third day thereafter. Eight days after *T. gondii* infection, I measured IFNγ production by $CD4^+$ T cell by flow cytometry and pathogen burden in the lung by Q-PCR. Importantly, cDC depletion was equivalent in DT-treated zDC- and CD11c-DTR bone marrow chimeras eight days after *T. gondii* infection (Figure 16A). Furthermore, $IFN\gamma^+CD4^+$ T cells were detectable but significantly reduced in the mesenteric lymph nodes and spleens of both types of mice (Figure 16B). However, $IFN\gamma^+CD4^+$ T cell response was significantly more reduced in CD11c-DTR compared to in zDC-DTR bone marrow chimeras. Accordingly, CD11c-DTR bone marrow chimeras displayed higher pathogen burden than zDC-DTR mice (Figure 16C), indicating CD11c-DTR mice mounted decreased overall levels of immunity to the pathogen. Therefore, DT treatment in CD11c-DTR mice impairs immune responses to *T. gondii* infection more so drastically than in zDC-DTR.

Figure 16. Immune responses to *Toxoplasma gondii* are more critically affected in CD11c-DTR than in zDC-DTR mice.

(A) Mice were treated with DT prior to infection with 15 *T. gondii* cysts by gavage and DT ablation was maintained until day eight after infection when mice were euthanized. The abundance of $Lin^{-}CD11c^{hi}$ cDCs in the spleens from DT-treated *T. gondii*-infected WT, zDC-DTR, and CD11c-DTR bone marrow chimeras determined by flow cytommetry.
(B) The percentage of $CD3^{+}CD4^{+}$ T cells producing IFNγ in the mesenteric lymph node and spleen quantified by intracellular cytokine staining after restimulation *in vitro.* Statistical significance was determined using a Student's t-test.
(C) Q-PCR of whole lung cDNA for *T. gondii* tachyzoite-specific SAG2 expression normalized to Gapdh. Statistical significance was determined by Student's t-test. *$p<0.01$; **$p<0.005$.

Figure 16

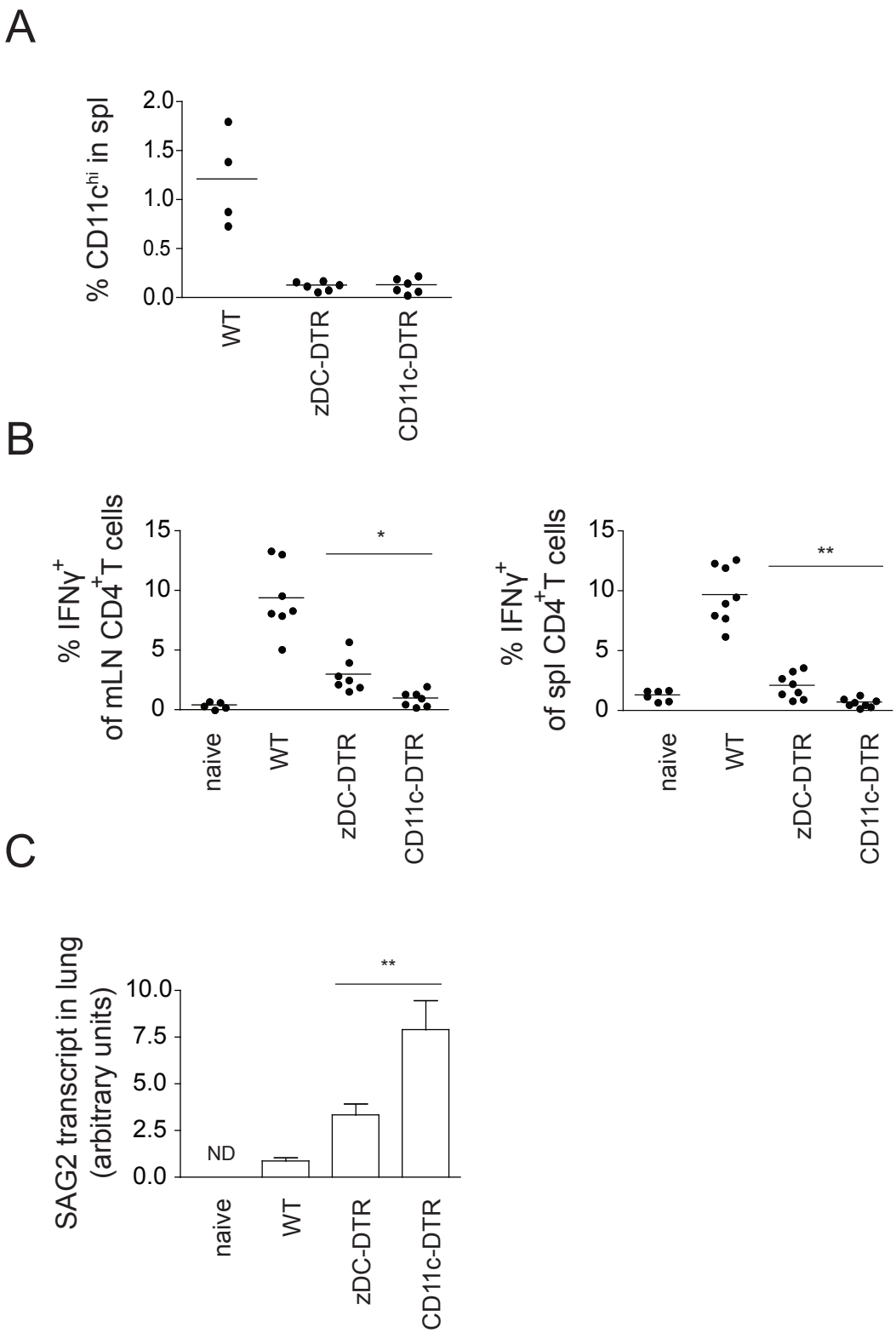
A
% CD11c^hi in spl
2.0
1.5
1.0
0.5
0.0
WT
zDC-DTR
CD11c-DTR
B
% IFNγ+ of mLN CD4+T cells
15
10
5
0
*
naive
WT
zDC-DTR
CD11c-DTR
% IFNγ+ of spl CD4+T cells
15
10
5
0
**
naive
WT
zDC-DTR
CD11c-DTR
C
SAG2 transcript in lung (arbitrary units)
10.0
7.5
5.0
2.5
0.0
**
ND
naive
WT
zDC-DTR
CD11c-DTR

Chapter 4.

RESULTS (PART III): zDC TARGET GENES

zDC ChIP-seq

zDC is a member of the BTB-ZF transcription factor family, and is therefore likely to function as a transcription factor. To identify genes regulated by zDC, I performed chromatin immunoprecipitation-sequencing (ChIP-seq) on steady state splenic cDCs. Genome-wide, zDC was enriched in a region 100 base pairs upstream of transcription start sites (TSS) (Figure 17A), which would optimally position it to interact with transcriptional machinery.

zDC contains two C2H2 zinc finger domains, each of which should bind a unique tri-nucleotide sequence(Bulyk et al. 2001), and therefore zDC would be predicted to recognize a six-nucleotide sequence motif. To identify zDC's DNA binding motif, I used MEME software to identify a consensus motif in the zDC ChIP-seq library (Bailey et al. 2009), which identified a ten-nucleotide sequence featuring a prominent six-nucleotide TGACGT core (Figure 17B). Gel shift assays confirmed this predicted motif as recombinant zDC bound double-stranded DNA probes containing the predicted binding motif but not control probe with a scrambled version of the motif (Figure 17C). Therefore, zDC binds its gene target at sequence-specific TGACGT motifs.

Figure 17. zDC localizes upstream of transcription start sites at a conserved DNA binding motif.

(A) Position of zDC-associated sequences relative to the closest gene's transcription start site (TSS). The number of genes at various distances from the TSS is shown on the y-axis.
(B) Consensus motif for zDC ChIP sequences determined by MEME analysis.
(C) Gel shift assays between recombinant zDC protein and probes containing predicted zDC motif or scrambled motif control. Because recombinant zDC was produced and purified as fusion protein with glutathione S-transferase (GST), GST protein was included as a control for GST:DNA binding.

Figure 17

A

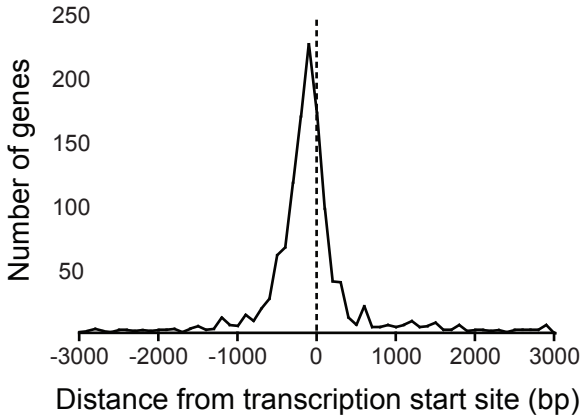

B

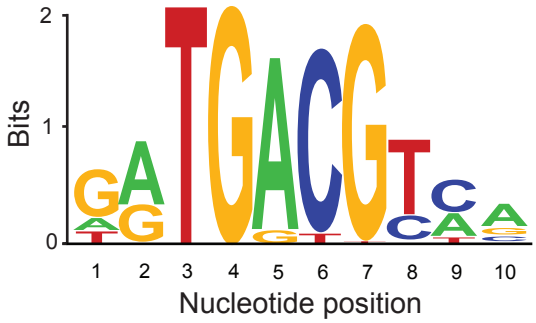

C

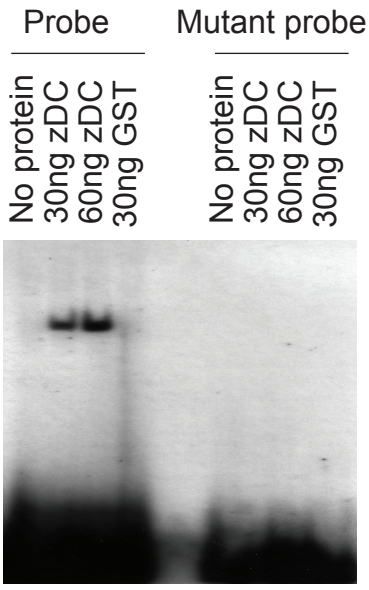

The ChIP-seq library identified 1,309 genes occupied by zDC, which represents a highly diverse group of gene families (Figure 18, Appendix I). The largest group of genes are implicated in the regulation of gene expression, including transcription factors, RNA processing factors, and chromatin regulators (Appendix II). A second large group of zDC-associated genes regulate protein metabolism, including kinases, peptidases, ubiquitin ligases, and phosphatases (Appendix III). Importantly, over 99% (1,304 of 1,309 target genes) contained the TGACGT consensus motif within one kilobase of the TSS ($p<0.01$).

Although zDC target genes were distributed throughout the genome, they were most abundant on chromosome 17 in the region of the mouse major histocompatibility (MHC) locus (Figure 19A). In fact, zDC is associated with nearly all MHC II genes expressed in C57BL/6 (Figure 19B). Therefore, zDC heavily occupies the MHC locus, including MHC II genes that are critical for cDC function.

Members of the BTB-ZF family are typically transcriptional repressors, but have also been shown to function as transcriptional activators (Beaulieu and Sant'Angelo 2011; Collins et al. 2001; Kelly and Daniel 2006). To begin to define the role of zDC in regulating gene expression *in vivo*, I compared the expression of zDC target gene mRNAs in fully differentiated cDCs and monocytes by gene array. Monocytes were selected for comparison because they are closely related to cDCs but lack zDC expression (Meredith, *et al.* submitted). Consistent with the

Figure 18. zDC ChIP-seq identified 1,309 target genes representing diverse gene families.

Pie chart shows distribution of zDC ChIP target genes. Gene ontologies for target genes were determined by PANTHER Classification (pantherdb.org). Numbers in parentheses indicate number of genes included in the indicated group.

Figure 18

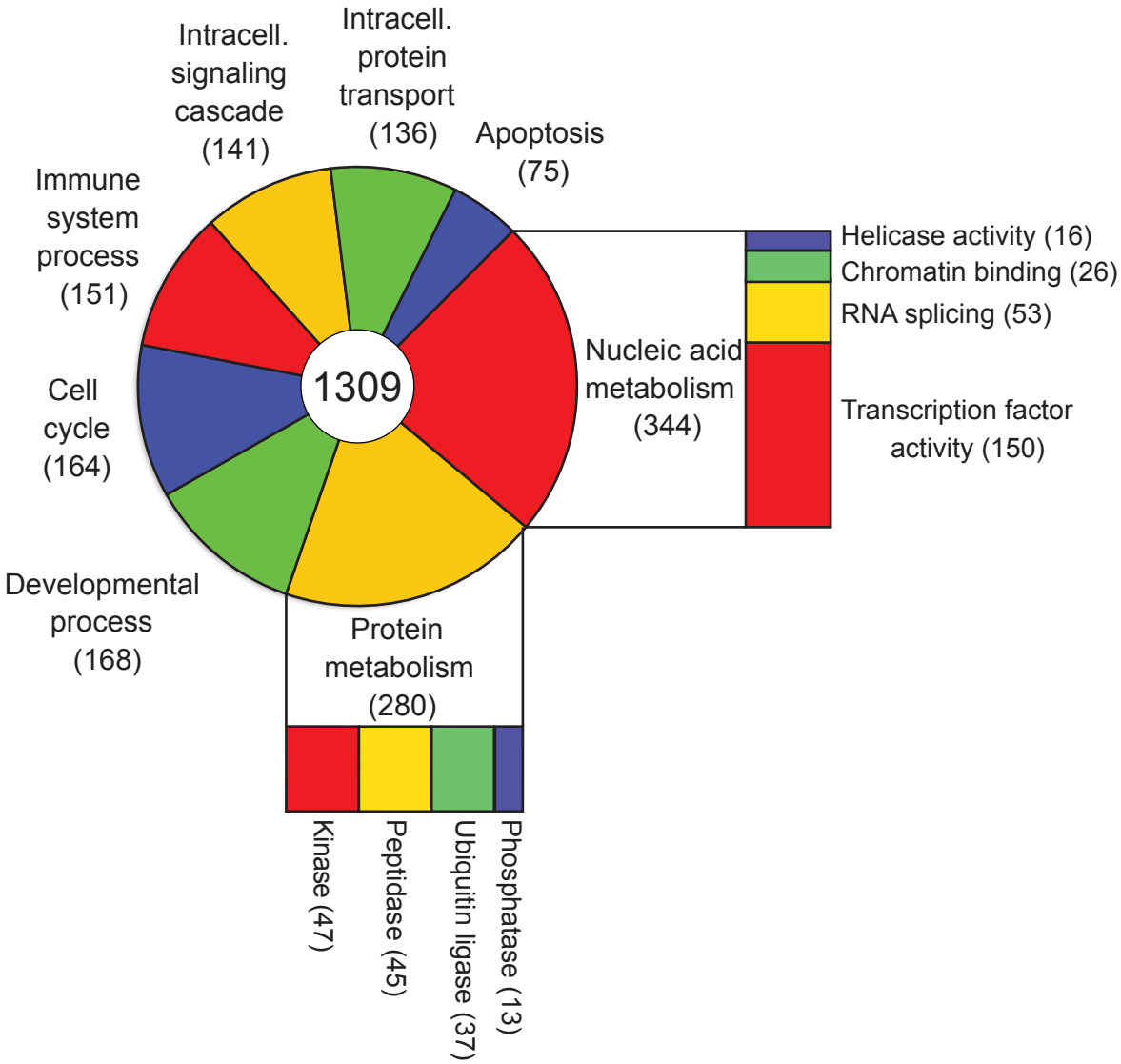
Intracell. signaling cascade (141)
Intracell. protein transport (136)
Apoptosis (75)
Immune system process (151)
Cell cycle (164)
Developmental process (168)
1309
Nucleic acid metabolism (344)
Protein metabolism (280)
Helicase activity (16)
Chromatin binding (26)
RNA splicing (53)
Transcription factor activity (150)
Kinase (47)
Peptidase (45)
Ubiquitin ligase (37)
Phosphatase (13)

Figure 19. zDC binds genes distributed throughout the genome, is especially abundant within the MHC locus on chromosome 17 including all expressed MHCII genes, and zDC target genes include many that are expressed higher in monocytes compared to cDCs.

(A) Genome-wide distribution of zDC target genes. The mouse genome was divided into 10 Mbp segments and the number of zDC target genes within each segment is shown. Alternating red and black portions and matching numbers indicate chromosome number.

(B) zDC ChIP reads relative to four classical MHC II genes expressed by C57BL/6 background. 1 kilobase scale bar included for each locus.

(C) Fold difference expression of zDC target gene probes by cDCs relative to monocytes. Red bars indicate probes expressed at higher levels in cDCs, and blue for those in monocytes. Probes expressed equally by cDCs and monocytes (ie less than two-fold difference) not shown.

Figure 19

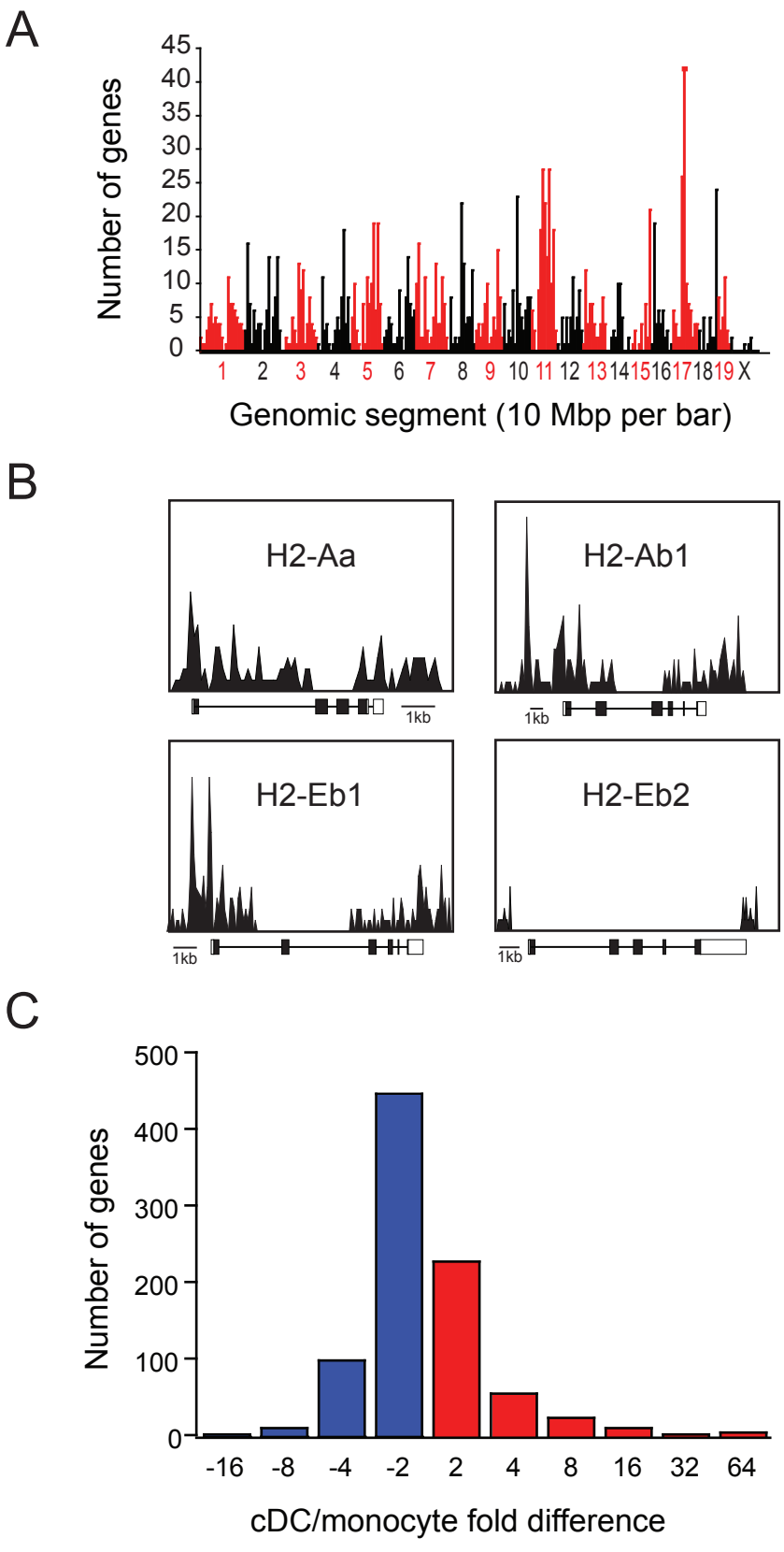
A
Number of genes
45
40
35
30
25
20
15
10
5
0
1 2 3 4 5 6 7 8 9 10 11 12 13 14 15 16 17 18 19 X
Genomic segment (10 Mbp per bar)
B
H2-Aa
H2-Ab1
H2-Eb1
H2-Eb2
1kb
C
Number of genes
500
400
300
200
100
0
-16 -8 -4 -2 2 4 8 16 32 64
cDC/monocyte fold difference

ability of BTB-ZF transcription factors to function as suppressors or activators, there was a broad range of differential gene expression of zDC target genes in cDC and monocytes. 564 zDC-associated gene probes were expressed at two- to four-fold higher levels in monocytes compared to cDCs (57% of ChIP target gene probes differentially expressed between cDCs and monocytes; Figure 19C). This pattern suggests zDC suppresses the expression of these genes in differentiated cDCs. Conversely, a smaller group of genes (381 probes; 40% of differentially expressed ChIP gene probes) was upregulated in cDCs compared to monocytes, representing targets that may be activated by zDC binding. Therefore, like other BTB-ZF family members, zDC represses the expression of many of its target genes but can also activate gene expression.

Chapter 5.

RESULTS (PART IV): zDC FUNCTION

zDC knockout mice

To examine the function of zDC *in vivo*, I produced a conditional knockout of zDC by flanking its second exon, which encodes the translational start site and the BTB protein-binding domain, with loxP sites (Figure 20A, $zDC^{lox/lox}$ mice). These mice were generated and maintained on the C57BL/6 background. $zDC^{lox/lox}$ mice were crossed with EIIA-Cre mice to produce mice that carry a zDC null mutation ($zDC^{-/-}$). $zDC^{-/-}$ mice were born below the expected Mendelian frequency from $zDC^{+/-}$ x $zDC^{+/-}$ crosses (15% versus expected 25%, p=0.0005), but once born appeared normal. zDC deletion was confirmed by western blot (Figure 20B).

zDC is not required for cDC development

Despite the absence of zDC protein in mutant mice, early cDC development was unaffected. Wildtype and $zDC^{-/-}$ mice contained comparable numbers of macrophage and dendritic cell progenitors (MDPs), common dendritic cell progenitors (CDPs) and pre-cDCs in the bone marrow (Figure 21A). Furthermore, the total number of cDCs in the spleen and skin-draining lymph nodes were similar in $zDC^{-/-}$ and wildtype littermates (Figure 21 B-C).

Figure 20. zDC knockout mice lack zDC protein expression in cDCs.

(A) Wildtype, conditional, and knockout zDC alleles. The BTB protein dimerization domain in exon 2 and two C2H2 zinc finger domains in exon 4 are labeled with arrows. Red triangles represent loxP sites.

(B) Western blot for zDC and Histone H4 loading control on purified splenic cDCs from $zDC^{+/+}$ and $zDC^{-/-}$ mice.

Figure 20

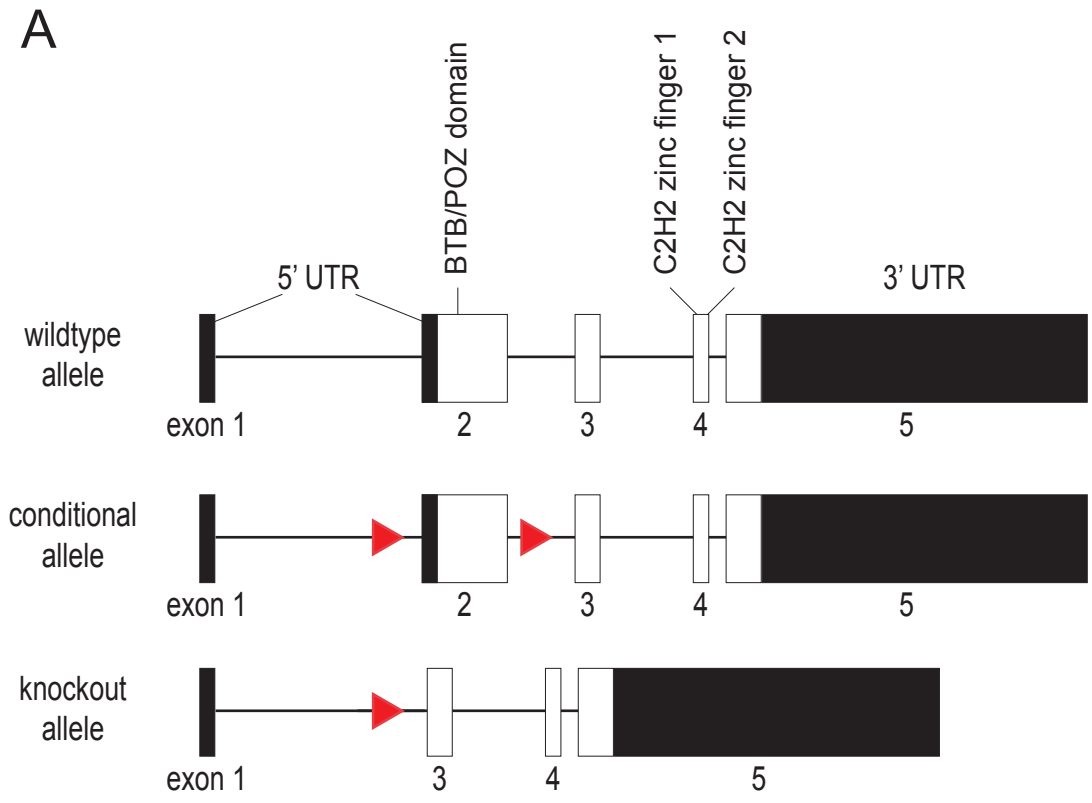
A
BTB/POZ domain
C2H2 zinc finger 1
C2H2 zinc finger 2
5' UTR
3' UTR
wildtype allele
exon 1
2
3
4
5
conditional allele
exon 1
2
3
4
5
knockout allele
exon 1
3
4
5

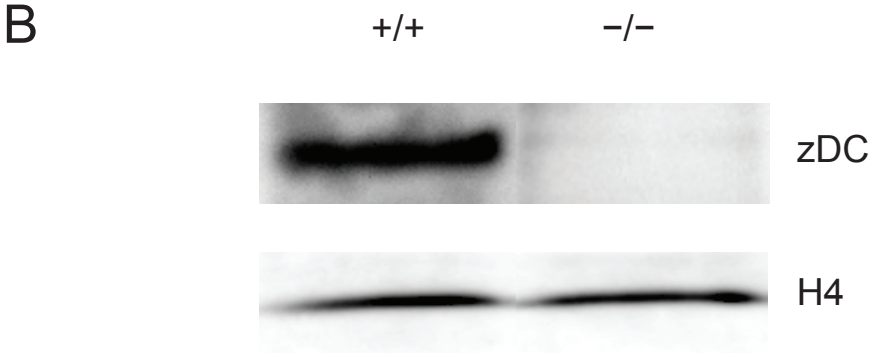
B
+/+
−/−
zDC
H4

Figure 21. cDC development is not impaired in zDC-deficient mice, though subset composition is altered which favors CD8 cDCs in the spleen and migratory DCs in the skin-draining lymph nodes.

(A) Percent abundance of $CD3^{-}B220^{-}NK1.1^{-}$("Lin^{-}")$Sca\text{-}1^{-}CD11b^{-}CD11c^{-}Flt3^{+}CD115^{+}$ $CD117^{hi}$ MDP, $Lin^{-}Sca\text{-}1^{-}CD11b^{-}CD11c^{-}Flt3^{+}CD115^{+}CD117^{lo}$ CDP, and $Lin^{-}MHCII^{-}CD11c^{+}Flt3^{+}$ pre-DC populations in bone marrow from wildtype (blue) and $zDC^{-/-}$ (red) mice.

(B) Flow cytometry plots of $CD11c^{hi}MHCII^{+}$ cDCs from the spleens of $zDC^{+/+}$, $zDC^{+/-}$, and $zDC^{-/-}$ mice. Numbers indicate percent of total spleen cells.

(C) As in (B), but in skin-draining lymph nodes. Numbers adjacent to $CD11c^{hi}MHCII^{+}$ cDC (red) and $CD11c^{hi}MHCII^{+}$ mDC gates (blue) indicate percent of skLN.

(D) Flow cytometry plots gated on $CD11c^{hi}MHCII^{+}$ splenic cDCs from $zDC^{+/+}$, $zDC^{+/-}$, and $zDC^{-/-}$ mice. Numbers adjacent to CD4 (green) and CD8 (orange) gates indicate percent of cDCs, and graph on the right shows percent of total spleen cells.

Figure 21

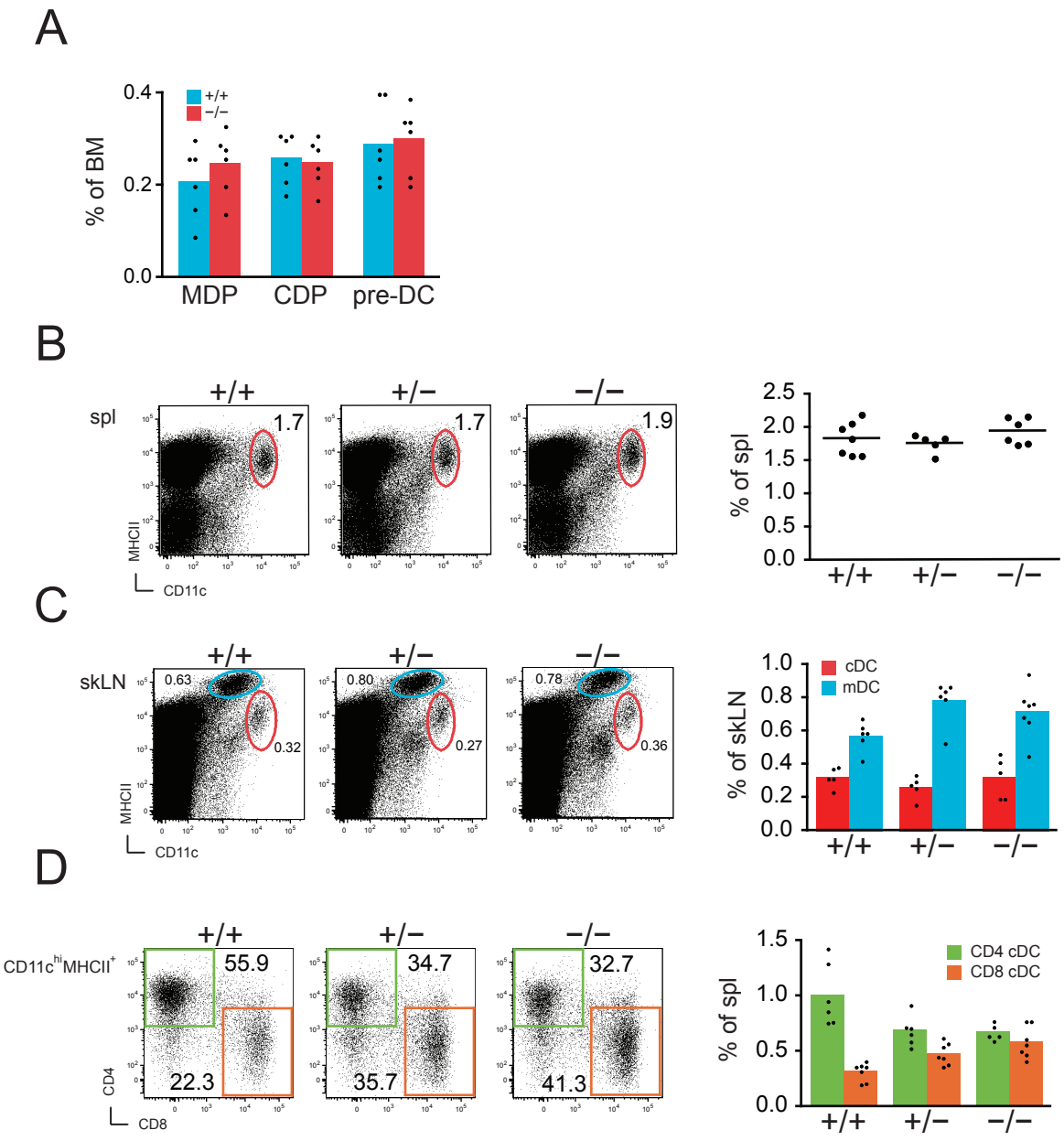
A
0.4
0.2
0.0
% of BM
+/+
−/−
MDP
CDP
pre-DC
B
+/+
+/−
−/−
spl
1.7
1.7
1.9
MHCII
CD11c
2.5
2.0
1.5
1.0
0.5
0.0
% of spl
+/+
+/−
−/−
C
+/+
+/−
−/−
skLN
0.63
0.32
0.80
0.27
0.78
0.36
MHCII
CD11c
1.0
0.8
0.6
0.4
0.2
0.0
% of skLN
cDC
mDC
+/+
+/−
−/−
D
+/+
+/−
−/−
CD11c^hiMHCII^+
55.9
22.3
34.7
35.7
32.7
41.3
CD4
CD8
1.5
1.0
0.5
0.0
% of spl
CD4 cDC
CD8 cDC
+/+
+/−
−/−

However, the number of $CD11c^{+}MHCII^{hi}$ migratory dendritic cells (mDCs), which arrive from the skin via CCR7-dependent migration following maturation (Alvarez et al. 2008), were slightly increased in the skin-draining lymph nodes of $zDC^{+/-}$ and $zDC^{-/-}$ mice (Figure 21C). Furthermore, although $zDC^{-/-}$ mice contained the same number of total cDCs as wildtype littermates, $zDC^{-/-}$ mice contained fewer splenic $CD4^{+}$ cDCs and reciprocally greater numbers of $CD8^{+}$ cDCs (Figure 21D). Whereas $CD4^{+}$ cDCs were three-fold more abundant than $CD8^{+}$ cDCs in wildtype littermates, zDC-deficient mice showed approximately equal numbers of $CD4^{+}$ and $CD8^{+}$ cDCs. Therefore, zDC is not required for cDC development, but zDC-deficiency alters the proportions of $CD4^{+}$ and $CD8^{+}$ cDCs in the spleen and results in a small increase in mDC numbers in the skin draining lymph nodes.

zDC regulation of gene expression

To determine the effects of zDC-deficiency on cDC gene expression genome-wide, I compared gene expression data from wildtype and zDC-deficient splenic $CD8^{+}$ and $CD4^{+}$ cDCs. Overall, 2,653 genes were upregulated while 1,195 genes were downregulated in $CD4^{+}$ $zDC^{-/-}$ cDCs relative to wildtype controls (Figure 22A). Similarly 2,333 genes were upregulated and 1,078 genes downregulated in $CD8^{+}$ $zDC^{-/-}$ cDCs (Figure 22B). These effects on gene expression in $zDC^{-/-}$ cDCs were highly correlated between $CD4^{+}$ and $CD8^{+}$ cDCs (Figure 22C; $m=0.78 \pm 0.0023$; $r^2=0.73$). Therefore, zDC-deficiency profoundly alters the transcriptional profiles of $CD4^{+}$ and $CD8^{+}$ cDCs, and these changes are shared in both subsets of cDCs.

Figure 22. cDC gene expression is significantly altered in the absence of zDC, including the upregulation of zDC target genes.

(A) Relative $\log_2$ expression of all Affymetrix Mouse 430 2.0 probes by wildtype $CD4^+$ cDCs on x-axis compared to $zDC^{-/-}$ CD4+ cDCs on y-axis. Each probe is represented by a single box. Bold red line represents equal expression, and probes located outside secondary red lines expressed at greater than two-fold difference.

(B) As in (A), but comparing wildtype $CD8^+$ cDCs with $zDC^{-/-}$ CD8+ cDCs.

(C) Ratio of expression between $zDC^{-/-}$ and wildtype cDCs for all Affymetrix Mouse 430 2.0 probes. Blue line represents linear regression of all points ($m=0.78 \pm 0.0023$; $r^2=0.74$)

(D) GSEA plot comparing gene array expression of zDC target genes by $zDC^{-/-}$ (left) and wildtype cDCs (right) ($p<0.001$).

Figure 22

A

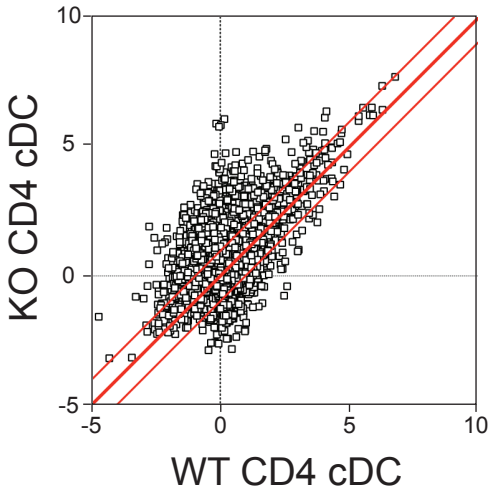

B

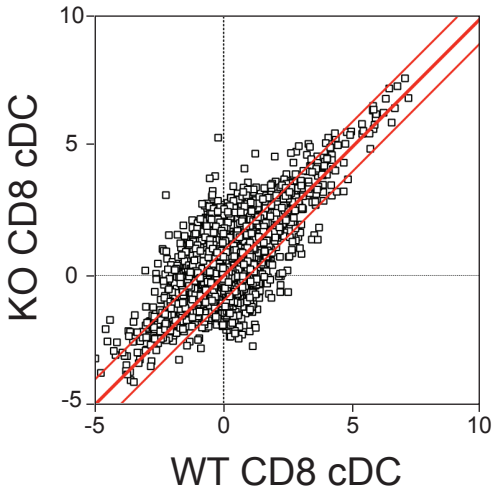

C

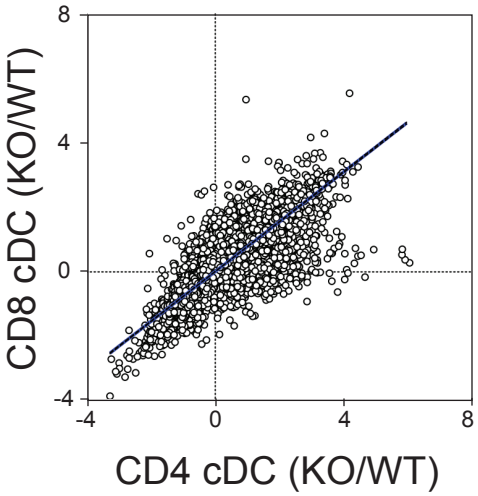

D

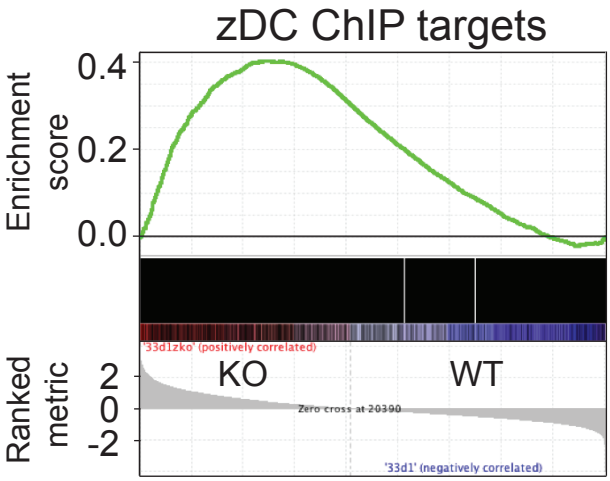

To better appreciate the function of zDC at its target genes, we compared the expression of zDC-bound genes identified by ChIP-seq with Gene Set Enrichment Analysis (GSEA) (Subramanian et al. 2005). Overall, zDC target genes were upregulated in zDC-deficient cDCs (Figure 22D; $p<0.001$). This upregulation of zDC-bound genes suggests zDC acts as a transcriptional repressor at many of its targets, similar to other members of the BTB-ZF family (Beaulieu and Sant'Angelo 2011; Collins et al. 2001; Kelly and Daniel 2006).

zDC-deficiency results in partial activation

cDCs express numerous pathogen recognition molecules and signaling receptors which allow them to sense pathogen- and self-derived activation signals. Signaling through these receptors induces cDC maturation, including the upregulation of MHC II and co-stimulatory markers, which enables cDCs to stimulate adaptive immune responses (Steinman 2007). GSEA software showed that multiple activation and inflammatory pathways are upregulated in zDC-deficient cDCs, including gene sets upregulated in response LPS (Foster et al. 2007) and by GM-CSF-cultured DCs treated with TNFα/IL-1β (Lindstedt et al. 2002) (Figure 23A; $p<0.005$). Furthermore, in addition to the transcriptional upregulation of these gene sets, $zDC^{-/-}$ cDCs expressed two-fold higher MHC II levels by flow cytometry compared to wildtype littermates (Figure 23B). Therefore, steady state zDC-deficient cDCs upregulate the expression of gene pathways normally expressed following activation.

Figure 23. zDC-deficient cDCs upregulate maturation gene pathways and MHCII expression, and wildtype cDCs lack zDC protein following immune stimulation.

(A) GSEA plots for inflammatory response after LPS exposure{Foster, 2007 #158} and DC maturation{Lindstedt, 2002 #159} gene sets significantly upregulated in $zDC^{-/-}$ compared to wildtype cDCs ($p<0.001$).

(B) Flow cytometry histograms depicting surface MHC II expression by splenic $CD11c^{hi}CD8^{+}$ and $CD11c^{hi}CD4^{+}$ cDCs. Shaded histogram represents wildtype and red line shows $zDC^{-/-}$.

(C) Western blot for zDC expression by CD11c-enriched splenic cDCs from naïve and TLR agonist-treated mice. Mice were injected i.v. with PBS, 30 μg poly I:C, 20 μg CpG in 15% DOTAP, or 50 μg LPS, and spleens were harvested three hours later. β-actin blot included as loading control.

Figure 23

A

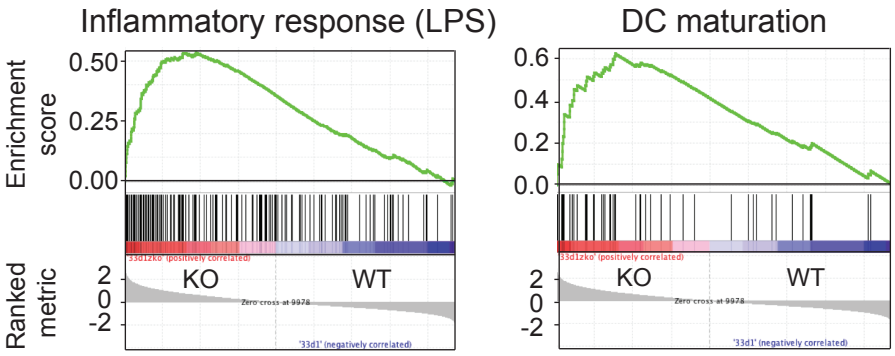

B

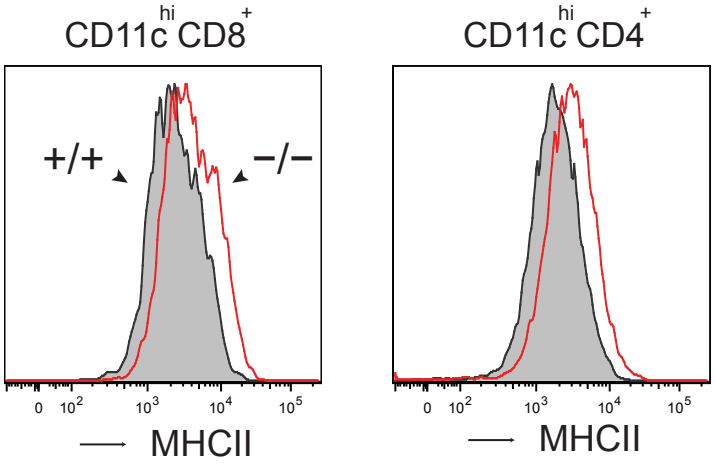

C

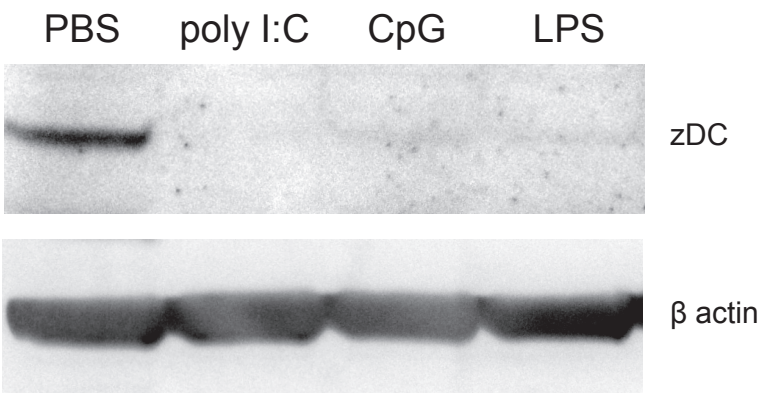

Since zDC-deficient steady state cDCs appear to phenocopy some aspects of cDC activation, I was curious if zDC expression is modulated during cDC activation. To determine the effect of cDC maturation on zDC expression, I injected mice with various TLR agonists and looked for zDC expression by western blot. As early as three hours after injection with poly I:C, CpG, or LPS, zDC protein could not be detected in splenic cDC lysates (Figure 23C). This loss of zDC protein is most likely due to protein degradation because zDC transcript levels remain elevated in cDCs isolated from poly I:C-injected and *Salmonella*-infected mice (immgen.org). Consistently, DTR expression in zDC-DTR mice is maintained in poly I:C-treated mice for up to 48 hours (Figure 24A), and neither pre-treatment with poly I:C nor *T. gondii* infection inhibit DT-mediated ablation (Figures 16A, 24B). Therefore, zDC protein is rapidly degraded following TLR stimulation, which is consistent with the upregulation of maturation pathways by zDC-deficient cDCs.

The choice between the induction of tolerance or adaptive immunity is in part determined by the activation state of cDCs (Steinman 2007). To examine the consequences of zDC deficiency during antigen presentation to T cells, I tested $zDC^{-/-}$ cDCs for the ability to induce OVA-specific OT-I T cell deletion (Dudziak et al. 2007; Hawiger et al. 2001). Specifically, wildtype and $zDC^{-/-}$ mice received 1-2 x 10^6 CFSE-labeled OT-I T cells and were immunized with 3μg DEC-205 antibody expressed as a fusion protein with OVA antigen (DEC-OVA). Two weeks after DEC-OVA immunization, OT-I cells were examined by flow

Figure 24. DTR expression is not downregulated in zDC-DTR mice following immune stimulation.

(A) Flow cytometry histograms showing DTR expression by $CD4^+$ cDCs from naïve wildtype (gray shaded), naïve zDC-DTR (red line), or zDC-DTR mice 12 hours (green) and 24 hours (blue) after poly I:C injection.

(B) As in (A), but by $CD8^+$ cDCs.

(C) WT, zDC-DTR, and CD11c-DTR bone marrow chimeras were treated with 30 μg poly I:C i.v., and DT 12 hours later i.p. Another 12 hours after DT treatment, the amount of cDC ablation in spleen was determined by flow cytometry. Gated on $B220^-CD3^-$.

Figure 24

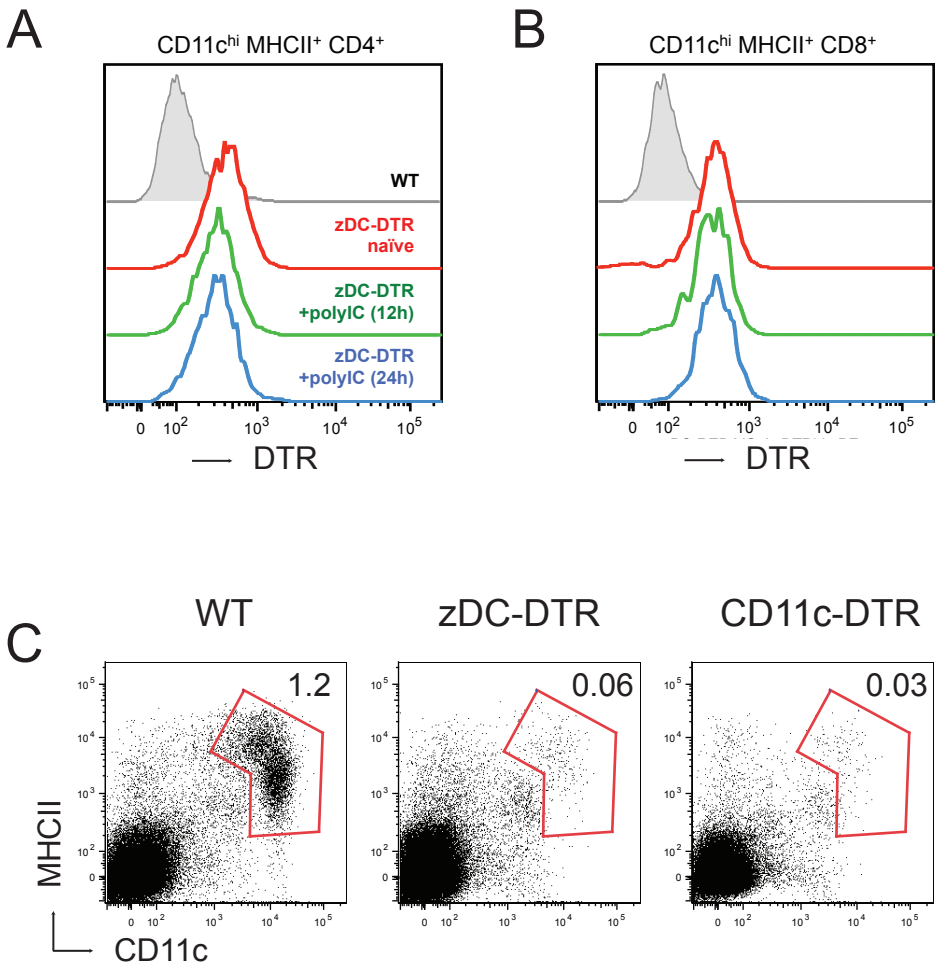
A
CD11c^hi MHCII+ CD4+
WT
zDC-DTR naïve
zDC-DTR +polyIC (12h)
zDC-DTR +polyIC (24h)
0 10^2 10^3 10^4 10^5
DTR
B
CD11c^hi MHCII+ CD8+
0 10^2 10^3 10^4 10^5
DTR
C
WT
zDC-DTR
CD11c-DTR
1.2
0.06
0.03
MHCII
CD11c

wildtype littermates were able to efficiently delete proliferated OT-I T cells, zDC-deficient mice contained significantly more surviving OT-I T cells as long as two weeks after DEC-OVA immunization (Figure 25A). These remaining OT-I T cells were $CFSE^{lo}$, and therefore did not represent naïve cells that had not proliferated (Figure 25B). Furthermore, the majority of surviving OT-I T cells collected from $zDC^{-/-}$ mice expressed low levels of CD62L (Figure 25C), suggesting these cells represent activated T cells with effector function. Conversely, naïve OT-I T cells from wildtype mice that did not receive DEC-OVA immunization, as well as the few remaining OT-I T cells from DEC-OVA-immunized wildtype mice, maintained a naïve phenotype indicated by high expression of CD62L. Therefore, antigen presentation by $zDC^{-/-}$ cDCs, which are more activated than wildtype cDCs, prevents efficient deletion of OT-I T cells in the steady state.

Increased lymphangiogenesis in $zDC^{-/-}$ mice

cDCs regulate lymph node expansion following immunization and re-quiescence upon return to steady state conditions (Tzeng et al. 2010; Webster et al. 2006). In addition to the upregulation of activation pathways in zDC-deficient cDCs, the skin-draining lymph nodes isolated from $zDC^{-/-}$ mice were significantly expanded in terms of size, weight, and cellularity (Figure 26 A-C). Furthermore, blood vessels associated with these enlarged lymph nodes were more prominent (Figure 26A). The spleens from wildtype and $zDC^{-/-}$ mice, however, were similar in size (Figure 26B). The enlarged skin-draining lymph nodes from $zDC^{-/-}$ mice

Figure 25. zDC$^{-/-}$ mice show impaired deletion of proliferated OT-I cells which encountered antigen in the steady state.

(A) Quantification of surviving CD8^{+}CD45.1^{+}Vα2^{+} OT-I T cells by flow cytometry in the spleens of wildtype and zDC$^{-/-}$ mice two weeks after immunization with 3 μg DEC-OVA.

(B) Histogram showing CFSE labeling and (C) CD62L expression by CD8^{+}CD45.1^{+}Vα2^{+} OT-I T cells described in (A). Gray shaded curve represents cells collected from unimmunized control, blue line from DEC-OVA-immunized wildtype mice, and red line from DEC-OVA-immunized zDC$^{-/-}$ mice.

Figure 25

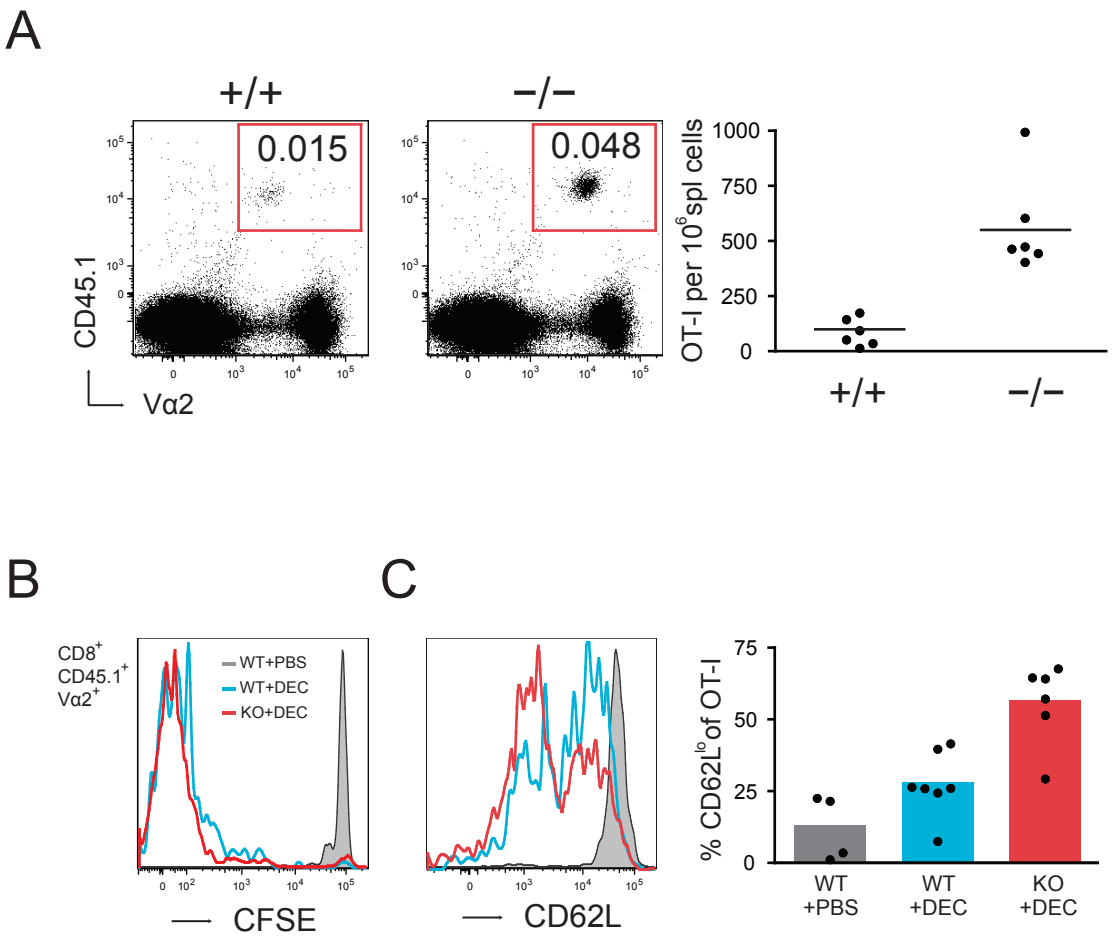
A
+/+
−/−
0.015
0.048
CD45.1
Vα2
OT-I per 10^6 spl cells
1000
750
500
250
0
+/+
−/−
B
CD8+
CD45.1+
Vα2+
WT+PBS
WT+DEC
KO+DEC
CFSE
C
CD62L
% CD62L^lo of OT-I
75
50
25
0
WT +PBS
WT +DEC
KO +DEC

Figure 26. The skin-draining lymph nodes of zDC$^{-/-}$ mice are significantly expanded.

(A) LEFT: Photograph of spleen, popliteal, inguinal, and axillary lymph nodes from wildtype and zDC-deficient mice. Ruler below shows millimeter increments. RIGHT: Axillary lymph nodes from wildtype (top right) and zDC-deficient (bottom right) mice showing increased vasculature in zDC$^{-/-}$ lymph nodes.

(B) Weights of spleens (spl), popliteal (popLN), inguinal (ingLN), and axillary (axiLN) lymph nodes from wildtype and zDC-deficient mice.

(C) Total cell counts from pooled skin-draining lymph nodes in wildtype and zDC-deficient mice.

(D) Percent composition of B and T lymphocytes in skin-draining lymph nodes from wildtype and zDC$^{-/-}$ mice determined by flow cytometry. Results pooled from four experiments.

Figure 26

A

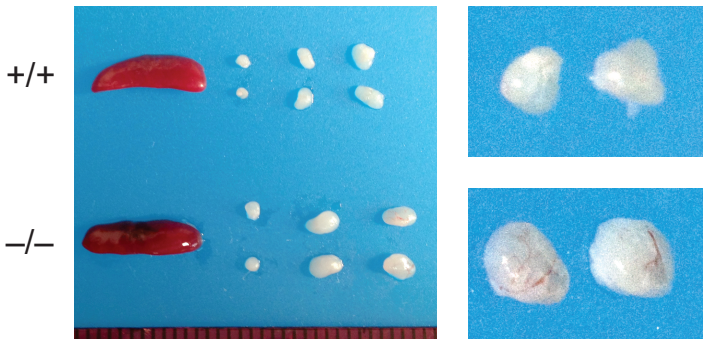

B

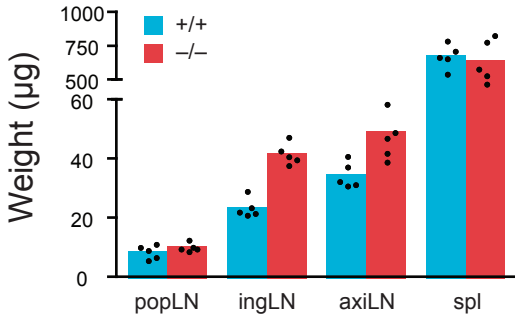

C

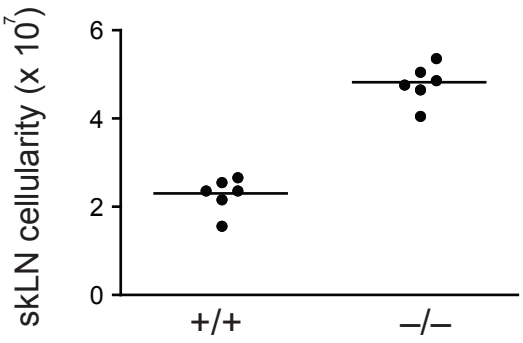

D

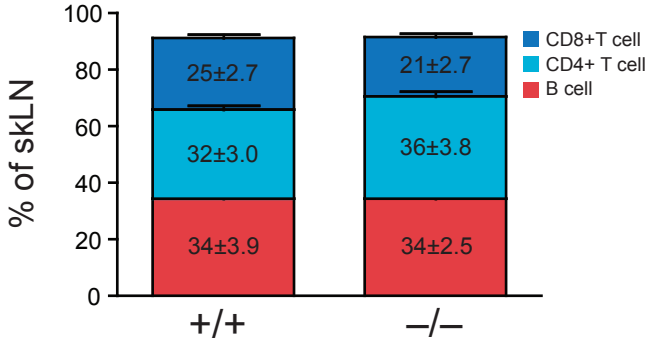

contained a proportional expansion of B and T lymphocytes (Figure 26D) without evident skewing of a particular population other than a small increase of mDCs (Figure 21C).

TLR-stimulated cDCs mediate lymph node enlargement and angiogenesis by producing vascular endothelial growth factor (VEGF) (Tzeng et al. 2010; Webster et al. 2006; Wendland et al. 2011). To determine if enhanced VEGF production by zDC-deficient cDCs contributes to lymph node expansion, I measured *Vegf* expression in $zDC^{-/-}$ cDCs. Gene array analysis suggested *Vegfc* is upregulated in $zDC^{-/-}$ $CD4^{+}$ cDCs (Figure 27A), and this was confirmed by Q-PCR (Figure 27B). Consistent with elevated *Vegfc* mRNA, popliteal lymph nodes collected from $zDC^{-/-} \rightarrow zDC^{+/+}$ bone marrow chimeras contained more VEGF than control bone marrow chimeras (Figure 27C), demonstrating zDC-deficient hematopoetic cells contribute to elevated VEGF levels in lymph nodes. However, *Vegfc* was not a zDC target identified by ChIP-seq. Therefore, elevated *Vegfc* expression by zDC-deficient cDCs is likely an indirect effect of cDC maturation.

Figure 27. Elevated VEGF expression by zDC-deficient cDCs.

(A) Log_2-scaled heat maps for three *Vegfc* probes showing *Vegfc* expression by splenic $CD4^+$ and $CD8^+$ cDCs collected from $zDC^{+/+}$ and $zDC^{-/-}$ mice.

(B) Q-PCR for *Vegfc* expression by splenic $CD4^+$ cDCs normalized to *Gapdh* expression.

(C) Western blot for VEGF protein from whole popliteal lymph node extracts collected from $zDC^{+/+}\rightarrow zDC^{+/+}$ and $zDC^{-/-}\rightarrow zDC^{+/+}$ bone marrow chimeras. β-actin is included as a loading control. Graph on right shows VEGF band quantification normalized to β-actin band intensity with ImageJ software from three experiments.

Figure 27

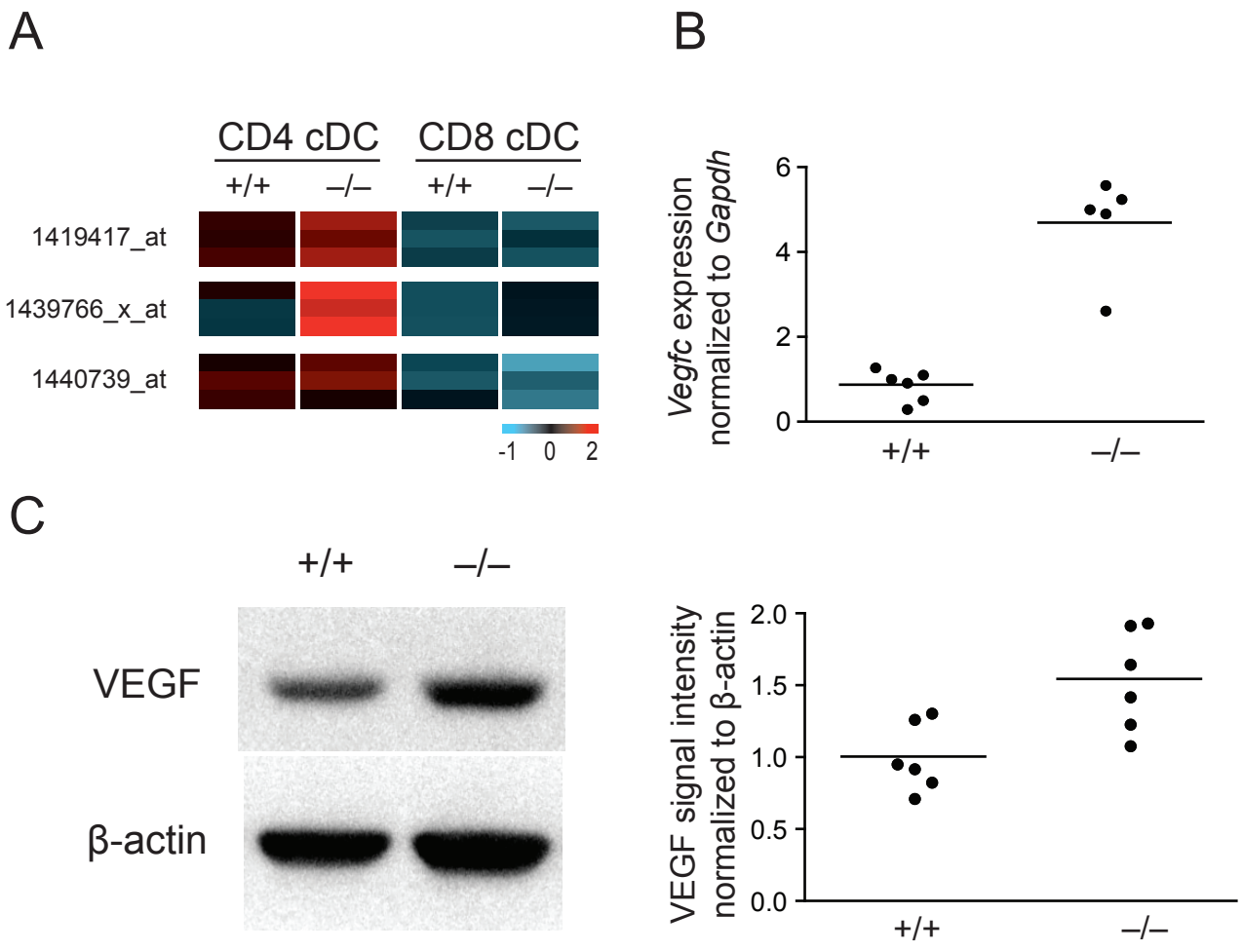
A
CD4 cDC
CD8 cDC
+/+
–/–
+/+
–/–
1419417_at
1439766_x_at
1440739_at
-1
0
2
B
Vegfc expression normalized to Gapdh
6
4
2
0
+/+
–/–
C
+/+
–/–
VEGF
β-actin
VEGF signal intensity normalized to β-actin
2.0
1.5
1.0
0.5
0.0
+/+
–/–

Chapter 6.

DISCUSSION

Since their initial description in 1973, the field of cDC biology has proven controversial. Much of the ensuing confusion arises from the complexity of the myeloid system and the lack of highly specific markers to distinguish its constituent populations. The distinction between monocytes/macrophages and cDCs has proven the most complicated, although pDCs also share key phenotypic markers with both. More important than phenotype, our understanding of monocyte/macrophage and cDC development and function has clarified that these two populations represent distinct lineages with unique functional specializations. However, even this progress can be slowed by the lack of clear markers to distinguish these populations.

CD11c is of course the most reliable and popular marker to identify cDCs, but is also the most misleading (Bradford et al. ; Geissmann et al. 2010). cDCs in steady state secondary lymphoid organs are distinctly $CD11c^{hi}$ compared to other CD11c-expressing populations, including pDCs, NK cells, and $Ly6C^{lo}$ monocytes, and some macrophage subsets (Figure 1). Inflammatory conditions, however, triggers the upregulation of CD11c on additional populations, including $Ly6c^{hi}$ monocytes and $CD8^{+}$ T cells. Moreover, MHC II expression is likewise upregulated in response to immune stimulation by several $CD11c^{+}$ populations, including pDCs and $Ly6C^{hi}$ monocytes. In this way, multiple populations can

display ‘definitive’ $CD11c^{+}MHCII^{+}$ cDC-like phenotypes. Furthermore, these phenotypes are best characterized in secondary lymphoid tissues and may not apply to some non-lymphoid organs, especially mucosal surfaces like the lung and gut which are constantly exposed to inflammatory stimuli. Therefore, additional markers to distinguish cDCs from other myeloid populations are necessary to define cDC function in these diverse tissue settings.

The distinction between cDCs and monocytes/macrophages is not trivial. These two populations serve distinct functional roles in the generation of immune responses. cDCs were initially recognized as a functionally distinct class of cells for their ability to potently stimulate the mixed leukocyte reaction (MLR) (Steinman and Witmer 1978). Conversely, some macrophage subsets dampen proliferative responses via the production of suppressive cytokines (Gordon and Taylor 2005; Hashimoto et al. 2011). More notably, cDCs are uniquely equipped to efficiently process and present antigens to T cells to prime adaptive immune responses (Dudziak et al. 2007; Nussenzweig et al. 1980). Other APCs, including B cells and activated monoctyes, are only able to initiate T cell responses when provided significantly more antigen (Kamphorst et al. 2010). For example, naïve $CD8^{+}$ T cells that interact with virus-infected lymph node macrophages undergo limited proliferation and do not upregulate activation markers in contrast to more productive stimulation provided by lymph node cDCs (Hickman et al. 2011). Although they are inefficient at priming primary T cell responses, antigen presentation by macrophages may contribute to the re-

stimulation of activated or memory T cells (Aderem and Underhill 1999; Mellman et al. 1998). The inefficiencies of macrophage antigen presentation are most likely not due to a lack of antigen access because macrophages are highly phagocytic. Instead, antigen processing is excessively degradative in the highly acidic and proteolytic lysosome compartments characteristic of macrophages (Savina and Amigorena 2007; Trombetta and Mellman 2005). Conversely, the generation of adaptive immune responses with limiting antigen suggests cDCs are critical to priming T cell responses under physiological conditions. The unique ability of cDCs to potently stimulate immune responses clearly distinguishes them from closely related and phenotypically similar monocytes/macrophages.

This thesis outlines the identification and characterization of the cDC-restricted zinc finger transcription factor 'zDC.' This factor was found to be upregulated in pre-DCs and differentiated cDCs, but absent in other myeloid and lymphoid populations. In this way, zDC expression is more specific to the cDC lineage compared to other markers including CD11c (Figure 28). The subsequent characterization of zDC expression and function involved three directions: (1) the generation and description of zDC-DTR knock-in mice to provide a system in which cDCs can be specifically depleted, (2) the identification of zDC target genes by ChIP-seq, and (3) the generation and description of $zDC^{-/-}$ mice to appreciate zDC function *in vivo*.

Figure 28. zDC more specifically defines the cDC lineage compared to CD11c.

cDC commitment occurs in the bone marrow with the differentiation into pre-DCs from CDPs. The expression of zDC is concomitantly upregulated with the transition from CDP to pre-DC, and zDC expression is maintained in differentiated cDCs. Therefore, zDC provides a more reliable marker for the cDC lineage compared to CD11c, which is expressed by pDCs, Ly6C^{lo} monocytes, some macrophage subsets, and activated Ly6C^{hi} monocytes.

Figure 28

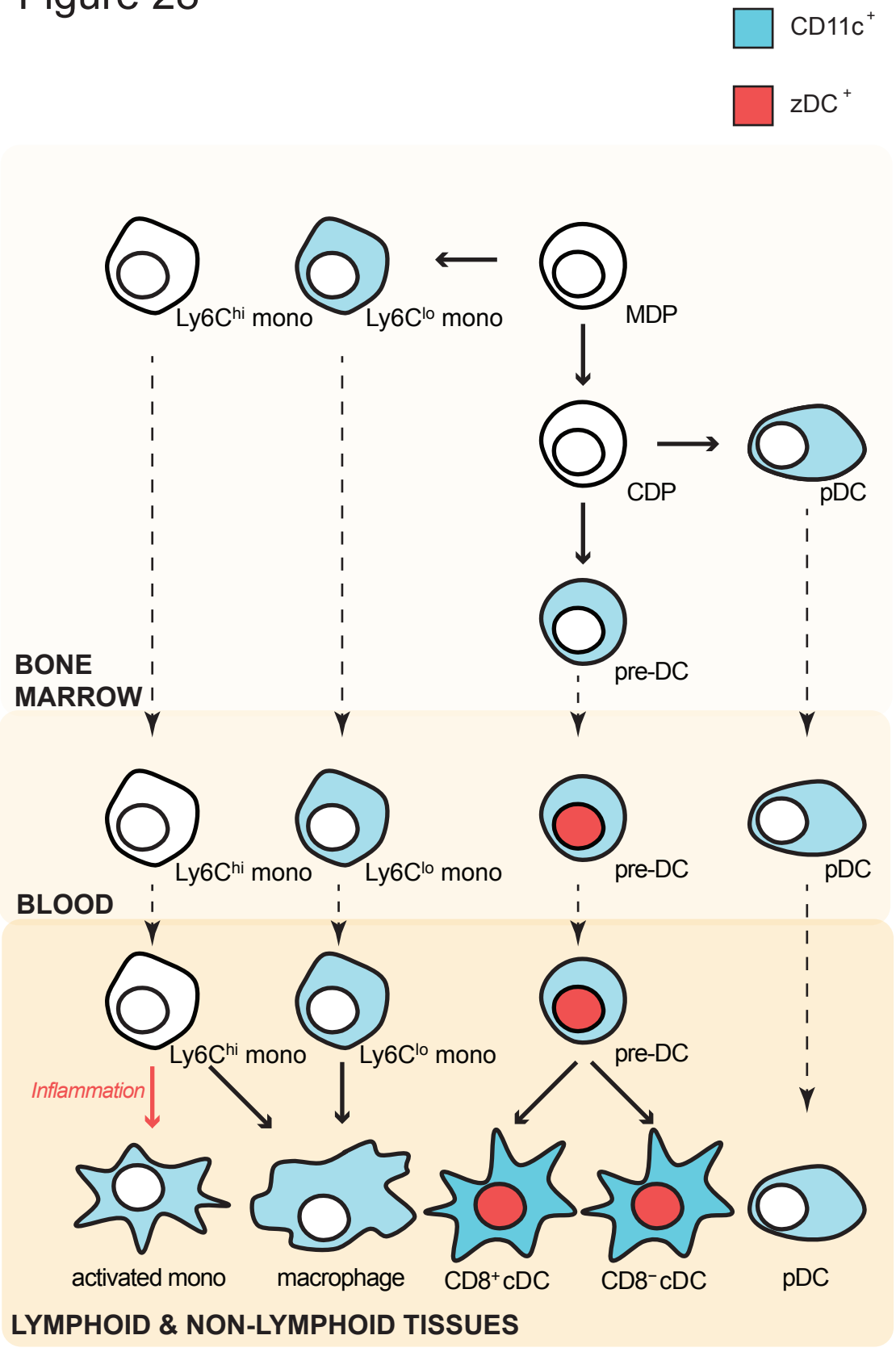
CD11c+
zDC+
Ly6Chi mono
Ly6Clo mono
MDP
CDP
pDC
pre-DC
BONE MARROW
Ly6Chi mono
Ly6Clo mono
pre-DC
pDC
BLOOD
Ly6Chi mono
Ly6Clo mono
pre-DC
Inflammation
activated mono
macrophage
CD8+ cDC
CD8− cDC
pDC
LYMPHOID & NON-LYMPHOID TISSUES

To identify a more reliable marker for the cDC lineage, I compared gene array data from populations representing various transitions during cDC development. To this end, I chose to enrich for genes that were upregulated with cDC commitment and expressed by both subsets of differentiated cDCs. Therefore, I first compared the expression of all gene probes between pre-DCs and monocytes. Because pre-DCs represent fully committed cDC precursors while monocytes do not demonstrate cDC potential (K. Liu et al. 2009), probes expressed at 10-fold or greater by pre-DCs were selected for subsequent analysis (Figure 2A). These pre-DC-upregulated probes were then compared in CDP and MDP progenitor populations. Because CDPs lack monocyte potential and are therefore one developmental 'step' closer to cDC differentiation relative to MDPs, I selected genes upregulated in CDPs. The transition from MDP to CDP involves fewer intermediates compared to the difference between pre-DCs and monoctyes (Figure 1). Therefore, probes upregulated in CDPs by two-fold or more were included for further characterization (Figure 2B). Finally, I compared the expression of these pre-DC- and CDP-enriched probes in differentiated $CD8^+$ and $CD4^+$ splenic cDCs. To select genes that would define both subsets of cDCs, gene probes which were expressed similarly by $CD8^+$ and $CD4^+$ cDCs (i.e. less than two-fold difference) were considered. This strategy identified the cDC marker CD11c in addition to an uncharacterized zinc finger transcription factor I call zDC (Zbtb46, Btbd4) (Figure 2C).

zDC belongs to a family of transcription factors known as bric-a-brac, tramtrack, and broadcomplex zinc finger (BTB-ZF) proteins. In the immune system, BTB-ZF transcription factors function as transcriptional repressors that regulate differentiation and activation (Beaulieu and Sant'Angelo 2011; Collins et al. 2001; Kelly and Daniel 2006). Lymphocyte development and function depend on the expression of multiple BTB-ZF factors including Bcl6, PLZF, ThPOK, PLZP, MARZ, BAZF, LRF and Miz. Bcl6 is a typical BTB-ZF transcriptional repressor that is required for germinal center B cell and follicular helper T cell development (Dent et al. 1997; Nurieva et al. 2009; Ye et al. 1997; Yu et al. 2009). Its effect on B cell differentiation is mediated in part through repression of Blimp-1, which is required for plasma cell development (Shaffer et al. 2000; Tunyaplin et al. 2004). Similarly, ThPOK is required for $CD4^+$ T cell lineage commitment and iNKT function (Engel et al. 2010; He et al. 2005). ThPOK-deficient thymocytes bearing TCRs that would normally become $CD4^+$ T cells or iNKT cells are instead diverted towards $CD8^+$ T cell commitment. This redirection is due to the loss of ThPOK-mediated repression of $CD8^+$ T cell determinants, including Runx3 (Beaulieu and Sant'Angelo 2011). On the other hand, the factor PLZP primarily modulates T cell proliferation and cytokine secretion following TCR stimulation (Piazza et al. 2004). PLZP-deficient $CD4^+$ T cells become hyperproliferative following TCR signaling and produce excessive IL-4, IL-5 and IL-13. Likewise, PLZP-deficient $CD8^+$ T cells hyperproliferate and produce more IFNγ. Although numerous BTB-ZF transcription factors are essential for lymphocyte development and function, less is known about what roles they play in myeloid cells.

zDC represents a BTB-ZF transcription factor which is uniquely expressed by pre-DCs and pre-DC-derived cDCs (Figure 3). Importantly, zDC is not expressed by steady state CD11c-expressing pDCs or monocytes/macrophages, and is not upregulated by activated monocytes. These phenotypically similar populations can therefore be better defined by the expression of zDC. zDC expression can be measured by multiple methods including gene array and Q-PCR for zDC transcription, western blot for protein expression, or flow cytometry for DTR reporter expression in zDC-DTR knock-in mice. Importantly, human ZDC is also restricted to cDCs among immune cells (Figure 4A), and can therefore provide a valuable marker for the on-going characterization of human cDC development and function.

zDC-DTR mice

The zDC locus provides an ideal promoter to drive the expression of reporters in cDCs. Therefore, to exploit this cDC-specific expression, I introduced DTR coding sequence into the 3'UTR of zDC to produce zDC-DTR knock-in mice (Figure 5A). In agreement with zDC mRNA and protein expression data, DTR expression was detectable by flow cytometry in $CD8^+$ and $CD4^+$ cDCs, but not pDCs, monocytes, or lymphocytes (Figure 6). Accordingly, DT injection selectively depleted differentiated pre-DCs and pre-DC-derived cDCs in lymphoid and non-lymphoid organs, but left other myeloid and lymphoid populations intact (Figures 8, 10, 11). Furthermore, cDC ablation in zDC-DTR mice is more

specific than currently available CD11c-DTR mice, in which multiple $CD11c^{+}$ myeloid and lymphoid populations can be heterogeneously ablated in addition to $CD11c^{hi}$ cDCs (Figure 11). Therefore, zDC-DTR mice provide a system with which to specifically interrogate cDC function *in vivo.*

However, DT injection in zDC-DTR knock-in mice revealed that zDC is expressed in some essential tissue because knock-in mice die within 24-48 hours following DT injection. Similarly, DT treatment in WT→zDC-DTR bone marrow chimeras also resulted in fatality within 24-48 hours, demonstrating that this vital population is radioresistant and not bone marrow-derived. Thus, although zDC expression is specific to cDCs within the immune system, this factor is also expressed by an undefined essential tissue. Therefore, similar to CD11c-DTR mice, long term experiments with zDC-DTR mice necessitate the production of zDC-DTR→WT bone marrow chimeras, which survive continued DT injection for two weeks (every 2-3 days to maintain cDC ablation) without noticeable side effects. For continuity, all experiments were performed with zDC-DTR bone marrow chimeras (20 ng DT per g bodyweight) alongside control WT (20 ng DT per g bodyweight) and CD11c-DTR bone marrow chimeras (4 ng DT per g bodyweight).

Direct comparison between DT treatment in zDC- and CD11c-DTR revealed both systems equivalently depleted pre-DCs and cDCs (Figure 10). However, CD11c-DTR further affected additional CD11c-expressing populations (Bennett and

Clausen 2007; Probst et al. 2005). Specifically, pDCs, NK cells, Ly6C^{lo} monocytes, activated Ly6C^{hi} monocytes, and multiple macrophage subsets were partially to completely depleted following DT treatment in CD11c-DTR, but are spared in zDC-DTR mice (Figures 11, 13, 14). All of these populations express at least low levels of CD11c, which can account for the activity of the CD11c promoter and consequent DTR expression by these populations in CD11c-DTR mice.

DT sensitivity of various CD11c^{+} populations in CD11c-DTR mice can complicate the interpretation of results obtained in these mice. Most notably, the difference between cDCs and monocytes/macrophages is not clear in CD11c-DTR mice due to heterogeneous expression of CD11c and varying DT sensitivity among monocyte and macrophage subsets. This distinction is critical considering the on-going confusion between these two lineages. For example, although the immune response to the parasite *Toxoplasma gondii* is critically impaired in DT-treated zDC- and CD11c-DTR mice, a significantly greater T_H1 response was generated in zDC-DTR mice compared to the nearly absent response (i.e. comparable to naïve controls) mounted by CD11c-DTR mice (Figure 16). This result confirms that cDCs are essential to prime these T cell responses, but further demonstrates that additional CD11c^{+} populations can less efficiently contribute to this process. There is substantial evidence that gut-resident CD103^{+} cDCs are essential for IL-12-dependent T_H1 responses to *T. gondii* (C. H. Liu et al. 2006; Mashayekhi et al. 2011). This scenario is consistent with the

reduction of T_H1 responses mounted by DT-treated zDC- and CD11c-DTR mice, both of which lack lamina propria $CD103^+$ cDCs.

However, the contributions of other myeloid populations during *T. gondii* infection are less defined. For example, monocyte-derived $CD11b^+$ DCs located in the intestinal lamina propria, the initial site of *T. gondii* infection, are intact in DT-treated zDC-DTR mice and conversely absent in DT-treated CD11c-DTR mice (Figure 10). These $CD11b^+$ DCs may be able to inefficiently prime T cell responses similar to other monocyte-derived APCs. For example, monocytes transferred into DT-treated CD11c-DTR mice are able to partially reconstitute OT II T cell proliferation in mesenteric lymph nodes when provided with high doses of OVA by gavage (Varol et al. 2009). Similarly, in addition to $CD103^+$ cDCs, peritoneal macrophages produce IL-12 within six hours of stimulation with *T. gondii* soluble tachyzoite antigen *in vitro* (Gazzinelli et al. 1994). Therefore, the minor T_H1 responses mounted by DT-treated, *T. gondii*-infected zDC-DTR mice could be coordinated by the monocyte-derived $CD11b^+$ DCs and macrophages, whereas these responses are absent in CD11c-DTR mice due to DT-sensitivity of these populations.

As a result of impaired T_H1-derived IFNγ responses, pathogen burden in both zDC- and CD11c-DTR mice was increased relative to wildtype controls. However, consistent with the generation of significantly more IFNγ-producing T_H1 $CD4^+$ T cells by zDC-DTR mice, zDC-DTR mice also demonstrated significantly

less tachyzoite burden compared to CD11c-DTR mice (Figure 16). Lower parasite load in zDC-DTR mice is likely the combined result of better T_H1 responses and the presence of macrophage populations. Macrophages are critical to the clearance of *T. gondii* tachyzoites, and IFNγ signaling increases nitric oxide production for enhanced tachyzoite killing (Aliberti 2005; Denkers 2003). Since CD11c-DTR mice fail to generate IFNγ-producing $CD4^+$ T cells and further lack multiple macrophage populations, these mice are unable to efficiently control parasite numbers.

In conclusion, zDC-DTR mice provide an alternative system in which cDC function can be more specifically interrogated. Conversely, CD11c-DTR mice also heterogeneously affect other $CD11c^+$ populations, most notably monocytes/macrophages, which can result in exaggerated conclusions regarding cDC function. For example, although *T. gondii*-induced IFNγ responses are significantly reduced in the absence of cDCs (zDC-DTR) or cDCs/macrophages (CD11c-DTR), a small but significant response is still mounted in mice lacking only cDCs (zDC-DTR) but not in mice lacking cDCs/macrophages (CD11c-DTR). Accordingly, parasite load is better controlled in mice lacking only cDCs (zDC-DTR) compared to the mice lacking both cDCs and macrophages (CD11c-DTR). Therefore, highly specific cDC ablation in zDC-DTR mice provides a means to more genuinely evaluate cDC function.

zDC target genes

To appreciate the effect of zDC on cDC gene expression, I identified its target genes in steady state cDCs by chromatin immunoprecipitation-sequencing (ChIP-seq). zDC-associated sequences mapped to regions upstream of transcription start sites (Figure 17A). These locations position zDC to interact with transcriptional machinery, where it serves primarily as a repressor of transcription similar to other BTB-ZF family members. zDC binds these regions at six-nucleotide TGACGT motifs (Figure 17 B-C), which is the expected footprint size of a transcription factor containing two C2H2 zinc finger domains (Bulyk et al. 2001). This motif was predicted by MEME analysis (Bailey et al. 2009) of the ChIP-seq library and confirmed by gel shift binding experiments between recombinant zDC and double-stranded DNA probes in gel shift assays. zDC bound DNA in a sequence-specific manner in that zDC bound DNA probe containing the MEME-predicted motif while no binding occurred with probe containing a mutated version of the motif. Therefore, zDC is a characteristic BTB-ZF that represses transcription of its target genes by binding upstream of transcription start sites at sequence-specific motifs.

zDC associated with the promoters of 1,309 genes in steady state splenic cDCs. Importantly, over 99% of these genes contained the zDC binding motif within one kilobase of the transcription start site. PANTHER Classification (Thomas et al. 2003) demonstrated these target genes belonged to diverse gene families (Figure 18). The largest group contained genes regulating gene expression,

including 150 transcription factors. This list included Stat3, which is critical for Flt3L-dependent cDC development and homeostasis. After transcription factors, a second large group were genes regulating protein post-translational modifications (PTMs), including multiple kinases, peptidases, ubiquitin ligases, and phophatases. The abundance of genes regulating gene expression and PTMs suggests zDC broadly influences the transcriptional and biochemical identity of cDCs.

zDC binding was most abundant on chromosome 17 within the region of the mouse MHC locus (Figure 19). In fact, the four classical MHC II genes expressed by C57BL/6 mice were occupied by zDC. The abundance of zDC binding within the MHC locus demonstrates it plays an important role in the regulation of cDC function. Specifically, zDC binding of MHC II genes acts as a repressor of steady state MHC II expression since $zDC^{-/-}$ cDCs express more MHC II in the steady state compared to wildtype littermates (Figure 23B). Analogously, cDC maturation via TLR stimulation results in rapid zDC protein degradation (Figure 23C). Therefore, zDC binding at MHC II promoters represses transcription, and the loss of zDC expression due to germline deletion or TLR stimulation consequently deregulates MHC II expression.

However, the mechanism of MHC II regulation by zDC is unclear. Although zDC motifs are located in the X2 box of MHC promoters, this position has been shown to be occupied by the MHC activator Creb1 (Handunnetthi et al. 2010; Krawczyk et al. 2008). This overlap suggests zDC and Creb1 compete for MHC promoter

binding. Furthermore, zDC also occupies the Creb1 promoter in steady state cDCs, and, accordingly, $zDC^{-/-}$ cDCs express higher Creb1 transcript levels than wildtype controls. Therefore, zDC may directly repress Creb1 expression by occupying its promoter, thus lowering Creb1 expression and allowing zDC to outcompete Creb1 for occupation of MHC II promoters in steady state cDCs. Following immune stimulation, zDC degradation would alleviate the competition for MHC binding, permitting Creb1 to freely associate with MHC promoters. This scenario is consistent with the kinetics of zDC downregulation within three hours of TLR stimulation (Figure 23C), and the short burst of MHC transcription that occurs during the first three to four hours following cDC maturation (Cella et al. 1997; Landmann et al. 2001). Further work is required to test whether zDC and Creb1 compete for MHC promoters, and whether this competition also occurs at other zDC target genes.

zDC knockout mice

To understand the role of zDC during cDC development and homeostasis, I generated a conditional knockout to produce zDC-deficient mice (Figure 20). cDC development does not depend on zDC expression, because cDC progenitors (MDPs, CDPs, and pre-DCs) were present at similar numbers in the bone marrow of zDC-deficient and wildtype littermates (Figure 21A). Likewise, total $CD11c^{hi}MHCII^{+}$ cDCs in the spleen and lymph nodes were present at normal frequencies (Figure 21 B-C). However, cDC subset composition in the spleen was altered such that $CD8^{+}$ and $CD4^{+}$ cDCs were present at similar

numbers in zDC-deficient mice in constrast to wildtype controls that contained these populations at a 1:3 ratio (Figure 21D). Therefore, although cDC development is not blocked by zDC deficiency, cDC subsets are altered by zDC deficiency such that the development or survival of $CD8^+$ cDCs is favored over $CD4^+$ cDCs.

BTB-ZF proteins are characteristically transcriptional repressors that block alternative lineage choices and limit lymphocyte activation (Beaulieu and Sant'Angelo 2011; Collins et al. 2001; Kelly and Daniel 2006). Like other BTB-ZF family members, zDC is primarily a transcriptional repressor since zDC-deficient cDCs upregulated many zDC target genes (Figure 22D). Moreover, global gene expression analysis demonstrated that steady state $zDC^{-/-}$ cDCs upregulated gene sets associated with TLR signaling and DC maturation (Figure 23A). Consistent with the expression of cDC maturation gene sets, MHC II expression was higher in steady state zDC-deficient cDCs compared to wildtype littermates (Figure 23B). Analogously, wildtype cDCs lack zDC protein during maturation. For example, within three hours of TLR stimulation, zDC protein cannot be detected in wildtype cDC lysates (Figure 23C). Therefore, upon immune stimulation, zDC protein is downregulated, removing transcriptional repression of its target genes. The upregulation of zDC target genes directly and indirectly results in the upregulation of maturation gene sets, including elevated MHC II expression. In this way, steady state zDC-deficient cDCs transcriptionally

resemble maturing wildtype cDCs. Thus, the repression of zDC target genes is necessary to prevent cDCs from undergoing maturation in the steady state.

Steady state cDCs promote tolerance for self and innocuous antigens, whereas activated cDCs prime adaptive immune responses. Tolerance in the steady state is maintained by instructing antigen-specific T cells to undergo deletion, anergy, or differentiation into regulatory T cells. For example, anti-DEC-205 targeting with OVA or hen egg lysozyme (HEL) in the steady state results in short-term proliferation of antigen-specific T cells (i.e. OVA-specific OT-I and OT-II, or HEL-specific 3A9) for about three days, followed by rapid deletion within seven or nine days after immunization (Dudziak et al. 2007; Hawiger et al. 2001). Deletion does not occur due to the loss of MHC:peptide complexes on cDCs because cDCs are able to present DEC-205-targeted antigen for up to 10 days after immunization (Dudziak et al. 2007), consistent with steady state cDC turnover every 10-14 days (K. Liu et al. 2007). Instead, deletion via bim-mediated apoptosis is a T cell-intrinsic default response following TCR signaling in the absence of co-stimulation (Davey et al. 2002; Steinman et al. 2003), similar to the deletion of auto-reactive thymocytes during T cell development (Bouillet et al. 2002). Conversely, immunization with adjuvants that stimulate cDC maturation impairs T cell deletion and proliferated T cells are detectable up to 20 days following immunization (Hawiger et al. 2001).

Consistent with the upregulation of maturation gene sets by zDC-deficient cDCs (Figure 23), the ability to delete responding OT-I T cells immunized with DEC-OVA was impaired in steady state zDC$^{-/-}$ mice. zDC-deficient mice maintained proliferated OT-I T cells two weeks after DEC-OVA immunization, whereas OT-I T cells were rare in wildtype controls by this time (Figure 25A). Importantly, these surviving OT-I T cells had proliferated as indicated by CFSE^{lo} fluorescence (Figure 25B), and thus did not represent naïve cells that had not received TCR signaling. Moreover, the surviving OT-I T cells isolated from zDC-deficient mice had acquired an effector phenotype indicated by the downregulation of CD62L (Figure 25C). In contrast, OT-I T cells from control unimmunized mice, as well as the few remaining OT-I T cells from wildtype DEC-OVA-immunized mice, remained CD62^{hi} naïve T cells. Therefore, antigen presentation by zDC-deficient steady state cDCs resulted in activation of OT-I T cells and impaired their subsequent deletion. This effect is consistent with the upregulation of maturation pathways by zDC-deficient cDCs.

Although zDC$^{-/-}$ mice demonstrate this break in peripheral tolerance, there was no indication of autoimmunity in these mice. zDC-deficient mice did not demonstrate aberrant steady state activation of endogenous CD4^{+} or CD8^{+} T cells, nor any change to Foxp3^{+} CD4^{+} regulatory T cell numbers. Similarly, there were no manifestations of autoimmune disease (proteinuria, glycosuria, weight loss) in zDC$^{-/-}$ mice aged for up to four months. Therefore, the steady state

activation of zDC-deficient cDCs is not sufficient to overcome other balances in the immune system, including central tolerance.

Similar to mice undergoing an immune response, zDC-deficient mice developed hyperplastic skin-draining lymph nodes (Figure 26). Lymph node enlargement was not the result of over accumulation of a single population, but instead involved the proportional expansion of B and T lymphocytes. Additionally, there was a small increase in mDC abundance (Figure 21C) reminiscent of increased mDC migration from the skin into skin-draining lymph nodes in response to inflammatory stimuli (Romani et al. 2010).

To accommodate adaptive immune responses in the skin-draining lymph nodes following immune stimulation, activated $CD11c^{+}$ DCs produce VEGF to induce lymph node vascularization and expansion (Webster et al. 2006; Wendland et al. 2011). Consistent with the enlargement of skin-draining lymph nodes isolated from $zDC^{-/-}$ mice, zDC-deficient $CD4^{+}$ cDCs expressed more *Vegfc* and total lymph node lysates contained elevated VEGF (Figure 27). Since *Vegfc* is not a direct target of zDC in the ChIP-seq library, the upregulation of VEGF is likely a downstream effect of cDC maturation due to zDC deficiency.

In summary, zDC serves a transcriptional repressor in steady state cDCs. Following stimulation, zDC protein is rapidly degraded which deregulates the repression of its target genes and results in cDC maturation. This process is

phenocopied in zDC-deficient cDCs, which express gene sets typically expressed in response to immune stimulation. As a result, $zDC^{-/-}$ mice are unable to maintain peripheral tolerance for steady state antigens and develop hyperplastic skin-draining lymph nodes. In these ways, zDC helps maintain cDCs from undergoing maturation in the steady state.

zDC is haploinsufficient, as indicated by altered cDC subset composition and elevated MHC II expression in $zDC^{+/-}$ heterozygotes (Figure 21). Mouse zDC dose dependence may be relevant to human disease since human ZDC expression is analogously cDC-restricted (Figure 4A). For example, a genome-wide association study identified single nucleotide polymorphisms (SNPs) on human chromosome 20q13, the locus containing the human ZDC gene, that are associated with pediatric-onset inflammatory bowel disease (IBD) (Kugathasan et al. 2008). Furthermore, colonic biopsies from IBD patients showed significantly increased ZDC transcript expression by gene array, suggesting altered ZDC expression can impact inflammatory disease. Although increased ZDC transcription associated with inflammatory disease is at first counterintuitive, the expression of ZDC mRNAs does not indicate normal ZDC function. For example, non-coding SNPs within the ZDC locus could produce splice variants that are sterile or encode protein truncations. Further work is necessary to address the effects of these SNPs on ZDC function, and to evaluate ZDC's role in IBD and other human inflammatory diseases.

Concluding remarks

The zinc finger transcription factor zDC provides a reliable marker for cDCs that is superior to the use of CD11c. zDC transcription is first upregulated in cDC-committed pre-DCs and is maintained in both steady state and activated cDCs. This additional parameter for the identification of cDCs will be useful in the on-going classification of mouse and human myeloid populations. zDC-DTR mice provide a reporter in which zDC expression can be detected by flow cytometry, and a system in which cDCs can be specifically ablated to interrogate cDC function. The generation of additional reporter mouse lines, including knock-in mice expressing brighter fluorescent proteins for flow cytometry analyses and *in vivo* imaging, or Cre recombinase for cDC-specific deletion of conditional knockout alleles, would be furter useful to appreciate cDC development and function.

In addition to its value as a reporter of the cDC lineage, zDC function is also critical to cDC homeostasis. zDC represses the transcription of its target genes and, in the absence of zDC-mediated repression in zDC-deficient or TLR-stimulated cDCs, these genes are upregulated and cDCs undergo maturation. Further work is necessary to understand the mechanism of zDC degradation and to determine which target gene or genes instigate cDC maturation. Most importantly, the possibility of human ZDC alleles influencing inflammatory diseases should be addressed to understand the potential role of cDCs in these diseases.

Chapter 7.

METHODS

Microarray. MDP, CDP, pre-DC, and monocytes were isolated from the bone marrow of C57BL/6 mice. $zDC^{-/-}$ cDCs were sorted from the spleens of Flt3L-treated mice. Total RNA extraction and hybridization on MOE-430 2.0 arrays (Affymetrix) were performed at Memorial Sloan-Kettering Cancer Center, New York, NY. Microarray data were analyzed using GeneSpring 10.0 software (Affymetrix). Triplicates of each population were collected and averaged in Genespring. Splenic B cell, T cell, and cDC array data were obtained previously (GEO accession: GSE6259 (Dudziak et al. 2007)).

Cell isolation. Myeloid progenitor (MP, $Lin^-(B220^-CD3^-NK1.1^-)CD11b^-CD11c^-Sca\text{-}1^-CD115^-Flt3^+CD117^{hi}$), macrophage and dendritic cell progenitor (MDP, $Lin^-CD11b^-CD11c^-Sca\text{-}1^-CD115^+Flt3^+CD117^{hi}$), common dendritic cell progenitor (CDP, $Lin^-CD11b^-CD11c^-Sca\text{-}1^-CD115^+Flt3^+CD117^{lo}$), and classical dendritic cell precursor (pre-DC, $Lin^-I\text{-}A/E^-CD11c^+Flt3^+CD172\alpha^{int}$) were sorted from bone marrow of C57BL/6 mice after MACS enrichment with Flt3-biotin and anti-biotin microbeads. Similarly, monocytes ($Lin^-CD11c^-Ly6G^-CD11b^+CD115^+Ly6C^{hi}$) were sorted from bone marrow of C57BL/6 mice after MACS enrichment with CD115-biotin and anti-biotin microbeads. $CD8^+$ classical dendritic cells ($CD8^+$ cDC, $Lin^-CD11c^{hi}I\text{-}A/E^{hi}CD8^+$), $CD11b^+$ cDC ($Lin^-CD11c^{hi}I\text{-}A/E^{hi}CD11b^+$), and plasmacytoid dendritic cells (pDC, $CD3^-CD19^-NK1.1^-CD11c^{int}B220^+$) were

sorted from spleen of C57BL/6 mice after MACS enrichment with CD11c microbeads.

Antibodies and other reagents. The following reagents were from BD Biosciences or eBioscience: anti-CD16-CD32 (2.4G2); anti-I-A/I-E (M5/114.15.2); anti-CD45R (RA3-6B2); anti-CD115 (AFS98); anti-Flt3 (A2F10); anti-CD3 (145-2C11); anti-CD4 (L3T4); anti-CD8 (53-6.7); anti-CD19 (1D3); anti-NK1.1 (PK136); anti-Ter119 (TER-119); anti-Sca-1 (D7); anti-CD11b (M1/70); anti-CD103 (2E7); anti-CD45.2 (104); anti-CD45.1 (A20); anti-CD14 (Sa2-8); anti-CD169 (MOMA-1); anti-F4/80 (BM8); anti-CD11c (N418); anti-CD172α (P84); anti-CD117 (2B8); anti-PDCA-1 (eBio927); anti-Ly6C (HK1.4); anti-Ly6G (1A8); and anti-IFNγ (XMG1.2). Anti-DEC-205 (NLDC145) was produced and kindly provided by C. Cheong. Biotin-conjugated anti-hDTR (hHB-EGF; R&D Systems) was used at a final concentration of 1μg/mL in PBS containing 2% FBS and 0.1% sodium azide, and streptavidin-PE (eBioscience) was used as a secondary.

BD Pharm Lyse lysing buffer, Cytoperm/Cytofix solution and Perm/Wash buffer were purchased from BD Biosciences. Anti-biotin, anti-CD11c, and anti-CD11b microbeads, and pDC isolation kit, were from Miltenyi Biotec. Other reagents included PBS, HBSS, FBS, ACK lysis buffer and EDTA (Gibco), Collagenase D (Roche) for spleen, skLN, mLN, lung and liver digestion (Ginhoux et al. 2009; K. Liu et al. 2009), and Collagenase VIII (Sigma) for small intestine digestion (Mucida et al. 2007).

Quantitative Real-time PCR. Total RNA was isolated from at least 5×10^4 FACS-sorted C57BL/6 primary cells with TRIzol (Invitrogen), from which cDNA libraries were reverse-transcribed using Superscript II (Invitrogen) and random primers. Murine zDC (Zbtb46) cDNA was amplified with primer located in exon 4 (forward: 5'-TCACATACTGGAGAGCGGC-3') and another in exon 5 (reverse: 5'-CCTCATCCTCATCCTCAACC-3'). Gapdh cDNA was also amplified to normalize zDC mRNA levels (forward: 5'-TGAAGCAGGCATCTGAGGG-3'; reverse: 5'-CGAAGGTGGAAGAGTGGGAG-3'). Murine Vegfc cDNA (forward: 5'-TGTGTCCAGCGTAGATGAGC-3'; reverse: 5'-TGGCATGCATTGAGTCTTTC-3') was also normalized to Gapdh cDNA. All quantitative PCR reactions were performed with Brilliant SYBR Green (Stratagene) on a Stratagene Mx3005P system.

Monoclonal antibody. Recombinant mouse zDC was produced as fusion protein to GST in BL21 competent cells (Promega) transformed with pGEX-6p-1 vector (GE Healthcare Life Sciences) containing the mouse zDC cDNA sequence. Glutathione sepharose beads and PreScission Protease (GE Healthcare Life Sciences) were used to purify zDC without the GST tag using the manufacturer's protocols.

Armenian hamsters were immunized with recombinant mouse zDC to produce specific antibodies by the Monoclonal Antibody Core Facility at Memorial Sloan

Kettering Cancer Center. Hybridomas were serially diluted and screened for zDC reactivity by ELISA. Antibodies were purified from hybridoma supernatants with Protein G (GE Healthcare).

Western blots. Whole cell or lymph node lysates were prepared by resuspension in RIPA buffer (50mM Tris-HCl, pH 8; 300mM NaCl; 1mM EDTA; 1% NaDOC; 0.2% SDS; 2% NP-40; 1mM DTT; 0.5mM PMSF) and sonication for 15 minutes on the high setting of a Diagenode Biorupter. Antibodies for western blots were purchased from the following: Armenian hamster anti-zDC (produced by hybridomas and purified with protein G sepharose (GE Healthcare)), rabbit anti-Histone H4 (Abcam), rabbit anti-VEGF (Abcam), mouse anti-β-actin (Merck), anti-Armenian hamster HRP (Jackson Immunoresearch), anti-rabbit HRP (Jackson Immunoresearch), anti-mouse HRP (Jackson Immunoresearch).

Dendrogram. Mouse (NP_081932.1), rat (NP_001101278.1), human (NP_079500.2), chimpanzee (XP_003317118.1), macaque (XP_001084247.1), cow (NP_001179093.1), chicken (XP_417431.2), frog (NP_001087165.1), zebra fish (XP_699124.4), and pufferfish (CAG11269.1) protein sequences were aligned and assembled into a neighbor joining tree using MacVector software.

Mice. zDC-DTR knockin mice were generated by homologous recombination in C57BL/6 albino embryonic stem (ES) cells at The Rockefeller University Gene Targeting Resource Center and maintained on a C57BL/6 background. The

targeting construct, assembled by PCR and cloning, consisted of two arms of homology—one 1.97 kb fragment spanning intron 4 up to the stop codon located in exon 5, and a second 8.25 kb fragment containing the 3'UTR of exon 5 and intergenic sequence—introduced into the pCON-ACN vector.

$zDC^{lox/lox}$ mice were produced by homologous recombination in C57BL/6 albino ES cells at The Rockefeller University Gene Targeting Resource Center and maintained on a C57BL/6 background. The targeting construct was assembled by traditional PCR and cloning of a 1.7 kb short arm within intron 1 (640 bp upstream of exon 2) and 5.9 kb long arm within intron 2 (520 bp downstream of exon 2) into a pCON-DTA vector to insert loxP sites flanking exon 2.

C57BL/6, C57BL/6.SJL, and CD11c-DTR mice were purchased from Jackson Laboratory. Bone marrow chimeras were reconstituted for at least 8-10 weeks after lethal irradiation (two doses of 525rad, three hours apart) and i.v. transfer of $5\text{-}10\times10^6$ bone marrow cells. $zDC^{+/DTR}$ and CD11c-DTR hemizygous mice were bred at The Rockefeller University for use in experiments and as bone marrow donors. C57BL/6 mice purchased from Jackson Laboratory were used as controls in experiments and as control bone marrow donors. All mice were housed in The Rockefeller University Comparative Bioscience Center under Specific Pathogen Free conditions. All experiments were performed in accordance with National Institutes of Health guidelines and approved by The Rockefeller University Animal Care and Use Committee.

Diptheria toxin. Diphteria toxin was purchased from Sigma. Importantly, every new batch of DT was titrated in zDC-DTR mice to determine the lowest effective dose due to variability between batches. For transient DT ablation, C57BL/6 (WT) and zDC-DTR bone marrow chimeras were injected i.p. with 20ng DT per g bodyweight, whereas CD11c-DTR bone marrow chimeras received 4ng DT per g. Mice were euthanized 12-24 hours after DT injection for analysis. To maintain DT ablation, mice received 4ng DT per g bodyweight on the third day after the initial DT injection and every third day thereafter.

Listeria monocytogenes. WT, zDC-DTR, and CD11c-DTR bone marrow chimeras were infected i.v. with 5×10^4 *L. monocytogenes* CFU and injected with DT i.p. 24-48 hours after infection. Spleens were collected 12 hours after DT injection and the abundance of $CD11b^+Ly6C^+CD11c^+MHCII^+$ activated monocytes was determined by flow cytometry.

Immunofluorescent staining. Tissues were fixed in 3% PFA/25% sucrose overnight, frozen in O.C.T Compound (Tissue-Tek,Sakura) and stored at -80°C. Frozen tissue was cut into 20µm thick sections, fixed for 10 minutes in ice-cold acetone and rehydrated in PBS for 30 minutes. Tissue sections were outlined with a Pap pen and stained for 2 hours at room temperature in 1% FCS in PBS. Antibody cocktail contained anti-CD16/CD32 blocking Ab (2.4G2, 1:100, BD Bioscience), FITC anti-CD45R/B220 (RA3-6B2, 1:200, BD Bioscience), and

either APC anti-F4/80 (BM8,1:100, eBioscience) or Alexa647 anti-CD169 (MOMA-1, 1:100, AbD Serotec). Sections were washed for 10 minutes 3× and mounted using ProLong Gold Antifade Reagent with DAPI (Invitrogen). Images were acquired on a wide-field fluorescent microscope (Zeiss) using MetaVue acquisition software (Molecular Devices) and a Hamamatsue Orca ER B/W digital camera, at the Rockefeller University Bio-Imaging Resource Center.

OT-I and OT-II proliferation *in vivo*. 2-5×10^6 CD45.1$^+$ OT-I and OT-II cells purified with CD8$^+$ T cell and CD4$^+$ T cell isolation kits (Miltenyi), respectively, were labeled with 2μM CFSE for 10 min at 37°C and transferred i.v. into CD45.2$^+$ WT, zDC-DTR, and CD11c-DTR bone marrow chimeras. The mice were treated with DT 24 hours after T cell transfer, and received 20μg LPS-free soluble OVA (Sigma) i.v. another 24 hours after DT treatment. Three days after OVA immunization, spleens and skin draining lymph nodes were collected to analyze CFSE dilution of transferred CD45.1$^+$ OT-I and OT-II cells by flow cytometry.

Mixed leukocyte reaction. 5×10^5 bulk CD45.2$^+$ C57BL/6 splenocytes from DT-treated WT, zDC-DTR, and CD11c-DTR bone marrow chimeras were co-cultured in complete RPMI with 5×10^4 CFSE-labeled T cells isolated by negative selection with Dynabeads (Invitrogen) from CD45.1$^+$ BALB/c mice. CFSE dilution due to proliferation of BALB/c T cells was measured by flow cytometry after 5 days *in vitro*. Bulk CD45.2$^+$ C57BL/6 splenocytes were lethally irradiated (1000rad) prior to co-culture.

Toxoplasma gondii. Twenty-four hours after DT treatment, WT, zDC-DTR, and CD11c-DTR bone marrow chimeras were infected with 15 *T. gondii* cysts by gavage in whole brain lysates from *T. gondii*-infected mice. During the course of infection, mice received DT every third day to maintain ablation.

After eight days of infection, the mesenteric lymph nodes and spleens of the infected mice were collected for analysis. Single cell suspensions were restimulated at 10^7 cells/mL *in vitro* with 50ng/mL PMA and 500ng/mL ionomycin (Sigma) and GolgiStop (BD Biosciences) in complete RPMI for 5 hours, and the proportion of $CD4^+$ T cells producing IFNγ was determined by ICS.

For *T. gondii* pathogen quantification, whole lung was homogenized in TRIzol (Invitrogen) to extract RNA for cDNA synthesis as described earlier. SAG2 levels were quantified by RT-PCR (Subauste and Remington 2001) and normalized to Gapdh.

ChIP-seq. 30 x 10^6 MACS-purified cDC (CD3, CD19, NK1.1, Gr1, CD45R-depleted, followed by CD11c enrichment) and B cells (CD43, CD11c-depleted, followed by CD19 enrichment) were isolated from Flt3L-injected and naïve C57BL/6 mice, respectively. Both populations were confirmed >95% by flow cytometry . Protein and DNA were crosslinked [fixed with 1% formaldehyde in PBS for 10 minutes at 37°C, and quenched with 125mM glycine] and genomic

DNA was sheared to 200-1000bp fragments [sonicated for 15 minutes at 4°C in RIPA buffer (50mM Tris-HCl, pH 8; 300mM NaCl; 1mM EDTA; 1% NaDOC; 0.2% SDS; 2% NP-40; 1mM DTT; 0.5mM PMSF) on the high setting of a Diagenode Biorupter]. Cell lysates were incubated overnight at 4°C while rocking with affinity-purified rabbit anti-mouse 'zDC exon 2 peptide' polyclonal antibody (peptide synthesis by The Rockefeller University Proteomics Resource Center, and immunization by Covance) conjugated to protein A Dynabeads (Invitrogen). The beads were washed rigorously [twice with RIPA buffer, twice with RIPA buffer + 0.2 M NaCl, twice with LiCl buffer (0.25M LiCl + 0.5% NP-40 + 0.5% NaDOC), once with TE buffer + 0.2% Triton X-100, and once with TE buffer], and protein was digested with 1mg/mL Proteinase K and 0.3% SDS in TE for 4 hours at 65°C. ChIP DNA was then isolated by phenol/chloroform extraction and ethanol precipitation. The purified DNA was resuspended in TE buffer and sequenced on an Illumina Genome Analyzer II.

zDC protein production and purification. Recombinant zDC was produced as fusion protein to GST in BL21 competent cells (Promega) transformed with pGEX-6p-1 vector (GE Healthcare Life Sciences) containing the mouse zDC cDNA sequence. Glutathione sepharose beads and PreScission Protease (GE Healthcare Life Sciences) were used to purify zDC without the GST tag using the manufacturer's protocols. GST control protein was purified from cells transformed with empty vector.

Gel shift assay. Double-stranded DNA probes containing the MEME-predicted motif (5'-ACGCGGT**GATGACGTCA**GGAGCCGCAA-3') and mutated motif (5'-ACGCGGT**ccattaaagc**GGAGCCGCAA-3') were labeled with γ-^{32}P ATP by T4 polynucleotidekinase (NEB). Binding reactions between labeled probes and recombinant zDC or GST control were performed in assay buffer [2mM TrisCl, pH 7.9; 10mM KCl; 0.02mM EDTA; 2% glycerol; 0.25mg/mL BSA; 1mM DTT; 0.1% NP40; 1mM PMSF] at 30°C for 30 minutes, run on 5% polyacrylamide gel, and exposed to photographic film overnight at -80℃.

TLR agonists. 30μg Poly I:C (Invitrogen), 50μg LPS serotype 0111:B4 (Sigma), or 20μg 1826 CpG plus 15% DOTAP (Roche) in PBS were injected i.v. Three hours after injection, mice were euthanized and the spleen DCs were enriched with CD11c beads (Miltenyi) for analysis by western blot.

OT-I deletion. OT-I T cells were isolated from CD45.1$^+$ OT-I mice using CD8+ T cell negative selection (Milyteni) and were labeled with 2μM CFSE (Molecular Probes). Each mouse received 1-2×10^6 CFSE-labeled OT-I T cells i.v., and 3μg DEC-OVA i.p. or footpad s.c. 12-18 hours after OT-I transfer. Two weeks after DEC-OVA immunization, the amount of CD8$^+$CD45.1$^+$Vα2$^+$ OT-I cells in the spleen were quantified by flow cytometry.

APPENDIX I. Total zDC target genes

AA543186	Arl6ip5	Bdp1	Cd74	Cox19	Dennd4b
AA987161	Arpc3	Bet1	Cd83	Cradd	Dgat1
Aaas	Arrb2	Bicd2	Cd86	Creb1	Dgcr14
Aamp	Arrdc2	Birc2	Cd97	Crem	Dguok
Aasdh	Arrdc3	Birc3	Cdadc1	Crkrs	Dhdds
Abce1	Ascc3	Birc6	Cdc2l1	Crlf2	Dhrs9
Abcf1	Ate1	Braf	Cdc2l5	Cry1	Dhx33
Abcf2	Atf3	Brca1	Cdc34	Cryzl1	Dhx40
Abhd11	Atf4	Brca2	Cdc42	Csde1	Diablo
Abt1	Atf6	Brd2	Cdc42bpb	Cse1l	Dimt1
Acbd5	Atf6b	Brd4	Cdc5l	Csf2ra	Dip2b
Aco2	Atg16l1	Bre	Cdc6	Csnk1g2	Dleu2
Acot2	Atg16l2	Brms1	Cdk2ap2	Cspp1	Dnajb12
Acox3	Atg5	Brpf1	Cdkl3	Csrnp1	Dnajb14
Actb	Atg7	Btaf1	Cdkn1a	Cst3	Dnajb2
Adam9	Atp13a3	Btbd1	Cdkn1b	Cstf1	Dnajc30
Adar	Atp2b1	Btbd6	Cdv3	Cstf2t	Dnttip1
Adipor2	Atp5d	Btbd9	Cebpb	Cstf3	Dnttip2
Adpgk	Atp5o	Btg1	Cenpp	Ctcf	Dok1
Aff1	Atp6v0a1	Btg2	Cenpq	Ctdp1	Dom3z
Aff4	Atp6v0c	Btla	Cep120	Ctnna1	Dot1l
Aftph	Atp9b	Bub1	Chd2	Ctsc	Dph1
Ahcyl1	Atpaf2	C1d	Chmp1b	Cul1	Dpm1
Al413782	Atrip	C230035I16Rik	Chmp4b	Cxcl9	Dscr3
Aldoa	Atxn1l	Calm3	Churc1	Cxxc1	Dtl
Alg9	Atxn2l	Casc3	Ciao1	Cyb5r3	Dullard
Ambra1	Atxn7l3	Casp8	Ciapin1	Cytip	Dus1l
Amn1	Azin1	Cbwd1	Cisd2	D16Ertd472e	Dus4l
Amz2	B4galt5	Ccbl1	Clcn3	D17Wsu92e	Dusp1
Anapc11	Banp	Ccdc101	Clcn4-2	D430020J02Rik	Dusp16
Ankrd11	Bap1	Ccdc124	Clec16a	D4Wsu53e	Dusp2
Ankrd13c	Bat1a	Ccdc134	Clec2i	D8Ertd738e	Dusp5
Ankrd17	Bat2	Ccdc19	Clec4a2	Dad1	Dyrk1a
Antxr2	Bat2d	Ccdc44	Clec9a	Dars2	E330016A19Rik
Ap1g1	Bat3	Ccdc45	Clic4	Dazap1	E4f1
Ap1s3	Bat5	Ccdc49	Clpb	Dazap2	Eapp
Ap2b1	Baz1b	Ccdc59	Clptm1l	Dbnl	Ecd
Ap2m1	Baz2a	Ccdc86	Cmas	Dcaf11	Ece1
Ap3m1	BC005537	Ccdc9	Cnbp	Dctn5	Eed
Apaf1	BC005624	Ccdc94	Cno	Ddx19b	Eftud2
Apbb1ip	BC013712	Ccnd3	Cnot1	Ddx23	EG547347
Apob48r	BC022687	Ccnh	Cnot10	Ddx27	Egr3
Appbp2	BC023814	Ccni	Cnot3	Ddx42	Ehd1
Aptx	BC031181	Ccnl1	Cnpy3	Ddx5	Eif1
Arf2	BC031781	Ccnt1	Cope	Ddx50	Eif2b1
Arhgdia	BC051142	Ccr1	Cops4	Ddx51	Eif2s1
Arid3a	Bcl2a1d	Ccr5	Cops8	Ddx54	Eif5a
Arih1	Bcl2l13	Ccrl2	Coq10b	Ddx55	Elk4
Arih2	Bcl2l2	Cd53	Coq2	Deb1	Ell
Arl5a	Bclaf1	Cd68	Cox18	Dennd4a	Ell2

APPENDIX I (ii). Total zDC target genes

Elmod2	Galnt11	H2-K1	Hspa8	Kdm6b	Map3k7
Elovl5	Gan	H2-M3	Htra2	Khsrp	Mapk3
Emg1	Gar1	H2-Ob	Htt	Kif11	Mapk8
Emp3	Gas5	H2-Q7	Idh3b	Kif2a	Mapkapk5
Enthd1	Gatc	H2afz	Ier2	Kif2c	Mapre1
Entpd6	Gga1	H3f3b	Ier5	Klf13	Mark2
Eprs	Gk5	Haus5	Ifitm2	Klf2	Mastl
Erlin1	Gle1	Haus8	Ifnar1	Klf4	Mat2a
Erp29	Glod4	Havcr2	Ifngr1	Klf6	Matr3
Errfi1	Gls	Hbp1	Ifngr2	Klhdc4	Mbd3
Esco1	Gm11202	Hbs1l	Ifrd1	Klhl12	Mbip
Esrra	Gm14005	Hdgf	Ift172	Klhl17	Mcl1
Esyt2	Gm2a	Hdgfrp2	Ikbkap	Klhl7	Mdn1
Etohd2	Gm6377	Hdlbp	Ikbkb	Klrk1	Mecr
Etv3	Gm6534	Heca	Il1b	Kpna4	Med13
Etv6	Gmeb2	Hexdc	Il1r2	Kptn	Med14
Evi2b	Gna11	Hexim1	Il6	Kras	Med20
Exd1	Gnas	Hexim2	Il6ra	Lancl2	Med27
F630110N24Rik	Gnb2l1	Hgs	Ilf3	Laptm5	Med29
Faf1	Golga1	Hiatl1	Impdh2	Larp4	Med31
Fahd2a	Gosr2	Hinfp	Ing3	Larp7	Med6
Fam100a	Gpam	Hint3	Ing4	Lasp1	Med9
Fam122a	Gpbp1	Hist1h1c	Ino80	Lats2	Mef2d
Fam18b	Gpd2	Hist1h1d	Inpp5k	Lcmt2	Mepce
Fam36a	Gpn3	Hist1h2bc	Ints12	Leng8	Mettl1
Fam49b	Gpr132	Hist1h2bh	Ints6	Letm2	Mib2
Fam82a2	Gpr55	Hist1h2bj	Ipo11	Lias	Midn
Fancd2	Gpr65	Hist1h3d	Irf2	Limk1	Mir142
Fastkd5	Gpx1	Hist1h3e	Irf2bp2	Lin54	Mir21
Fau	Grasp	Hist1h4a	Irgq	Lmbr1	Mir212
Fbxo33	Gsk3a	Hist1h4h	Isca2	Lmbr1l	Mir22
Fbxo34	Gtf2a1	Hist2h4	Iscu	Lmbrd1	Mir339
Fbxw4	Gtf2f1	Hivep2	Isy1	Lmna	Mkks
Fcho2	Gtf2h5	Hmg20a	Itga4	Lonp1	Mlec
Fdxacb1	Gtf3c2	Hmga1	Ivns1abp	Lrrc14	Mlf2
Fkbp2	Gtf3c6	Hmga1-rs1	Jdp2	Lrrc8c	Mlst8
Fkbpl	Gtpbp10	Hmgcl	Jmjd5	Lrrc8d	Mmab
Fmc1	Gtpbp2	Hnrnpa2b1	Josd1	Lsm2	Mms19
Fndc7	Guf1	Hnrnpa3	Josd2	Lsm4	Mnt
Fos	Guk1	Hnrnpc	Jtb	Lsp1	Morf4l1
Fosb	Gusb	Hnrnpl	Jun	Luc7l2	Mpdu1
Foxk2	H2-Aa	Homer1	Junb	Lyrm7	Mpeg1
Foxo3	H2-Ab1	Hpgds	Jund	Maff	Mrm1
Fuz	H2-D1	Hps4	Kat2b	Mafk	Mrpl1
Fxr2	H2-DMa	Hps5	Katnb1	Magoh	Mrpl17
Fyco1	H2-DMb1	Hspa14	Kctd12	Magohb	Mrpl2
Fzr1	H2-DMb2	Hspa1a	Kctd20	Malat1	Mrpl20
G3bp2	H2-Eb1	Hspa2	Kdm2a	Map3k1	Mrpl34
Gabarap	H2-Eb2	Hspa4	Kdm2b	Map3k11	Mrpl4
Galk2	H2-gs10	Hspa5	Kdm5a	Map3k2	Mrpl41

APPENDIX I (iii). Total zDC target genes

Mrps17	Nlrp3	Pdcd10	Ppfia1	Pxmp4	Rg9mtd2
Mrps23	Nme1	Pdcd5	Ppig	Qpctl	Rgl2
Mrps27	Nol10	Pdcd7	Ppil4	Qrich1	Rgs1
Mrrf	Nolc1	Pdlim5	Ppme1	Qtrtd1	Rgs2
Mtap4	Nr4a1	Pef1	Ppp1r10	Rab1	Rhbdd3
Mthfsd	Nr4a2	Peli1	Ppp1r15a	Rab11a	Rheb
Mtmr15	Nrbf2	Pelp1	Ppp1r15b	Rab11b	Rhoa
Mul1	Nrd1	Per1	Ppp2ca	Rab11fip1	Rhoq
Muted	Nsmce2	Pet117	Ppp2r5a	Rab33b	Rilpl2
Mvd	Nsmce4a	Pex3	Ppp4c	Rab3a	Rin3
Myl6b	Nsun6	Pfas	Ppp6c	Rab3gap1	Ring1
Mylip	Nt5c2	Pfdn2	Ppwd1	Rab43	Riok1
Mynn	Nt5dc3	Pfkfb3	Prcc	Rab5a	Rmrp
Myo1c	Ntan1	Phf15	Prcp	Rab6	Rnasek
Myo1g	Nub1	Phf20l1	Prdm4	Rab7l1	Rnf139
Myst2	Nubp2	Phf23	Prdx5	Rab8a	Rnf141
Nab2	Nubpl	Phospho2	Prdx6	Rabepk	Rnf166
Nacc1	Nudt19	Pi4k2a	Preb	Rabggta	Rnf167
Nadk	Nudt6	Picalm	Prex1	Rabl3	Rnf170
Napa	Nufip1	Pigg	Prkacb	Rad17	Rnf34
Nat10	Nufip2	Pigl	Prkag1	Rad51c	Rnf44
Nat11	Nup133	Pik3cg	Prkar2a	Raf1	Rnps1
Nat6	Nup153	Pim1	Prkce	Ralgapa1	Rnu11
Nbeal1	Nup155	Pip5k1a	Prkrip1	Ranbp2	Rnu7
Ncbp2	Nup214	Pip5k1c	Prmt7	Ranbp6	Rock1
Ndel1	Nup54	Pitpna	Prpf38a	Rap1b	Rod1
Ndufa10	Nup98	Pja2	Prpf4	Rap2a	Rpl21
Ndufa13	Nupl1	Pkn1	Prr3	Rapgef6	Rpl22
Ndufa5	Oaz1	Pknox1	Prss43	Rasal2	Rpl23
Ndufb6	Obfc2a	Pla2g15	Pskh1	Rasip1	Rpl27
Ndufb9	Ocel1	Pla2g6	Psma1	Rbm14	Rpl3
Ndufs1	Ogdh	Plaa	Psmb2	Rbm15	Rpl34
Ndufs3	Opa3	Plbd2	Psmb8	Rbm22	Rpl37
Ndufs7	Ormdl3	Plek	Psmd3	Rbm3	Rplp0
Ndufv1	Osbpl8	Plekhf2	Psme2	Rbm39	Rplp2
Neat1	Otud6b	Plekhg2	Psme3	Rbm42	Rprd2
Necap1	P2rx4	Plekho2	Psmg4	Rbm5	Rps19
Nek1	P2ry10	Pmaip1	Ptbp1	Rbm7	Rps26
Nek8	P2ry14	Pmvk	Ptcd1	Rbm8a	Rps29
Nfatc3	P4hb	Pnpla8	Pten	Rbms2	Rps3
Nfil3	Pabpc1	Pnpo	Ptgr2	Rccd1	Rps6ka5
Nfkb2	Pacrgl	Pnrc1	Ptma	Rce1	Rps6kb2
Nfkbib	Pafah1b1	Pogz	Ptp4a1	Rdbp	Rps9
Nfkbid	Pak1ip1	Polb	Ptp4a2	Rel	Rpusd2
Nfkbie	Palb2	Polg2	Ptpn11	Relb	Rraga
Nfx1	Parp8	Polk	Ptprc	Rfc1	Rrm1
Nfyc	Pcbp2	Polr2a	Ptprj	Rfc4	Rrp1
Nhej1	Pcf11	Pomt1	Pura	Rft1	Rrp1b
Nhp2l1	Pcna	Pop7	Purb	Rfx1	Rsbn1
Nipa2	Pcnp	Por	Pus10	Rfx7	Rsf1

APPENDIX I (iv). Total zDC target genes

Runx1	Slc35e1	Ssr4	Tgif1	Trim39	Uqcrq
Rwdd1	Slc38a1	Sssca1	Tgoln2	Trim65	Use1
S100pbp	Slc38a2	Ssu72	Thap6	Trim8	Usf1
Safb2	Slc39a13	Stag1	Thoc1	Trmt12	Uso1
Sap30bp	Slc3a2	Stap1	Thrap3	Trmt2a	Usp12
Sass6	Slc41a1	Stat3	Thumpd1	Trmt5	Usp28
Sbds	Slc43a2	Stk11	Tifab	Trmt61a	Usp36
Scaf1	Slc44a1	Stk16	Timm44	Trmt61b	Usp38
Scfd2	Slc7a5	Stk38l	Tinf2	Trpm7	Usp42
Sclt1	Smchd1	Stoml2	Tle3	Trpv2	Usp48
Scrn3	Smek1	Strap	Tlr6	Trub2	Usp52
Scyl2	Smg7	Stt3a	Tmbim4	Tsc22d2	Usp8
Sdccag8	Smndc1	Stx12	Tmem107	Tssc4	Utp15
Sec16a	Smu1	Stx16	Tmem109	Ttc1	Utp3
Sec22b	Snapc1	Sugt1	Tmem123	Ttc5	Uvrag
Sec31a	Snapc5	Sumo2	Tmem147	Ttll5	Vamp1
Secisbp2	Snora78	Supt4h1	Tmem167b	Tuba1a	Vamp3
Senp2	Snord49b	Supv3l1	Tmem183a	Tuba1c	Vamp4
Senp3	Snrnp27	Surf4	Tmem203	Tubb6	Vasp
Senp5	Snrnp40	Surf6	Tmem206	Tubgcp6	Vav3
Sept7	Snrnp70	Syf2	Tmem209	Tulp4	Vcpip1
Serinc3	Snrpc	Synj1	Tmem39a	Twistnb	Vprbp
Sertad2	Snrpg	Tacc1	Tmem49	Txndc11	Vps18
Sertad3	Snx11	Taf11	Tmem66	Txnl4b	Vps26a
Sesn2	Snx14	Taf13	Tmem69	U2af1	Vps28
Sestd1	Snx15	Taf3	Tmem97	Uba52	Vps37a
Setd1a	Snx17	Taf5l	Tmtc2	Uba6	Vps37b
Sf1	Snx18	Tank	Tmub2	Ubap2l	Vps4b
Sf3b5	Snx20	Tap1	Tnf	Ubc	Vps52
Sfrs1	Socs4	Tarbp2	Tnfaip1	Ube2h	Vps72
Sfrs11	Socs5	Tatdn2	Tnfaip3	Ube2j1	Wbp11
Sfrs5	Sos1	Tbc1d15	Tnfrsf1a	Ube2n	Wbp2
Sgk3	Sp1	Tbc1d17	Tnni2	Ube2q1	Wdfy2
Sh2b3	Spag9	Tbc1d23	Tnrc6b	Ube2s	Wdr12
Sh3gl1	Spcs3	Tbc1d7	Tob2	Ube2v1	Wdr4
Sh3glb1	Spen	Tbc1d9	Tom1l2	Ube3c	Wdr43
Siah2	Sphk2	Tbck	Tomm6	Ube4a	Wdr45l
Sik1	Spop	Tbl2	Tor1aip1	Ubl3	Wdr53
Sik2	Sptlc1	Tbl3	Tpp2	Ubn2	Wdr5b
Sik3	Spty2d1	Tbp	Tpr	Ubp1	Wdr61
Sike1	Sqstm1	Tbrg4	Tpt1	Ubr4	Wdr67
Siva1	Srgap2	Tcf25	Tra2a	Ubxn2a	Wdr70
Skap2	Srgn	Tcf3	Traf1	Ubxn4	Wdr74
Skil	Srp19	Tes	Traf4	Uchl5	Wdr75
Slc15a3	Srp9	Tesk1	Trafd1	Ucp2	Wdr90
Slc16a6	Srpr	Tet2	Trak2	Uhrf1bp1l	Whsc2
Slc25a16	Srrm1	Tex2	Trap1	Unc13a	Wsb1
Slc25a3	Srrm2	Tfip11	Trib1	Unc84b	Xab2
Slc25a37	Ssbp4	Tgfb1	Trim12	Unk	Xcr1
Slc35b1	Ssna1	Tgfbrap1	Trim35	Uqcrfs1	Xpnpep3

APPENDIX I (v). Total zDC target genes

Xrcc6	Zscan21	6430531B16Rik
Xrn2	Zswim6	6820431F20Rik
Yars2	Zswim7	9130023H24Rik
Yeats2	Zzef1	9530068E07Rik
Yipf6	0610010K14Rik	A230051G13Rik
Ypel5	0610011L14Rik	A430005L14Rik
Ywhag	0610040B10Rik	A530054K11Rik
Ywhaz	1110003E01Rik	A630001G21Rik
Yy1	1110004E09Rik	A730011L01Rik
Zbtb11	1110014N23Rik	
Zbtb7a	1110038B12Rik	
Zc3h10	1110049F12Rik	
Zc3h12a	1110059G10Rik	
Zc3h13	1300018I05Rik	
Zc3h18	1500010J02Rik	
Zc3h3	1700012B15Rik	
Zc3hav1	1700020C11Rik	
Zcchc11	2010106G01Rik	
Zcchc2	2010321M09Rik	
Zdhhc3	2210018M11Rik	
Zer1	2310001A20Rik	
Zfand2a	2310033P09Rik	
Zfand5	2310035K24Rik	
Zfat	2310044H10Rik	
Zfc3h1	2410001C21Rik	
Zfp1	2510012J08Rik	
Zfp143	2610027L16Rik	
Zfp295	2610028A01Rik	
Zfp335	2610101N10Rik	
Zfp36	2700099C18Rik	
Zfp36l1	2810408A11Rik	
Zfp36l2	2810422J05Rik	
Zfp384	2900064A13Rik	
Zfp438	3110043O21Rik	
Zfp457	3110082I17Rik	
Zfp593	4632411B12Rik	
Zfp622	4930519G04Rik	
Zfp653	4930544D05Rik	
Zfp667	4930583K01Rik	
Zfp687	4933421E11Rik	
Zfp868	4933433P14Rik	
Zfp869	5430405H02Rik	
Zfpl1	5430435G22Rik	
Zfyve20	5730419I09Rik	
Zfyve27	5730422E09Rik	
Zh2c2	5730455O13Rik	
Zkscan14	5830433M19Rik	
Zmynd11	6330407A03Rik	
Znhit3	6330577E15Rik	
Znrd1	6330578E17Rik	

APPENDIX II. zDC target genes: Transcription factor activity (TF), RNA splicing factory activity (RNA), Chromatin binding (Chrom), and Helicase activity (Heli)

TF		
A630001G21Rik	Hmg20a	Rbm14
AA987161	Ing3	Rel
Aff1	Ing4	Relb
Aff4	Irf2	Rfx1
Arid3a	Ivns1abp	Ring1
Arih1	Jdp2	Rnf44
Arih2	Jun	Runx1
Atf3	Junb	Safb2
Atf4	Jund	Sap30bp
Atf6b	Klf13	Sf1
Bap1	Klf2	Skil
Bat2	Klf4	Sp1
Bclaf1	Klf6	Spop
Brca1	Klhdc4	Stat3
Btbd1	Klhl12	Supt4h1
Btbd6	Klhl17	Taf11
Btbd9	Klhl7	Taf13
C1d	Maff	Taf5l
Ccbl1	Mafk	Tbp
Ccnh	Med13	Tcf3
Ccnl1	Med14	Tgif1
Ccnt1	Med27	Thrap3
Cd86	Med6	Tle3
Cdc5l	Mef2d	Ubp1
Cebpb	Mms19	Usf1
Cnot1	Mnt	Xab2
Cnot3	Morf4l1	Yeats2
Creb1	Mynn	Yy1
Crem	Myst2	Zbtb11
Ctcf	Nab2	Zbtb7a
Dnttip1	Nfatc3	Zer1
E4f1	Nfil3	Zfat
Eed	Nfkb2	Zfc3h1
Egr3	Nfx1	Zfp1
Elk4	Nfyc	Zfp143
Ell	Nr4a1	Zfp295
Ell2	Nr4a2	Zfp36
Esrra	Nrbf2	Zfp438
Etv3	Ocel1	Zfp457
Etv6	Per1	Zfp653
Fos	Phf15	Zfp667
Fosb	Phf20l1	Zfp687
Foxk2	Pknox1	Zfp868
Gan	Plekhf2	Zfp869
Gtf2a1	Prdm4	Zfpl1
Gtf2f1	Pura	Zfyve27
Hbp1	Purb	Zkscan14
Hdgf	Qrich1	Zmynd11
Hdgfrp2	Rabepk	Znhit3
Hivep2	Rap1b	Zscan21

RNA
Ascc3
Ccdc94
Dazap1
Hnrnpa2b1
Hnrnpa3
Hnrnpc
Hnrnpl
Hspa1a
Isy1
Khsrp
Lsm4
Nrd1
Pabpc1
Pafah1b1
Pak1ip1
Pcbp2
Prpf4
Ptbp1
Rbm14
Rbm3
Rbm39
Rbm42
Rbm8a
Rbms2
Rnps1
Rod1
Sf1
Sfrs1
Sfrs5
Snrnp70
Snrpg
Spen
Tbl2
Tfip11
Tra2a
Ubp1
Ucp2
Usp12
Usp28
Usp36
Usp38
Usp48
Usp8
Wdr43
Wdr53
Wdr5b
Xab2
Zer1

Chrom
A630001G21Rik
Baz1b
Baz2a
Brd2
Brd4
Deb1
Hist1h2bc
Hist1h3d
Hist1h3e
Hist1h4a
Hist1h4h
Hmg20a
Ing3
Ing4
Klhdc4
Morf4l1
Myst2
Nfyc
Pim1
Rabepk
Rccd1
Safb2
Sass6
Spty2d1
Supt4h1
Yeats2

Heli
Ascc3
Bat1a
Ccnl1
Ddx27
Ddx42
Ddx5
Ddx50
Ddx51
Ddx54
Ddx55
Dhx33
Dhx40
Hspa1a
Ino80
Supv3l1
Xrcc6

APPENDIX III. zDC target genes: Kinase activity, Peptidase activity, Ubiquitin-ligase activity, and Phosphatase activity

Kinase	Peptidase	Ubiquitin-ligase	Phosphatase
Bap1	Abhd11	Arih1	Bdp1
Braf	Adam9	Arih2	Dusp1
Bub1	Bap1	Cd86	Dusp2
Ccr1	Btbd1	Cdc34	Ppp2ca
Cdc2l1	Btbd6	Cul1	Ppp2r5a
Cdc2l5	Btbd9	Mib2	Ppp4c
Cdc42bpb	Casp8	Pafah1b1	Ppp6c
Cdkl3	Clpb	Pak1ip1	Pten
Crkrs	Ctsc	Rnf139	Ptp4a1
Csnk1g2	Ece1	Rnf167	Ptp4a2
Dyrk1a	Gan	Rnf34	Ptpn11
Gsk3a	Htra2	Siah2	Ptprc
Ikbkb	Ivns1abp	Tbl2	Ptprj
Lats2	Klhl12	Trim12	
Lias	Klhl17	Trim35	
Limk1	Klhl7	Trim39	
Map3k1	Lonp1	Trim65	
Map3k11	Mbd3	Trim8	
Map3k2	Mbd3	Ube2h	
Mapk3	Napa	Ube2j1	
Mapk8	Nrd1	Ube2n	
Mapkapk5	Pef1	Ube2s	
Mark2	Pim1	Ube2v1	
Mastl	Prcp	Ube3c	
Nek1	Psma1	Ubl3	
Nek8	Psmb2	Ubp1	
Pef1	Psmb8	Ubr4	
Pim1	Rce1	Use1	
Pkn1	Senp2	Usp12	
Prkacb	Senp3	Usp28	
Prkce	Senp5	Usp36	
Pskh1	Sp1	Usp38	
Ptcd1	Spop	Usp48	
Raf1	Tpp2	Usp8	
Riok1	Ubp1	Wdr43	
Rock1	Uchl5	Wdr53	
Rps6ka5	Ucp2	Wdr5b	
Rps6kb2	Usp12		
Sgk3	Usp28		
Stk11	Usp36		
Stk16	Usp38		
Stk38l	Usp48		
Tesk1	Usp52		
Tgfb1	Usp8		
Trib1	Zh2c2		

References

Aderem, A. and Underhill, D. M. (1999), 'Mechanisms of phagocytosis in macrophages', *Annu Rev Immunol,* 17, 593-623.

Akbari, O., DeKruyff, R. H., and Umetsu, D. T. (2001), 'Pulmonary dendritic cells producing IL-10 mediate tolerance induced by respiratory exposure to antigen', *Nat Immunol,* 2 (8), 725-31.

Aliberti, J. (2005), 'Host persistence: exploitation of anti-inflammatory pathways by Toxoplasma gondii', *Nat Rev Immunol,* 5 (2), 162-70.

Alvarez, D., Vollmann, E. H., and von Andrian, U. H. (2008), 'Mechanisms and consequences of dendritic cell migration', *Immunity,* 29 (3), 325-42.

Asselin-Paturel, C., et al. (2001), 'Mouse type I IFN-producing cells are immature APCs with plasmacytoid morphology', *Nat Immunol,* 2 (12), 1144-50.

Auffray, C., et al. (2009), 'CX3CR1+ CD115+ CD135+ common macrophage/DC precursors and the role of CX3CR1 in their response to inflammation', *J Exp Med,* 206 (3), 595-606.

Bailey, T. L., et al. (2009), 'MEME SUITE: tools for motif discovery and searching', *Nucleic Acids Res,* 37 (Web Server issue), W202-8.

Barchet, W., Cella, M., and Colonna, M. (2005), 'Plasmacytoid dendritic cells--virus experts of innate immunity', *Seminars in immunology,* 17 (4), 253-61.

Beaulieu, A. M. and Sant'Angelo, D. B. (2011), 'The BTB-ZF family of transcription factors: key regulators of lineage commitment and effector function development in the immune system', *J Immunol,* 187 (6), 2841-7.

Belz, G. T. and Nutt, S. L. (2012), 'Transcriptional programming of the dendritic cell network', *Nat Rev Immunol,* 12 (2), 101-13.

Bennett, C. L. and Clausen, B. E. (2007), 'DC ablation in mice: promises, pitfalls, and challenges', *Trends Immunol,* 28 (12), 525-31.

Birnberg, T., et al. (2008), 'Lack of conventional dendritic cells is compatible with normal development and T cell homeostasis, but causes myeloid proliferative syndrome', *Immunity,* 29 (6), 986-97.

Blasius, A., et al. (2004), 'A cell-surface molecule selectively expressed on murine natural interferon-producing cells that blocks secretion of interferon-alpha', *Blood,* 103 (11), 4201-6.

Bogunovic, M., et al. (2009), 'Origin of the lamina propria dendritic cell network', *Immunity,* 31 (3), 513-25.

Bouillet, P., et al. (2002), 'BH3-only Bcl-2 family member Bim is required for apoptosis of autoreactive thymocytes', *Nature,* 415 (6874), 922-6.

Bouloc, A., et al. (2000), 'Triggering CD101 molecule on human cutaneous dendritic cells inhibits T cell proliferation via IL-10 production', *Eur J Immunol,* 30 (11), 3132-9.

Bradford, B. M., et al. (2011), 'Defining the anatomical localisation of subsets of the murine mononuclear phagocyte system using integrin alpha X (Itgax, CD11c) and colony stimulating factor 1 receptor (Csf1r, CD115) expression fails to discriminate dendritic cells from macrophages', *Immunobiology,* 216 (11), 1228-37.

Brasel, K., et al. (2000), 'Generation of murine dendritic cells from flt3-ligand-supplemented bone marrow cultures', *Blood,* 96 (9), 3029-39.

Bulyk, M. L., et al. (2001), 'Exploring the DNA-binding specificities of zinc fingers with DNA microarrays', *Proc Natl Acad Sci U S A,* 98 (13), 7158-63.

Carotta, S., et al. (2010), 'The transcription factor PU.1 controls dendritic cell development and Flt3 cytokine receptor expression in a dose-dependent manner', *Immunity,* 32 (5), 628-41.

Cella, M., et al. (1997), 'Inflammatory stimuli induce accumulation of MHC class II complexes on dendritic cells', *Nature,* 388 (6644), 782-7.

Cella, M., et al. (1999), 'Plasmacytoid monocytes migrate to inflamed lymph nodes and produce large amounts of type I interferon', *Nat Med,* 5 (8), 919-23.

Cheong, C., et al. (2010), 'Microbial stimulation fully differentiates monocytes to DC-SIGN/CD209(+) dendritic cells for immune T cell areas', *Cell,* 143 (3), 416-29.

Collins, T., Stone, J. R., and Williams, A. J. (2001), 'All in the family: the BTB/POZ, KRAB, and SCAN domains', *Mol Cell Biol,* 21 (11), 3609-15.

Colonna, M., Trinchieri, G., and Liu, Y. J. (2004), 'Plasmacytoid dendritic cells in immunity', *Nature immunology,* 5 (12), 1219-26.

Coombes, J. L., et al. (2007), 'A functionally specialized population of mucosal CD103+ DCs induces Foxp3+ regulatory T cells via a TGF-beta and retinoic acid-dependent mechanism', *J Exp Med,* 204 (8), 1757-64.

Corcoran, L., et al. (2003), 'The lymphoid past of mouse plasmacytoid cells and thymic dendritic cells', *Journal of immunology,* 170 (10), 4926-32.

D'Amico, A. and Wu, L. (2003), 'The early progenitors of mouse dendritic cells and plasmacytoid predendritic cells are within the bone marrow hemopoietic precursors expressing Flt3', *J Exp Med,* 198 (2), 293-303.

Darrasse-Jeze, G., et al. (2009), 'Feedback control of regulatory T cell homeostasis by dendritic cells in vivo', *J Exp Med,* 206 (9), 1853-62.

Davey, G. M., et al. (2002), 'Peripheral deletion of autoreactive CD8 T cells by cross presentation of self-antigen occurs by a Bcl-2-inhibitable pathway mediated by Bim', *J Exp Med,* 196 (7), 947-55.

Denkers, E. Y. (2003), 'From cells to signaling cascades: manipulation of innate immunity by Toxoplasma gondii', *FEMS Immunol Med Microbiol,* 39 (3), 193-203.

Denkers, E. Y. and Gazzinelli, R. T. (1998), 'Regulation and function of T-cell-mediated immunity during Toxoplasma gondii infection', *Clin Microbiol Rev,* 11 (4), 569-88.

Dent, A. L., et al. (1997), 'Control of inflammation, cytokine expression, and germinal center formation by BCL-6', *Science,* 276 (5312), 589-92.

Diao, J., et al. (2004), 'Characterization of distinct conventional and plasmacytoid dendritic cell-committed precursors in murine bone marrow', *J Immunol,* 173 (3), 1826-33.

Dudziak, D., et al. (2007), 'Differential antigen processing by dendritic cell subsets in vivo', *Science,* 315 (5808), 107-11.

Dustin, M. L., Chakraborty, A. K., and Shaw, A. S. (2010), 'Understanding the structure and function of the immunological synapse', *Cold Spring Harb Perspect Biol,* 2 (10), a002311.

Engel, I., et al. (2010), 'Co-receptor choice by V alpha14i NKT cells is driven by Th-POK expression rather than avoidance of CD8-mediated negative selection', *J Exp Med,* 207 (5), 1015-29.

Fitzgerald-Bocarsly, P. (1993), 'Human natural interferon-alpha producing cells', *Pharmacology & therapeutics,* 60 (1), 39-62.

Fogg, D. K., et al. (2006), 'A clonogenic bone marrow progenitor specific for macrophages and dendritic cells', *Science,* 311 (5757), 83-7.

Foster, S. L., Hargreaves, D. C., and Medzhitov, R. (2007), 'Gene-specific control of inflammation by TLR-induced chromatin modifications', *Nature,* 447 (7147), 972-8.

Galli, S. J., Borregaard, N., and Wynn, T. A. (2011), 'Phenotypic and functional plasticity of cells of innate immunity: macrophages, mast cells and neutrophils', *Nat Immunol,* 12 (11), 1035-44.

Gallucci, S. and Matzinger, P. (2001), 'Danger signals: SOS to the immune system', *Curr Opin Immunol,* 13 (1), 114-9.

Gazzinelli, R. T., et al. (1994), 'Parasite-induced IL-12 stimulates early IFN-gamma synthesis and resistance during acute infection with Toxoplasma gondii', *Journal of immunology,* 153 (6), 2533-43.

Geissmann, F., Jung, S., and Littman, D. R. (2003), 'Blood monocytes consist of two principal subsets with distinct migratory properties', *Immunity,* 19 (1), 71-82.

Geissmann, F., et al. (2010a), 'Unravelling mononuclear phagocyte heterogeneity', *Nat Rev Immunol,* 10 (6), 453-60.

Geissmann, F., et al. (2010b), 'Development of monocytes, macrophages, and dendritic cells', *Science,* 327 (5966), 656-61.

Ginhoux, F., et al. (2009), 'The origin and development of nonlymphoid tissue CD103+ DCs', *J Exp Med,* 206 (13), 3115-30.

Gordon, S. and Taylor, P. R. (2005), 'Monocyte and macrophage heterogeneity', *Nat Rev Immunol,* 5 (12), 953-64.

Handunnetthi, L., et al. (2010), 'Regulation of major histocompatibility complex class II gene expression, genetic variation and disease', *Genes Immun,* 11 (2), 99-112.

Hashimoto, D., Miller, J., and Merad, M. (2011), 'Dendritic cell and macrophage heterogeneity in vivo', *Immunity,* 35 (3), 323-35.

Hawiger, D., et al. (2004), 'Immunological unresponsiveness characterized by increased expression of CD5 on peripheral T cells induced by dendritic cells in vivo', *Immunity,* 20 (6), 695-705.

Hawiger, D., et al. (2001), 'Dendritic cells induce peripheral T cell unresponsiveness under steady state conditions in vivo', *J Exp Med,* 194 (6), 769-79.

He, X., et al. (2005), 'The zinc finger transcription factor Th-POK regulates CD4 versus CD8 T-cell lineage commitment', *Nature,* 433 (7028), 826-33.

Helft, J., et al. (2010), 'Origin and functional heterogeneity of non-lymphoid tissue dendritic cells in mice', *Immunol Rev,* 234 (1), 55-75.

Hickman, H. D., et al. (2011), 'Chemokines control naive CD8+ T cell selection of optimal lymph node antigen presenting cells', *J Exp Med,* 208 (12), 2511-24.

Hildner, K., et al. (2008), 'Batf3 deficiency reveals a critical role for CD8alpha+ dendritic cells in cytotoxic T cell immunity', *Science,* 322 (5904), 1097-100.

Hohl, T. M., et al. (2009), 'Inflammatory monocytes facilitate adaptive CD4 T cell responses during respiratory fungal infection', *Cell Host Microbe,* 6 (5), 470-81.

Inaba, K., et al. (1992a), 'Generation of large numbers of dendritic cells from mouse bone marrow cultures supplemented with granulocyte/macrophage colony-stimulating factor', *J Exp Med,* 176 (6), 1693-702.

Inaba, K., et al. (1992b), 'Identification of proliferating dendritic cell precursors in mouse blood', *J Exp Med,* 175 (5), 1157-67.

Iparraguirre, A., et al. (2008), 'Two distinct activation states of plasmacytoid dendritic cells induced by influenza virus and CpG 1826 oligonucleotide', *J Leukoc Biol,* 83 (3), 610-20.

Julia, V., et al. (2002), 'A restricted subset of dendritic cells captures airborne antigens and remains able to activate specific T cells long after antigen exposure', *Immunity,* 16 (2), 271-83.

Jung, S., et al. (2002), 'In vivo depletion of CD11c+ dendritic cells abrogates priming of CD8+ T cells by exogenous cell-associated antigens', *Immunity,* 17 (2), 211-20.

Kamphorst, A. O., et al. (2010), 'Route of antigen uptake differentially impacts presentation by dendritic cells and activated monocytes', *J Immunol,* 185 (6), 3426-35.

Kassim, S. H., et al. (2006), 'In vivo ablation of CD11c-positive dendritic cells increases susceptibility to herpes simplex virus type 1 infection and diminishes NK and T-cell responses', *J Virol,* 80 (8), 3985-93.

Kawai, T. and Akira, S. (2006), 'TLR signaling', *Cell Death Differ,* 13 (5), 816-25.

Kelly, K. F. and Daniel, J. M. (2006), 'POZ for effect--POZ-ZF transcription factors in cancer and development', *Trends Cell Biol,* 16 (11), 578-87.

Kraal, G., et al. (1986), 'Langerhans' cells, veiled cells, and interdigitating cells in the mouse recognized by a monoclonal antibody', *J Exp Med,* 163 (4), 981-97.

Krawczyk, M., et al. (2008), 'Identification of CIITA regulated genetic module dedicated for antigen presentation', *PLoS Genet,* 4 (4), e1000058.

Kretschmer, K., et al. (2005), 'Inducing and expanding regulatory T cell populations by foreign antigen', *Nat Immunol,* 6 (12), 1219-27.

Krug, A., et al. (2004), 'Herpes simplex virus type 1 activates murine natural interferon-producing cells through toll-like receptor 9', *Blood,* 103 (4), 1433-7.

Kugathasan, S., et al. (2008), 'Loci on 20q13 and 21q22 are associated with pediatric-onset inflammatory bowel disease', *Nat Genet,* 40 (10), 1211-5.

Landmann, S., et al. (2001), 'Maturation of dendritic cells is accompanied by rapid transcriptional silencing of class II transactivator (CIITA) expression', *J Exp Med,* 194 (4), 379-91.

Leon, B., Lopez-Bravo, M., and Ardavin, C. (2007), 'Monocyte-derived dendritic cells formed at the infection site control the induction of protective T helper 1 responses against Leishmania', *Immunity,* 26 (4), 519-31.

Lian, Z. X., et al. (2003), 'Heterogeneity of dendritic cells in the mouse liver: identification and characterization of four distinct populations', *Journal of immunology,* 170 (5), 2323-30.

Lieberman, L. A. and Hunter, C. A. (2002), 'The role of cytokines and their signaling pathways in the regulation of immunity to Toxoplasma gondii', *Int Rev Immunol,* 21 (4-5), 373-403.

Lindstedt, M., Johansson-Lindbom, B., and Borrebaeck, C. A. (2002), 'Global reprogramming of dendritic cells in response to a concerted action of inflammatory mediators', *Int Immunol,* 14 (10), 1203-13.

Liu, C. H., et al. (2006), 'Cutting edge: dendritic cells are essential for in vivo IL-12 production and development of resistance against Toxoplasma gondii infection in mice', *J Immunol,* 177 (1), 31-5.

Liu, K. and Nussenzweig, M. C. (2010), 'Origin and development of dendritic cells', *Immunol Rev,* 234 (1), 45-54.

Liu, K., et al. (2007), 'Origin of dendritic cells in peripheral lymphoid organs of mice', *Nat Immunol,* 8 (6), 578-83.

Liu, K., et al. (2009), 'In vivo analysis of dendritic cell development and homeostasis', *Science,* 324 (5925), 392-7.

Lucas, M., et al. (2007), 'Dendritic cells prime natural killer cells by trans-presenting interleukin 15', *Immunity,* 26 (4), 503-17.

Maldonado-Lopez, R., et al. (1999), 'CD8alpha+ and CD8alpha- subclasses of dendritic cells direct the development of distinct T helper cells in vivo', *J Exp Med,* 189 (3), 587-92.

Maraskovsky, E., et al. (1996), 'Dramatic increase in the numbers of functionally mature dendritic cells in Flt3 ligand-treated mice: multiple dendritic cell subpopulations identified', *J Exp Med,* 184 (5), 1953-62.

Maraskovsky, E., et al. (2000), 'In vivo generation of human dendritic cell subsets by Flt3 ligand', *Blood,* 96 (3), 878-84.

Mashayekhi, M., et al. (2011), 'CD8alpha(+) dendritic cells are the critical source of interleukin-12 that controls acute infection by Toxoplasma gondii tachyzoites', *Immunity,* 35 (2), 249-59.

McKenna, H. J., et al. (2000), 'Mice lacking flt3 ligand have deficient hematopoiesis affecting hematopoietic progenitor cells, dendritic cells, and natural killer cells', *Blood,* 95 (11), 3489-97.

Mellman, I. and Steinman, R. M. (2001), 'Dendritic cells: specialized and regulated antigen processing machines', *Cell,* 106 (3), 255-8.

Mellman, I., Turley, S. J., and Steinman, R. M. (1998), 'Antigen processing for amateurs and professionals', *Trends Cell Biol,* 8 (6), 231-7.

Metlay, J. P., et al. (1990), 'The distinct leukocyte integrins of mouse spleen dendritic cells as identified with new hamster monoclonal antibodies', *J Exp Med,* 171 (5), 1753-71.

Mitamura, T., et al. (1995), 'Diphtheria toxin binds to the epidermal growth factor (EGF)-like domain of human heparin-binding EGF-like growth factor/diphtheria toxin receptor and inhibits specifically its mitogenic activity', *J Biol Chem,* 270 (3), 1015-9.

Mosier, D. E. (1967), 'A requirement for two cell types for antibody formation in vitro', *Science,* 158 (3808), 1573-5.

Mucida, D., et al. (2007), 'Reciprocal TH17 and regulatory T cell differentiation mediated by retinoic acid', *Science,* 317 (5835), 256-60.

Murphy, K. M. (2011), 'Comment on "Activation of beta-catenin in dendritic cells regulates immunity versus tolerance in the intestine"', *Science,* 333 (6041), 405; author reply 05.

Naik, S. H., Corcoran, L. M., and Wu, L. (2005a), 'Development of murine plasmacytoid dendritic cell subsets', *Immunology and cell biology,* 83 (5), 563-70.

Naik, S. H., et al. (2006), 'Intrasplenic steady-state dendritic cell precursors that are distinct from monocytes', *Nat Immunol,* 7 (6), 663-71.

Naik, S. H., et al. (2005b), 'Cutting edge: generation of splenic CD8+ and CD8- dendritic cell equivalents in Fms-like tyrosine kinase 3 ligand bone marrow cultures', *J Immunol,* 174 (11), 6592-7.

Naik, S. H., et al. (2007), 'Development of plasmacytoid and conventional dendritic cell subtypes from single precursor cells derived in vitro and in vivo', *Nat Immunol,* 8 (11), 1217-26.

Nurieva, R. I., et al. (2009), 'Bcl6 mediates the development of T follicular helper cells', *Science,* 325 (5943), 1001-5.

Nussenzweig, M. C., et al. (1980), 'Dendritic cells are accessory cells for the development of anti-trinitrophenyl cytotoxic T lymphocytes', *J Exp Med,* 152 (4), 1070-84.

Nussenzweig, M. C., et al. (1982), 'A monoclonal antibody specific for mouse dendritic cells', *Proc Natl Acad Sci U S A,* 79 (1), 161-5.

Nussenzweig, M. C., et al. (1981), 'Studies of the cell surface of mouse dendritic cells and other leukocytes', *J Exp Med,* 154 (1), 168-87.

O'Keeffe, M., et al. (2003), 'Dendritic cell precursor populations of mouse blood: identification of the murine homologues of human blood plasmacytoid pre-DC2 and CD11c+ DC1 precursors', *Blood,* 101 (4), 1453-9.

O'Keeffe, M., et al. (2002), 'Mouse plasmacytoid cells: long-lived cells, heterogeneous in surface phenotype and function, that differentiate into CD8(+) dendritic cells only after microbial stimulus', *J Exp Med,* 196 (10), 1307-19.

Onai, N. and Manz, M. G. (2008), 'The STATs on dendritic cell development', *Immunity,* 28 (4), 490-2.

Onai, N., et al. (2007), 'Identification of clonogenic common Flt3+M-CSFR+ plasmacytoid and conventional dendritic cell progenitors in mouse bone marrow', *Nat Immunol,* 8 (11), 1207-16.

Piazza, F., et al. (2004), 'Disruption of PLZP in mice leads to increased T-lymphocyte proliferation, cytokine production, and altered hematopoietic stem cell homeostasis', *Mol Cell Biol,* 24 (23), 10456-69.

Probst, H. C., et al. (2005), 'Histological analysis of CD11c-DTR/GFP mice after in vivo depletion of dendritic cells', *Clin Exp Immunol,* 141 (3), 398-404.

Randolph, G. J., et al. (1999), 'Differentiation of phagocytic monocytes into lymph node dendritic cells in vivo', *Immunity,* 11 (6), 753-61.

Rathinam, C., et al. (2005), 'The transcriptional repressor Gfi1 controls STAT3-dependent dendritic cell development and function', *Immunity,* 22 (6), 717-28.

Rissoan, M. C., et al. (2002), 'Subtractive hybridization reveals the expression of immunoglobulin-like transcript 7, Eph-B1, granzyme B, and 3 novel transcripts in human plasmacytoid dendritic cells', *Blood,* 100 (9), 3295-303.

Robbins, S. H., et al. (2008), 'Novel insights into the relationships between dendritic cell subsets in human and mouse revealed by genome-wide expression profiling', *Genome Biol,* 9 (1), R17.

Romani, N., Clausen, B. E., and Stoitzner, P. (2010), 'Langerhans cells and more: langerin-expressing dendritic cell subsets in the skin', *Immunol Rev,* 234 (1), 120-41.

Saito, M., et al. (2001), 'Diphtheria toxin receptor-mediated conditional and targeted cell ablation in transgenic mice', *Nat Biotechnol,* 19 (8), 746-50.

Sallusto, F. and Lanzavecchia, A. (1994), 'Efficient presentation of soluble antigen by cultured human dendritic cells is maintained by granulocyte/macrophage colony-stimulating factor plus interleukin 4 and downregulated by tumor necrosis factor alpha', *J Exp Med,* 179 (4), 1109-18.

Sancho, D., et al. (2009), 'Identification of a dendritic cell receptor that couples sensing of necrosis to immunity', *Nature,* 458 (7240), 899-903.

Savina, A. and Amigorena, S. (2007), 'Phagocytosis and antigen presentation in dendritic cells', *Immunol Rev,* 219, 143-56.

Schlenner, S. M., et al. (2010), 'Fate mapping reveals separate origins of T cells and myeloid lineages in the thymus', *Immunity,* 32 (3), 426-36.

Schmid, M. A., et al. (2010), 'Instructive cytokine signals in dendritic cell lineage commitment', *Immunol Rev,* 234 (1), 32-44.

Schmid, M. A., et al. (2011), 'Bone marrow dendritic cell progenitors sense pathogens via Toll-like receptors and subsequently migrate to inflamed lymph nodes', *Blood,* 118 (18), 4829-40.

Schulz, C., et al. (2012), 'A Lineage of Myeloid Cells Independent of Myb and Hematopoietic Stem Cells', *Science*.

Schulz, O. and Reis e Sousa, C. (2002), 'Cross-presentation of cell-associated antigens by CD8alpha+ dendritic cells is attributable to their ability to internalize dead cells', *Immunology,* 107 (2), 183-9.

Serbina, N. V., et al. (2003), 'TNF/iNOS-producing dendritic cells mediate innate immune defense against bacterial infection', *Immunity,* 19 (1), 59-70.

Shaffer, A. L., et al. (2000), 'BCL-6 represses genes that function in lymphocyte differentiation, inflammation, and cell cycle control', *Immunity,* 13 (2), 199-212.

Shigematsu, H., et al. (2004), 'Plasmacytoid dendritic cells activate lymphoid-specific genetic programs irrespective of their cellular origin', *Immunity,* 21 (1), 43-53.

Steinman, R. M. (2007), 'Lasker Basic Medical Research Award. Dendritic cells: versatile controllers of the immune system', *Nat Med,* 13 (10), 1155-9.

Steinman, R. M. and Cohn, Z. A. (1973), 'Identification of a novel cell type in peripheral lymphoid organs of mice. I. Morphology, quantitation, tissue distribution', *J Exp Med,* 137 (5), 1142-62.

Steinman, R. M. and Witmer, M. D. (1978), 'Lymphoid dendritic cells are potent stimulators of the primary mixed leukocyte reaction in mice', *Proc Natl Acad Sci U S A,* 75 (10), 5132-6.

Steinman, R. M., Hawiger, D., and Nussenzweig, M. C. (2003a), 'Tolerogenic dendritic cells', *Annu Rev Immunol,* 21, 685-711.

Steinman, R. M., et al. (1979), 'Identification of a novel cell type in peripheral lymphoid organs of mice. V. Purification of spleen dendritic cells, new surface markers, and maintenance in vitro', *J Exp Med,* 149 (1), 1-16.

Steinman, R. M., et al. (2003b), 'Dendritic cell function in vivo during the steady state: a role in peripheral tolerance', *Ann N Y Acad Sci,* 987, 15-25.

Subauste, C. and Remington, J. (2001), 'Animal models for Toxoplasma gondii infection', *Curr Protoc Immunol,* Chapter 19, Unit 19 3.

Subramanian, A., et al. (2005), 'Gene set enrichment analysis: a knowledge-based approach for interpreting genome-wide expression profiles', *Proc Natl Acad Sci U S A,* 102 (43), 15545-50.

Sun, C. M., et al. (2007), 'Small intestine lamina propria dendritic cells promote de novo generation of Foxp3 T reg cells via retinoic acid', *J Exp Med,* 204 (8), 1775-85.

Thomas, P. D., et al. (2003), 'PANTHER: a browsable database of gene products organized by biological function, using curated protein family and subfamily classification', *Nucleic Acids Res,* 31 (1), 334-41.

Tian, T., et al. (2005), 'In vivo depletion of CD11c+ cells delays the CD4+ T cell response to Mycobacterium tuberculosis and exacerbates the outcome of infection', *J Immunol,* 175 (5), 3268-72.

Tittel, A. P., et al. (2012), 'Functionally relevant neutrophilia in CD11c diphtheria toxin receptor transgenic mice', *Nat Methods*.

Trombetta, E. S. and Mellman, I. (2005), 'Cell biology of antigen processing in vitro and in vivo', *Annu Rev Immunol,* 23, 975-1028.

Tunyaplin, C., et al. (2004), 'Direct repression of prdm1 by Bcl-6 inhibits plasmacytic differentiation', *J Immunol,* 173 (2), 1158-65.

Tzeng, T. C., et al. (2010), 'CD11c(hi) dendritic cells regulate the re-establishment of vascular quiescence and stabilization after immune stimulation of lymph nodes', *J Immunol,* 184 (8), 4247-57.

Varol, C., et al. (2007), 'Monocytes give rise to mucosal, but not splenic, conventional dendritic cells', *J Exp Med,* 204 (1), 171-80.

Varol, C., et al. (2009), 'Intestinal lamina propria dendritic cell subsets have different origin and functions', *Immunity,* 31 (3), 502-12.

Waskow, C., et al. (2008), 'The receptor tyrosine kinase Flt3 is required for dendritic cell development in peripheral lymphoid tissues', *Nat Immunol,* 9 (6), 676-83.

Webster, B., et al. (2006), 'Regulation of lymph node vascular growth by dendritic cells', *J Exp Med,* 203 (8), 1903-13.

Wendland, M., et al. (2011), 'Lymph node T cell homeostasis relies on steady state homing of dendritic cells', *Immunity,* 35 (6), 945-57.

Xu, Y., et al. (2007), 'Differential development of murine dendritic cells by GM-CSF versus Flt3 ligand has implications for inflammation and trafficking', *Journal of immunology,* 179 (11), 7577-84.

Yamaizumi, M., et al. (1978), 'One molecule of diphtheria toxin fragment A introduced into a cell can kill the cell', *Cell,* 15 (1), 245-50.

Yamazaki, S., et al. (2008), 'CD8+ CD205+ splenic dendritic cells are specialized to induce Foxp3+ regulatory T cells', *Journal of immunology,* 181 (10), 6923-33.

Ye, B. H., et al. (1997), 'The BCL-6 proto-oncogene controls germinal-centre formation and Th2-type inflammation', *Nat Genet,* 16 (2), 161-70.

Yu, D., et al. (2009), 'The transcriptional repressor Bcl-6 directs T follicular helper cell lineage commitment', *Immunity,* 31 (3), 457-68.

Zaft, T., et al. (2005), 'CD11chigh dendritic cell ablation impairs lymphopenia-driven proliferation of naive and memory CD8+ T cells', *J Immunol,* 175 (10), 6428-35.

Zammit, D. J., et al. (2005), 'Dendritic cells maximize the memory CD8 T cell response to infection', *Immunity,* 22 (5), 561-70.

Zhang, J., et al. (2006), 'Characterization of Siglec-H as a novel endocytic receptor expressed on murine plasmacytoid dendritic cell precursors', *Blood,* 107 (9), 3600-8.